AN ABSTRACT OF THE THESIS OF

Ahmed I. M. Rushdi for the degree of Doctor of Philosophy in Oceanography presented on May 26, 1989.

Title: Kinetics and Equilibria of Magnesian Calcite in Seawater-like Solutions: Laboratory Studies

Redacted for Privacy

Abstract Approved: _____
Ricardo M. Pytkowicz

The effects of magnesium ion concentrations and the degree of saturation in artificial seawater (ASW) upon the kinetics and the equilibria of calcium carbonate solid have been studied. Also, the effects of calcium and magnesium ion concentrations on the equilibrium state of the system H_2CO_3-H_2O have been investigated. It is shown that magnesium ions delay the spontaneous precipitation of calcium carbonates from supersaturated seawater to such an extent that only biological removal is possible from the open ocean. Low magnesian calcite is favored at low degrees of supersaturation and low concentration of magnesium. Aragonite is observed to form at magnesium concentration of natural seawater. The presence of magnesium ions in ASW produces acicular crystals rather than the equant morphology of calcium carbonate.

The measured first and second apparent dissociation constants of carbonic acid, K_1' and K_2', increase with increasing concentrations of calcium and magnesium in ASW. The estimated $(\gamma HCO3^-)_T$ and $(\gamma CO3^{2-})_T$ at $I_T = 0.718$ and $T = 25^oC$ decrease as a function of Mg:Ca concentration ratios in ASW. The results also show that Ca^{2+} has a greater effect on the apparent dissociation constants of carbonic acid than magnesium,

suggesting that Ca^{2+} associates more strongly with bicarbonate and carbonate than magnesium.

Calcite precipitation results from overgrowth interface in the presence as well as in the absence of Mg^{2+} in ASW. The reaction is second order in Mg-free ASW and third order in the presence of magnesium ion in ASW. The overgrowth reaction rates decrease with increasing Mg^{2+} concentration in ASW. The decrease of reaction rate and the shift from a second order to a third order reaction confirm the involvement of magnesium ions in the overgrowth reaction by magnesian calcite.

The apparent solubility products of pure calcite, when exposed to different Mg:Ca concentration ratios in ASW, increase with Mg^{2+} concentration in ASW. Their solubility product values further increase by increasing the degree of supersaturation at the same Mg^{2+} concentration in the test solution. The increase of surface areas, that are exposed to the same volume of the solution under the same condition lowers the apparent solubility product values. This implies a shift from a kinetic steady-state to a thermodynamic equilibrium. The thermodynamic solubility products that are estimated from the ion association model and the activity of calcite and magnesite in the test ASW show that the activity coefficient of magnesite is much higher than that of calcite, which indicates that a nonideal solid solution is formed. The estimated incongruent solid-solution thermodynamic constants of magnesian calcite increase significantly with Mg^{2+} concentrations in ASW which suggests that the outermost layer of calcite is probably of higher magnesium concentration than those determined.

KINETICS AND EQUILIBRIA OF MAGNESIAN CALCITE IN SEAWATER-LIKE SOLUTIONS: LABORATORY STUDIES

by

Ahmed I. M. Rushdi

A THESIS

Submitted to

Oregon State University

In partial fulfillment of

the requirement for the degree of

Doctor of Philosophy

Completed May 26, 1989

Commencement June 1990

APPROVED:

Redacted for Privacy

Professor of Oceanography in Charge of Major

Redacted for Privacy

Dean of College of Oceanography

Redacted for Privacy

Dean of Graduate School

Date thesis is presented May 26, 1989

ACKNOWLEDGEMENTS

First, I would like to thank my major advisor, Ricardo Pytkowicz. He was a great support and source of encouragement throughout all stages of this thesis. Many of the ideas presented in this work were developed in discussions with him. His friendship and guidance have helped make my experience here a pleasure one. I thank Erwin Suess for his personal interest and his invaluable inputs during the first stages of this thesis. Arthur Boucot, Bob collier, Peter Nelson and Roman Schmitt are sincerely appreciated for their time and energy they spent as members of my committee.

The support I received from friends, faculty and fellow students was one the most satisfying and reassuring products of this thesis. Arthur Chen has been willing and helpful. Chih-An Huh was generous when I needed a laboratory space to finish the final phase of this research. Technical assistance was provided by Andy Ungerer, who was extremely helpful. He taught me how to use the atomic adsorption spectrophotometer and X-ray diffractiometer.

Jim McManus, who kept me playing out-door and in-door soccer and Johnny Sharp, whose great spirits were always around; they still owe me a house-to-go. Kaijun Lin, with him I had wonderful times. My class-mates Orest Kawka, Luis Pinto and Calvin Mordy.

I am grateful to my family. I would like to thank my wife Fiaza, for her encouragement, friendship. She has tolerated the tensions and stresses with love. My lovely daughter Eman, had been reminding me to wash my hands from chemicals at the end of the day.

My sincere thank to my parents. My mother and my father who encouraged me to science and sports since the childhood. My father in-law Ahmed Al-Saaidi and my mother in-law, who gave us the love, guidance and encouragements.

A very special acknowledgement to (Khalou) Ali Basahi for his always being a long distance phone calls. Special thanks to my friend Mohammed Mutahar for taking care of the things when I needed him.

Financial support was provided by U.S. AID program in Sana'a , Yemen Arab Republic and Oceanography Department, Faculty of Science, Sana'a University.

TABLE OF CONTENTS

LIST OF FIGURES

INTRODUCTION

CHAPTER 1.

CHAPTER 2.

CHAPTER 3.

CHAPTER 4.

LIST OF TABLES

INTRODUCTION

CHAPTER 1.

CHAPTER 2.

CHAPTER 3.

CHAPTER 4.

LIST OF APPENDIX FIGURES

LIST OF APPENDIX TABLES

KINETICS AND EQUILIBRIA OF MAGNESIAN CALCITE IN SEAWATER-LIKE SOLUTIONS: LABORATORY STUDIES

INTRODUCTION AND OUTLINE

Introduction

The $CaCO_3$-H_2O system has been extensively studied by chemists, sanitary engineers, as well as geochemists and oceanographers, because of its buffering behavior *(Horne, 1970; Riley and Skirrow, 1975; Stumm and Morgan, 1982; Butler, 1982*), its relation to water hardness *(Snoeyink and Jenkins, 1980; Butler, 1982),* and biogeochemical processes in natural waters *(Berner, 1966a; Bathurst, 1975; Mackenzie et al., 1982; Broecker and Peng, 1982; 1987).* The chemical behavior of calcium carbonate in aqueous solution is important for understanding geochemical principles, because of the effect of the CO_2-system on major metal concentrations, major minerals and biological activities. The biological activities and both, chemical and physical processes make the system very complicated to predict and to apply the geochemical principles in the marine environment *(Bathurst, 1964; Mackenzie et al., 1982).*

The carbonate system is characterized by the following species: gaseous $CO_{2(g)}$, aqueous $CO_{2(l)}$ and H_2CO_3, HCO_3^- and CO_3^{2-} in solution; and a solid form represented by $RCO_{3(s)}$, where R refers to a divalent metal such as Ca^{2+}. The following reactions define the carbonate system in simple solution:

$$CO_{2(g)} \Longleftrightarrow CO_{2(l)} \qquad (1)$$

$$CO_{2(l)} + H_2O \Longleftrightarrow H_2CO_3 \qquad (2)$$

$$H_2CO_3 \Longleftrightarrow H^+ + HCO_3^- \qquad (3)$$

$$HCO_3^- \Longleftrightarrow H^+ + CO_3^{2-} \qquad (4)$$

$$R^{2+} + CO_3^{2-} \Longleftrightarrow RCO_{3(s)} \qquad (5)$$

Morphology and Mineralogy of CaCO3(s)

In nature there are three common polymorphic forms of calcium carbonate, which are shown in Table 1. Each solid of these compounds has a different solubility, which makes the carbonate equilibrium relationship somewhat difficult to be treated as a simple system. Calcite is the stable phase at 25°C and one atmospheric pressure *(Brooks et al., 1951; Jamieson 1953; Garrels et al., 1961).* Aragonite is only stable at hydrostatic pressure of about 4kbar, at 25°C *(Clark, 1957).* At low pressures, aragonite is metastable and inverts to calcite when heated *(Jamieson, 1953; 1957; Clark, 1957; Boettcher and Wyllie, 1968).* The standard free energy of formation, ΔG_f^o, for aragonite is less than calcite, since it is related to the thermodynamic equilibrium constant, K_{so}, by:

$$\Delta G_f^o = RT \ln K_{so} \qquad (6)$$

The estimated values of ΔG_f^o of aragonite and calcite are -269.6 kcal. mole^{-1} and -269.8 kcal. mole^{-1} respectively *(Garrels et al., 1961).* Recent carbonate sediments are composed to a large extent of aragonite, it may contain about 50% aragonite and or, a variety of high magnesian calcite *(Land, 1967; Schmalz, 1967).* One of the few inorganic precipitates formed from seawater is believed to occur as the aragonite mud found on the Bahamas shelf*(Kitano et al., 1962; Taft and Harbaugh, 1964; Milliman, 1967; Pytkowicz, 1973; Moller and Rajagopalan, 1975).* It is also believed that the aragonite mud of Bahamas shelf is of an inorganic precipitate from seawater *(Cloud, 1962b; Broecker and Takahashi, 1966; Budd, 1988).* Some aragonite needles precipitated by organisms are chemically and morphologically indistinguishable from aragonite precipitated inorganically *(Lowenstam, 1955; Lowenstam and Esptein, 1957; Stockman et al., 1967).*

Table 1

Calcium carbonate polymorphs (from: Dana and Ford, 1951).

Name	Composition	Ionic structure
Calcite	$CaCO_3$	Trigonal System, Hexagonal, Scalenohedral class.
Aragonite	$CaCO_3$	Orthorhombic system.
Vaterite	$CaCO_3$	Hexagonal, also called μ-calcite.

Magnesian Calcite in Marine Environment

The concentration of magnesium ion in natural seawater is about 0.052 mole.kg^{-1}. It is the third major ion in seawater and it is five times the concentration of calcium ion which is about 0.01 mole.kg^{-1}. Magnesium is directly involved in the formation of the $CaCO_3$ solid. Natural calcite contains a range of magnesium in solid solution which is usually, named magnesian calcite. The skeletal magnesian calcites in biogenic hard parts, and marine magnesian calcite in cements are the most important occurrences of these phases *(Silliman, 1846; Chave, 1952; 1954a,b; 1981; Land, 1967; Schmalz, 1967; Pigott and Land, 1986; Anderson and Dyrssen, 1987).* The most important contributors of skeletal magnesian calcite to shallow-water marine sediments are the skeletons of calcareous red algae, benthic foraminifera, bryozoans, echiniods and barnacles *(Chave, 1981). Chave, (1954b; 1981)* estimated that the ranges in magnesium content of the most common magnesian calcite secreting organisms are :

Calcareous red algae:	10-25%
Echinoderms:	10-15%
Foraminifera:	1-15%
Barnacles:	1-5%
Bryozoans (mixture of calcite/aragonite):	≈ 0-11%

The data from the major organism groups *(Chave, 1954b)* showed a general decrease in magnesian content of the skeletal magnesian calcite from the tropics to the poles, and as function of environmental temperature of the growth. This trend may be interpreted as the influence of growth rates, which are dependent on temperature and other physiological factors *(Moberly, 1968)*, and seawater saturation state *(Broecker et al., 1979; Smith and Roth, 1979)*, because the fact is that the increase of (CO_3^{2-}) influences the reaction rate.

State of Degree of Saturation

The degree of saturation, Ω, of natural waters is defined as the ratio of ionic products of the calcium carbonate to its solubility product in the solution. Accordingly the following equation is defined, for $CaCO_{3(s)}$:

$$\Omega = \frac{(Ca^{2+})_T(CO_3^{2-})_T}{K_{Sp}} \qquad (7)$$

and

$$K_{Sp} = (Ca^{2+})_{T,e}(CO_3^{2-})_{T,e} \qquad (8)$$

the subscripts T and e refer to the total dissolved concentrations and the concentrations at equilibrium respectively.

Various natural waters, such as spring waters, ground waters, oceanic surface waters and pore waters are often to be supersaturated with respect to both calcite and aragonite *(Weyl, 1961; Back, 1963; Schmalz, 1963; MacIntyre and Platford, 1964; Barnes 1965; Pytkowicz, 1965; Berner, 1975; 1966a; Plath and Pytkowicz, 1980).* Surface seawater is apparently supersatured with respect to calcite; with Ω ranging between 150-300% supersaturated *(Garrels et al., 1961; MacIntyre and Platford, 1964).* Saturometry measurements of interstitial waters from neritic carbonate sediments indicate slight supersaturation and saturation with respect to calcite *(Berner,1966a).* Interstitial waters, which were squeezed from cores of bottom sediments were undersaturated or saturated with respect to carbonates *(Schmalz, 1963).*

A fine-grained size 3-10μm diameter of $CaCO_{3(s)}$ should recrystallize within hours or days as calculated by *Weyl, (1958; 1964)* and *Pantin, (1965)*, but Ancient fine-grained limestones have not recrystallized to coarser fabric. The retention of supersaturation of surface seawater and very slow diagenetic transformation of sediments and rocks are the observations that led many investigators to study the influence of organic compounds *(Chave and Suess, 1970; Suess, 1970; 1973)*, and inorganic additives *(Kitano et al., 1962; Pytkowicz, 1965; 1973; Bischoff, 1968; Bischoff and Fyfe, 1968; Katz, 1973; Mucci and Morse, 1984a)*, upon the chemical and physical behavior of calcium carbonate minerals.

Previous Work

It is well established that magnesium ion has a direct effect on the mineral behavior of $CaCO_{3(s)}$ and its solubility. Scientists have mostly used the inorganic phases as the mineral system to form the basis for their interpretation. Laboratory studies showed that magnesium ion in solution plays a significant role in controlling the behavior of carbonate solid solution. Magnesium ion concentrations influence the kinetics of precipitation and dissolution, the crystal morphology and mineralogy, the solubility behavior and the diagenesis of carbonate minerals *(Chave et al., 1962; Kitano and Hood, 1962; Simkiss, 1964; Pytkowicz, 1965; 1973; Weyl, 1966; Bischoff, 1968; Bischoff and Fyfe, 1968; Folk, 1974; 1978; Lahann 1978a,b: Mackenzie et al., 1982; Mucci and Morse, 1984b; Mucci et al., 1985).*

Retention of Supersaturation

Investigations on the solubilities and on the degree of saturation in seawater with respect to calcium carbonate solids started with the work of *Pytkowicz and Connors*

(1964), and Pytkowicz (1965). A problem of considerable interest is why the near-surface oceanic water remains metastable with respect to both calcite and aragonite, e.g. the degree of saturation is over 200% *(Weyl, 1961; MacIntyre and Platford, 1964; Pytkowicz, 1965). Pytkowicz (1965; 1973)* conducted experiments to find out the induction time of near-surface oceanic waters versus the degree of supersaturation and the time required for precipitation onset in the ocean. He also used various amounts of magnesium in synthetic seawater in another set of experiments in order to determine directly, the effect of magnesium on the time of nucleation of the precipitate. The total ionic strength was maintained constant by adding NaCl. The results show that magnesium has a strong retarding effect on the precipitation of magnesian calcite. Because of the lack of mineralogical analysis except for that of the magnesium-to-calcium concentration ratio of seawater, which showed only pure aragonite was precipitated, he suggested that the magnesium retardation was probably attributed to a composite of several factors: the inhibition of aragonite nucleation by adsorption of magnesium ions on the surfaces of nuclei which slows down their growth because magnesium ion does not fit in the aragonite lattice; and because the formation of ion pairs increases in the presence of magnesium ions which increase the solubility and decrease the degree of saturation, and slow down the precipitation of aragonite.

The role of magnesium upon the crystal growth of carbonate was further examined by *Berner (1975).* He attributed the retardation in the crystal growth to the easier fit of the magnesium ion into the calcite lattice than into that of aragonite. Probably two concurrent processes are causing this retardation; first, the magnesium ion is adsorbed as a hydrated ion at the surface kinks and inhibits the spread of growth dislocations, second when the magnesium content of the surface layer increases there is an increase in the solubility of calcite.

However, it is interesting to observe that the open near-surface ocean water remains supersaturated in presence of calcareous organisms. This can be explained by either the organic coatings on the test *(Chave, 1965; Chave and Suess, 1970; Suess, 1970)*, which prevent equilibration with the solution, or the formation of high magnesian calcite coating and the increase the particle solubility.

Solubility of Magnesian Calcite

Study of carbonate behavior in seawater was started with the work of *Chave et al., (1962)* and*Weyl (1967). Chave et al., (1962)*, showed that the solubility of carbonates increases in the order of pure calcite, low magnesian calcite, aragonite, and high magnesian calcite. The behavior of calcite and aragonite and their solubility at earth surface temperature are fairly well known .

Magnesian calcite equilibrium solubility products have been studied extensively *(for example; Chave et al., 1962; Chave and Schmalz, 1966; Land, 1967; Schmalz, 1967; Weyl, 1967; Ingle et al., 1973; Plummer and Mackenzie, 1974; Berner, 1975; Moller and Parekh, 1975; Garrels et al., 1980; Plath et al .,1982; Koch and Disteche, 1984; Walter and Morse, 1984; Mucci and Morse, 1984a,b).* Biogenic magnesian calcites were used in most of the experimental investigations of their dissolution in distilled water, Ca-Mg-CO_2-H_2O system and seawater. There were also precipitation reactions studies. These solubility measurements are compiled in Figure 1, in which the solubility is expressed as:

$$^{(Mg\text{-}calcite)}IAP = a_{Ca^{2+}}^{(1-x)}\, a_{Mg^{2+}}^{(x)}\, a_{CO_3^{2-}} \qquad (9)$$

where $(Mg\text{-}calcite)IAP$ is the ionic activity product of magnesian calcite, a_i represents the activity of i and x is the mole fraction of $MgCO_3$ in the solid.

There are many factors that may cause the scatter in Figure 1: like experimental techniques, different solutions, different materials and analytical procedures. The use of different approaches for aqueous carbonate system could be the main source of these discrepancies between the results of different authors. The incongruent behavior of magnesian carbonate in solutions led to a disagreement in the theoretical interpretation of the experimental data *(Chave et al., 1962; Land, 1967; Plummer and Mackenzie, 1974; Thorstenson and Plummer, 1977).*

In the following I shall summarize the dissolution experiments of magnesian calcite solubility by *Chave et al., (1962), Land (1967)* and *Plummer and Mackenzie (1974),* which involved dissolution of biogenic magnesian calcite in distilled water, and the precipitation experiments by *Mucci and Morse, (1984a; 1984b),* and finally I shall introduce the purpose of my experimental work.

Dissolution Experiments

Chave et al., (1962) used the pH-drift method during the dissolution of biogenic magnesian calcite and the final pH was estimated at infinite time, following the *Garrels et al., (1961)* approach by extrapolation of pH versus the reciprocal square root of time. They claimed that only relative solubility was obtained, by comparing the method with the estimated pH for calcite and aragonite. However, the dissolution of magnesian calcites showed that the (Ca^{2+})-to-(Mg^{2+}) concentration ratio in solution at steady-state equilibrium with solid was similar to the ratio of the solid which indicated a congruent dissolution *(Land, 1967).* In a careful study of magnesian calcite behavior during

dissolution *(Plummer and Mackenzie, 1974)* showed three stages of dissolution. The first stage was congruent dissolution and was believed to be the most reactive one, the second was a stage where there was dissolution as well as a precipitation of low magnesian calcite and the third stage was, presumably, the precipitation of magnesian calcite.

Plummer and Mackenzie (1974), used only the congruent segment of the reactions to estimate their pHs following the approach of pH versus the reciprocal of the square root of time. These obtained pH values were used to calculate solubilities of Mg-calcite. The reported pH values by *Plummer and Mackenzie (1974)* were much higher than the values obtained by *Land (1967)*. Although *Plummer and Mackenzie (1974)*, used very fine particles and low solid-to-solution ratios.

Precipitation Experiments

Solubility data for various magnesian calcites, precipitated on synthetic calcite from supersaturated solution were obtained by pH-stat *(Mucci and Morse, 1984a)* and by free drift experiments *(Mucci and Morse, 1984b)*. They suggested that the free-drift experiments may be used to represent thermodynamic equilibria. Then, they determined the overgrowth composition by atomic adsorption spectrophotometry and X-ray diffraction. The magnesium contents of overgrowths varied with (Mg^{2+})-to-(Ca^{2+}) concentration ratios in solution. The magnesium contents of overgrowth were later verified by Auger spectroscopy analysis *(Mucci et al., 1985)*. The results of overgrowth compositions of magnesian calcite are shown in Table 2. Their data (Figure 1) showed an increase in calcite solubility with magnesium content, but much less than the data obtained

Figure 1

The ionic activity products of magnesian calcite, defined by equation (9) as a function of mole% $MgCO_3$, obtained by different authors.

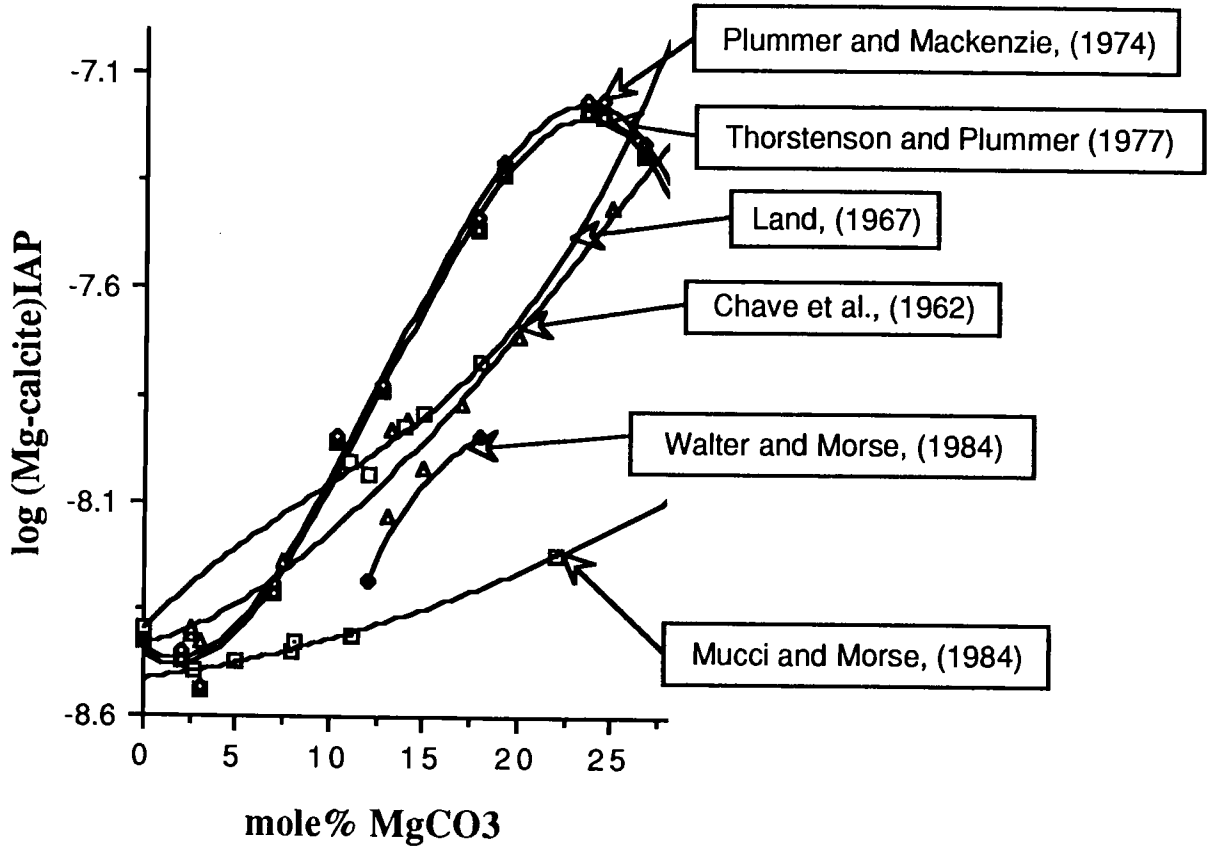
Plummer and Mackenzie, (1974)
Thorstenson and Plummer (1977)
Land, (1967)
Chave et al., (1962)
Walter and Morse, (1984)
Mucci and Morse, (1984)
-7.1
-7.6
-8.1
-8.6
0
5
10
15
20
25
log (Mg-calcite)IAP
mole% MgCO3

Figure 1

Table 2

Magnesian calcite overgrowth composition Mucci et al., 1985.

$[(Mg2+)/(Ca2+)]_{soln}$	Mole% MgCO3			
	On polished crystal		On powder	
	Ω	Auger. Anal.	Ω	Auger. Anal.
0	-	-	-	-
1.0	-	-	3.2-5.8	2.7±.2
2.5	1.2	5.0±.6	4.5-8.2	4.9±.4
5.13	1.2	7.4±.2	7.5-13.4	8.1±1.7
	8	7.7±.5		
7.5	1.2	8.5±.2	8.0-13.5	8.2±.5
10.3	1.2	11.4±.4	9.9-17.2	11.2±.7
20.0	1.2	22.3±2.6	-	21.0±3.9

from the dissolution experiments by *Plummer and Mackenzie (1974)*, and *Land (1967)*, however, the closest data were that of *Land, (1967)*. At this point the high solubility values obtained from the dissolution of biogenic magnesian calcite and the low solubility obtained from the precipitation on seed remained unexplained. It has been suggested that themagnesian calcites that inorganically precipitated were in metastable exchange equilibrium with the solution *(Mucci and Morse, 1984a)*. Another discrepancy of the data may be caused by the extrapolation method of the initial dissolution data to an infinite time *(for example: Chave et al, 1962; Plummer and Mackenzie, 1974; and others)*. Later on it was claimed by *Thorstenson and Plummer (1977)* that the extrapolation approach represents a state of stoichiometric saturation, and the thermodynamic equilibrium conditions can not be calculated from congruent dissolution data. I think the only, reasonable, approach that may explain the discrepancy of the above results is the one that was introduced by *Wollast and Reinh-Deire (1977)* which is discussed in chapter 4 for precipitation reaction of magnesian calcite.

Purposes of This Study

The purpose of this work was to study the effects (Mg^{2+}) in solutions on the kinetics of homogeneous behavior of carbonates, on the heterogeneous kinetic behavior and the solubility of pure calcite when exposed to seawater-like solutions. The results have been examined to give a better understanding of the possible kinetic factors that might influence the equilibrium state of carbonate. Also the results of the solubility studies have been used to predict the thermodynamic equilibria from an ion-pairs model in ASW.

Artificial seawater of different (Mg^{2+})-to-(Ca^{2+}) concentration ratios was used in these investigations, and the ionic strength was maintained at 0.72M by adding NaCl.

Homogeneous Precipitation

The same approach of *Pytkowicz (1965; 1973)* was used to determine the induction time, and to evaluate the metastability of supersaturated near-surface seawater by extrapolation. The mineralogy of the incipient precipitate was examined by X-ray diffraction analysis (XRDA) and Atomic Adsorption Spectroscopy (AAS). The morphology and the size of the precipitate were also, examined by Scanning Electron Microscopy (SEM). The data obtained were combined to link the mineralogies of precipitates as kinetic factors.

Heterogeneous Precipitation (Overgrowth)

Synthetic analytical grade calcites were used as seeds in a closed system. The reaction rate was followed by monitoring the pH with time. The rate constant, k_n, and the total order, n, of the reaction at various (Mg^{2+}) concentrations were determined. This was to examine, in presence of (Mg^{2+}), the validity of the conventional equation of the reaction rate that was used for pure $CaCO_{3(s)}$ in simple solution. The conventional equation was:

$$\frac{\partial C}{\partial t} = - k_n A (C_t - C_\infty)^n \qquad (10)$$

where A is the specific area of the seeds and C_t and C_∞ are the concentrations at time t and infinity respectively.

Solubility of Magnesian Calcite

The solubility product of calcite was measured in ASW of different Mg:Ca concentration ratios at 25°C. Different solid-to-solution ratios were introduced to the test solution at two different degrees of supersaturation; one similar to that of natural seawater, and another higher supersaturation. This was to differentiate between equilibrium control and kinetic control of the overgrowth. The overgrowth coating compositions were determined by AAS analysis method because, I couldn't locate the Scanning Auger Spectroscope for the purpose of this work.

The values of the first and the second dissociation constants of carbonic acid were also measured at different Mg:Ca concentration ratios. They were used to estimate the carbonate species in the different phases of this work.

Chapter 1.

THE EFFECTS OF MAGNESIUM-TO-CALCIUM RATIOS IN ARTIFICIAL SEAWATER, AT DIFFERENT IONIC PRODUCTS, UPON THE INDUCTION TIME, MINERALOGY AND MORPHOLOGY OF CALCIUM CARBONATE: A LABORATORY STUDY.

1.1 Introduction:

The precipitation, conversion of minerals, and the cementation of carbonate rocks in an aqueous solution at the Earth's surface temperatures and pressures are mainly affected by the dissolution and reprecipitation of different calcium carbonate minerals. The rates of dissolution and reprecipitation are controlled by the nucleation and the growth of the solid phases.

Earlier it was found that the presence of magnesium ion in solution affects the time of nucleation and the mineralogy of calcium carbonate. *Pytkowicz (1965;1973)* studied the problem of spontaneous precipitation and found that magnesium ions in seawater inhibit the precipitation of calcium carbonate. He concluded that magnesium adsorption delays the nucleation for long periods. *Bischoff and Fyfe (1968)* and *Bischoff (1968)* suggested that the presence of magnesium ion in solution retarded the nucleation of calcite during the dissolution of aragonite and precipitation of calcite. *Moller and Rajagapolan (1975)* showed that the induction time increased with the increase of magnesium ions in solution.

Mucci and Morse (1984a) concluded that the magnesian content of calcite is dominantly influenced by the (Mg^{2+})-to-(Ca^{2+}) ratio in the water from which it precipitates. *Berner (1975;1978)* and *Thorstenson and Plummer (1977)* suggested that magnesian calcite composition is controlled by growth rates.

Leitmeir (1919), Taft and Harbaugh (1964), Kitano et al (1962), Kitano and Hood (1962), and Pytkowicz (1965a) observed that aragonite precipitated spontaneously from normal seawater. *Kitano et al (1962)* could synthesize pure aragonite at (Mg^{2+})-to-(Ca^{2+}) concentration ratio of more than 3.82. *Moller and Rajagapolan (1975)* found that aragonite precipitates when the (Mg^{2+})-to-(Ca^{2+}) ratio was more than 4. *Mucci and Morse (1984a*

and 1984b) stated that the magnesium concentration affects the mineralogy of bulk solids or the overgrowth on calcites.

It has been suggested that magnesium controls the diagenetic aragonite-calcite transformation *(Monaghan and Lytle 1956; Simkiss, 1964; Bischoff and Fyfe, 1968; Bischoff, 1968; Berner, 1974;1971).*

Recently, some authors correlated the mineralogy and the morphology of abiogenic carbonate precipitates to chemical processes in nature. For example, *Folk (1974), Sandberg (1975) and Wilkinson (1979),* suggested that that the mineralogy must be related to the hydrospheric (Mg^{2+})-to-(Ca^{2+}) activity ratio. *Mackenzie and Pigott (1981)* and *Sandberg (1983)* proposed that pCO_2 is the most important parameter to be considered in the formation of $CaCO_3$ minerals, their crystal habit and mineral chemistry in nature.

Folk (1974), Longman (1980) and Given and Wilkinson (1985) showed that the magnesium concentration and the rate of precipitation have significant effects upon the morphology of calcium carbonates. They suggested that pure calcite, low-magnesian calcite and dolomite form equant crystals and the high-magnesian calcite and aragonite are acicular ones.

Weyl (1967) showed that magnesium ion affects the solution behavior of carbonate minerals in seawater. He concluded that seawater does not equilibrate thermodynamically with the solids, but that their surfaces are altered by magnesium uptake and that this uptake is rate controlled.

The purposes of the present work were :

a) to study he effects of magnesium ions in solution upon the induction time for spontaneous nucleation, that is, the time between perpetration of the solutions and the onset of precipitation;

b) to show why the near-surface oceanic waters can remain supersaturated with respect to calcium carbonate without spontaneous precipitation such as would occur in synthetic solution;

c) to study the mineralogy of calcium carbonate that is controlled by magnesium ions in solution and by the degree of supersaturation;

d) to examine the morphology of calcium carbonate resulting from the presence of magnesium in solution and the rate of the precipitation reaction.

1.2 Theory

Crystallization of salts from supersaturated solutions, such as in seawater, involves two steps; nucleation and growth. Nucleation is the process in which initially, small clusters of ions or molecules build up to a critical size beyond which growth can occur *(Newkirk, 1957; Dufour and Defay, 1963; Nancollas and Purdie, 1964; Stumm and Morgan, 1982; Pytkowicz 1983).*

1.2.1. Spontaneous Crystallization

Spontaneous crystallization or precipitation is a process that occurs in the intentional absence of an initial solid phase, serving as nucleus. In theory there are two steps, spontaneous nucleation which occurs in the body of solution followed by growth. Dust and other particles often provide nucleation sites so that nucleation, usually, is not homogeneous. Four steps can be distinguished in the formation of crystals *(Stumm and Morgan, 1982)*:

1. Ions and molecules interact to form clusters:

$$A + A \quad \Longleftrightarrow A_2$$

rather than to serve as nuclei *(Pytkowicz 1983b). Toschev, (1973)* pointed out that the fast nucleation that occurs when concentrated solutions are mixed may have advantages over homogeneous nucleation due to the velocity of the reaction.

1.2.2. Heterogeneous Crystallization

Heterogeneous nucleation occurs by design on the surface of a foreign body. Physically, it does not differ from the spontaneous nonhomogeneous precipitation. In the latter case, however, the heterogeneous nucleation is not intentional. If the nuclei and the surface of the solid have a good fit then the interfacial energy between those two phases is small. Therefore, a smaller degree of saturation is required for the formation of critical nuclei and subsequent crystal growth.

1.3. Methods

Ten liters of Mg-free artificial seawater were prepared using the method of *Kester et al., (1967)*. The concentrations of different constituents are shown in Table 1.1. Air was diffused through the solution for two days to equlilibrate the solution with atmospheric carbon dioxide. Varying quantities of Mg^{2+} ions were added to test their effect upon the induction time, upon the mineralogy, and upon the morphology of precipitated calcium carbonate. Different amounts of 0.1 molar Na_2CO_3 from a freshly prepared stock solution were added to the artificial seawater to increase the rate of the reaction.

Artificial seawater was used to avoid in part, the presence of natural organic matter and the presence of the small particles which may serve as surface sites for calcium carbonate precipitation. Still, the nucleation was heterogeneous on the surface of the glass of the container and on dust particles. Homogeneous nucleation would require an

exceedingly long time. The artificial seawater corresponds roughly to natural seawater of 35‰ salinity after adding NaCl. NaCl was added to replace $MgCl_2.6H_2O$ and to maintain the ionic strength at 0.72M. This avoided in part, the effect of changes in the ionic strength on the rate of the reaction when magnesium is reduced *(Bischoff, 1968; Syales and Fyfe, 1973; Kitano, 1962).* The experiment was carried out in a water bath (Aminco Constant Temperature bath, #4-8605) at 25.0± 0.4 °C.

The runs were made by placing 100 ml of artificial seawater in Erlenmyer flasks to which varying amounts of magnesium were added. Then the desired amount of Na_2CO_3 was added with stirring.

1.3.1 Determination of the Induction Time

The initial time was set when Na_2CO_3 was added. The pH was followed with a Corning SemiMicro combination pH-electrode, a research pH Meter and strip chart recorder. The time ranges for the onsets of the precipitation used in this work correspond to the interval between the addition of Na_2CO_3 and the time when cloudiness in the solution occurred. The detection of the cloudiness was obtained by observing an applied light beam through the solution with a dark black background. In this work I also used the discontinuity in the pH against time by an extrapolation of the initial horizontal segments and the pH decay curves to a common point. The time at this point is TN and also is the onset of precipitation, which is illustrated in Figures 1.1a,b,c,d and e. The uncertainty of this method increases at low supersaturations where it is hard to determine the first appearance of the cloudiness and only the discontinuity of the pH against time is used. All solutions are at least 250% supersaturated like near-surface oceanic waters even without addition of Na_2CO_3. The degree of saturation of each solution with respect to calcite can be roughly, estimated from:

$$\Omega \approx (Na_2CO_3 \text{ molar added }) \text{ X } 2.2E+4.$$

Table 1.1

Artificial seawater prepared, using the Kester et al., Method (1967).

Salt	Molarity
NaCl	0.4017
$NaSO_4$	0.0276
KCl	0.0089
KBr	0.0080
H_3BO_3	0.0004
NaF	0.00007
$NaHCO_3$	0.00229
$CaCl_2$	0.00993
$SrCl_2$	0.00015

1.3.2. Identification of the Mineralogy of the Precipitates and Determination of the Weight Percent of Each Phase (e.g. Calcite and Aragonite)

The precipitates were collected by filteration and identified by X-ray diffraction immediately, after the first massive precipitations. The mole percent of $MgCO_3$ (mole % $MgCO_3$) in calcite was calculated from the empirical relationship:

$$mole\%\ MgCO_3 = 376.6\ X\ (3.039 - d_{100}) \qquad (1.1)$$

where d_{100} is the d-spacing of the major reflector (100) which is directly proportional to the amount of substitution of the smaller Mg-ion for Ca^{2+} in the crystal lattice *(Chave, 1952)*. The starting angle 2 theta (2θ) was 25° and the ending one was 34°.

Each precipitate was dissolved in HCl (0.10N) and the amount of Mg^{2+} was determined by standard atomic adsorption spectroscopy. To account for the residual (Mg^{2+}) in the precipitate it was assumed that pure aragonite had a maximum of 1.5 mole% $MgCO_3$ and the excess (Mg^{2+}) was residual.

The Weight percent (wt%) of calcite was calculated for each sample using the following equation:

$$wt\%\ calcite = \left(\frac{b\ X\ 84.3}{24.3}\right) + \left(\frac{b\ X\ 100.1}{24.3}\right) X \left(\frac{100.0 - a}{a}\right) \qquad (1.2)$$

where a is the mole % $MgCO_3$ in calcite, calculated from X-ray diffraction (XRD) using equation (1.1) and b is the weight percent of Mg^{2+} in the total sample, determined by AAS. Therefore, the weight percent of aragonite is 100 - wt% calcite.

Other precipitation runs were kept in a water bath for thirty-five days at a temperature of 25 ± .4 °C. They were examined by XRD during the 35 days to test the transformation of their mineralogy throughout this period. The XRD runs were made once each week up to a month. In this case the same equations (1.1) and (1.2) were used to determine the mole% $MgCO_3$ and the weight percent of calcite in each sample. Quantities of the transient vaterite and of aragonite were determined from, the intensity ratio of aragonite to vaterite.

$$\frac{I_{(arag.)}}{I_{(vater.)}} \qquad (1.3)$$

I is the height at 2θ for each mineral from XRD assuming that the height is a function of the amount of the mineral in the mixture.

1.3.3. Examination of the Morphologies of Calcium Carbonate Precipitates

Twelve samples from these precipitates were selected for the morphological and size examination. The samples were selected from low and high degree of supersaturations and at (Mg2+)-to-(Ca2+) ratios in solution from 0 to 5, to test the effect of these parameters, i.e. of the (Mg2+)-to-(Ca2+) and the rate of growth upon the morphology of the crystals. The precipitates were examined under the Scanning Electron Microscope (SEM).

Figure 1.1.

Visual range (time range of the cloudness appearance in the solution and before settling on the bottom of the beaker) and pH determination of the induction time, when 4.72 mM Na_2CO_3 areadded for:

a) (Mg^{2+}:Ca^{2+}) ratio = 0:1

b) (Mg^{2+}:Ca^{2+}) ratio = 1:1

c) (Mg^{2+}:Ca^{2+}) ratio = 2:1

d) (Mg^{2+}:Ca^{2+}) ratio = 4:1

e) (Mg^{2+}:Ca^{2+}) ratio = 5:1

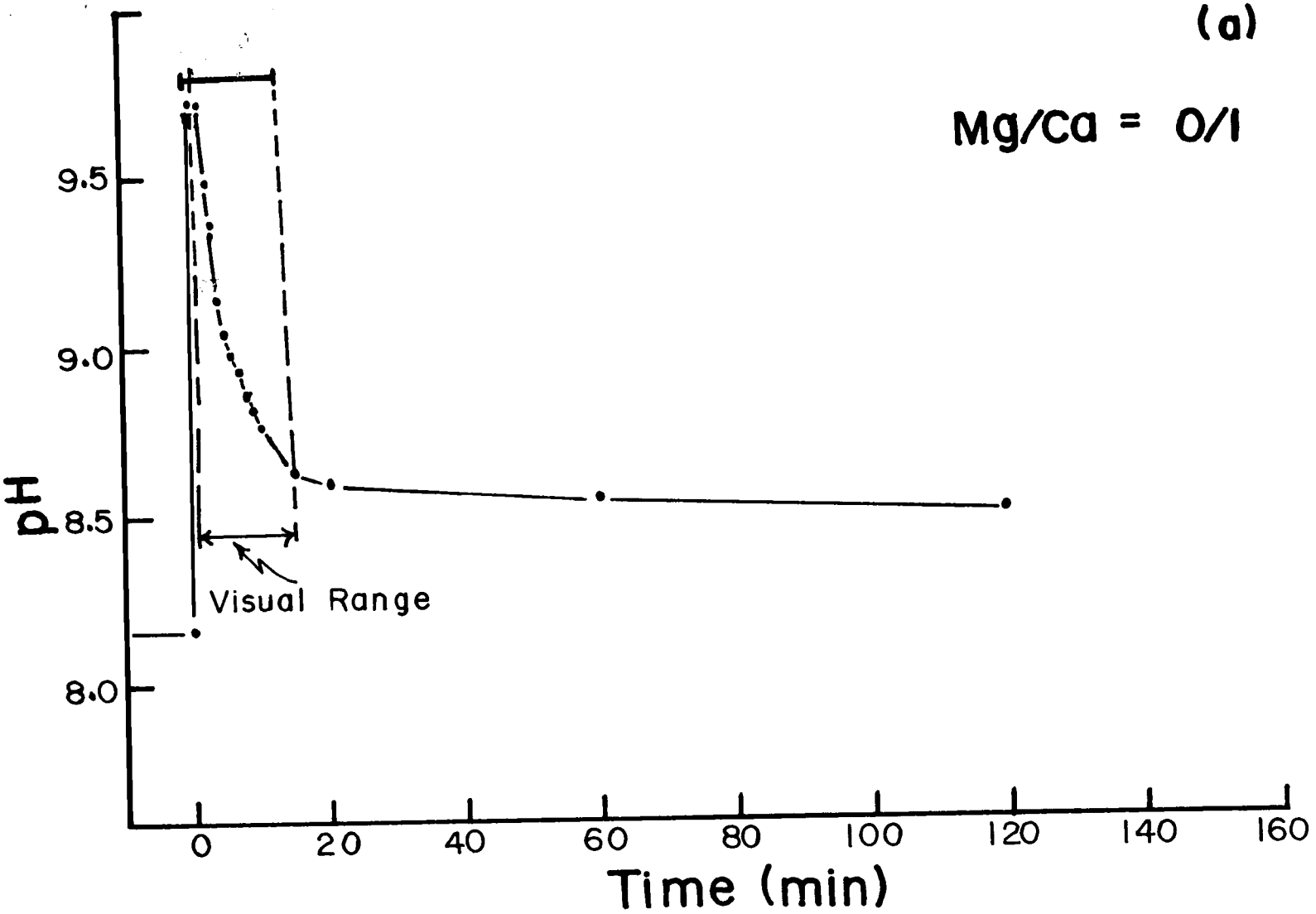
(a)
Mg/Ca = 0/1
9.5
9.0
8.5
8.0
pH
Visual Range
0
20
40
60
80
100
120
140
160
Time (min)

Figure 1.1

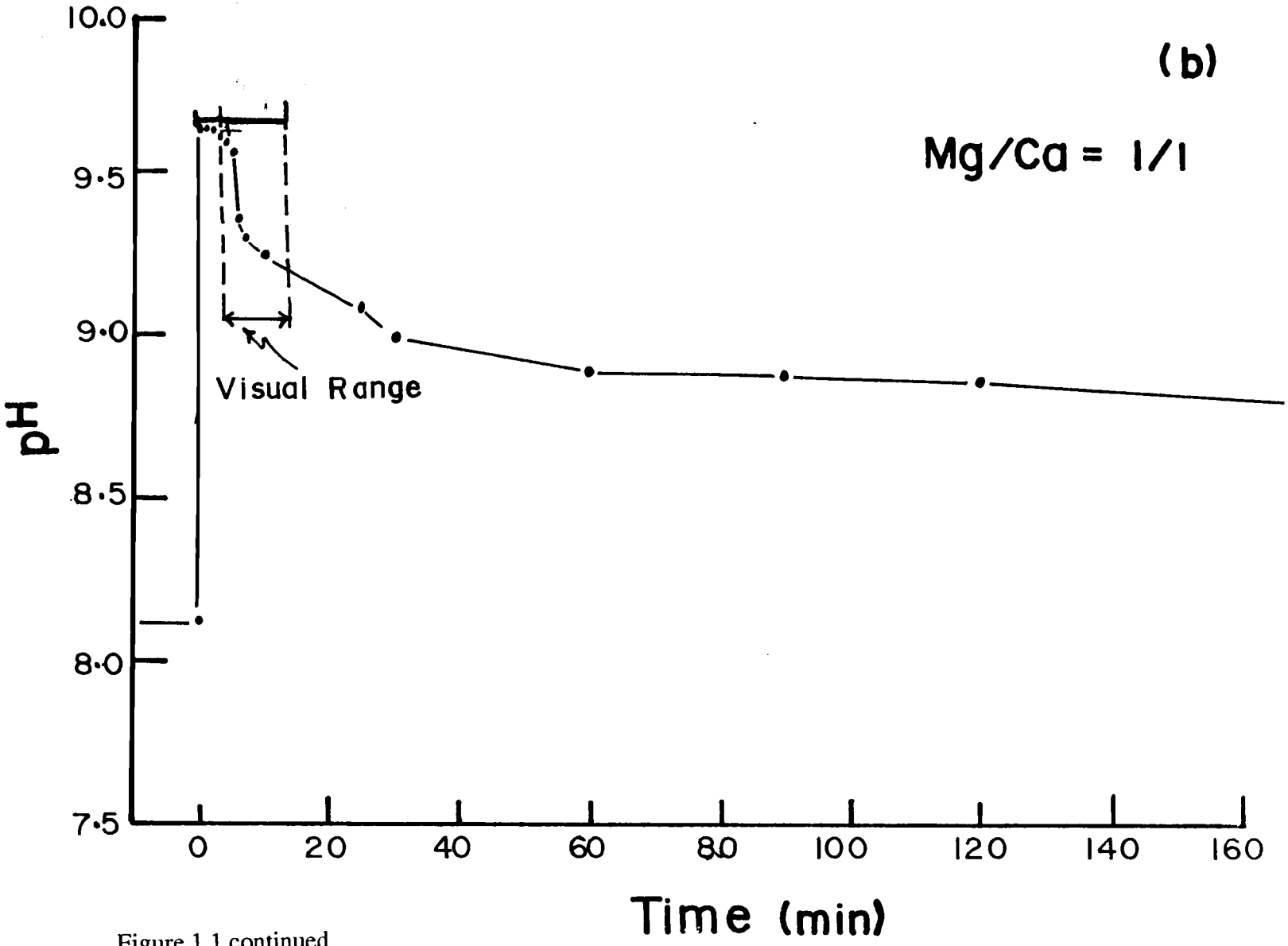

Figure 1.1 continued

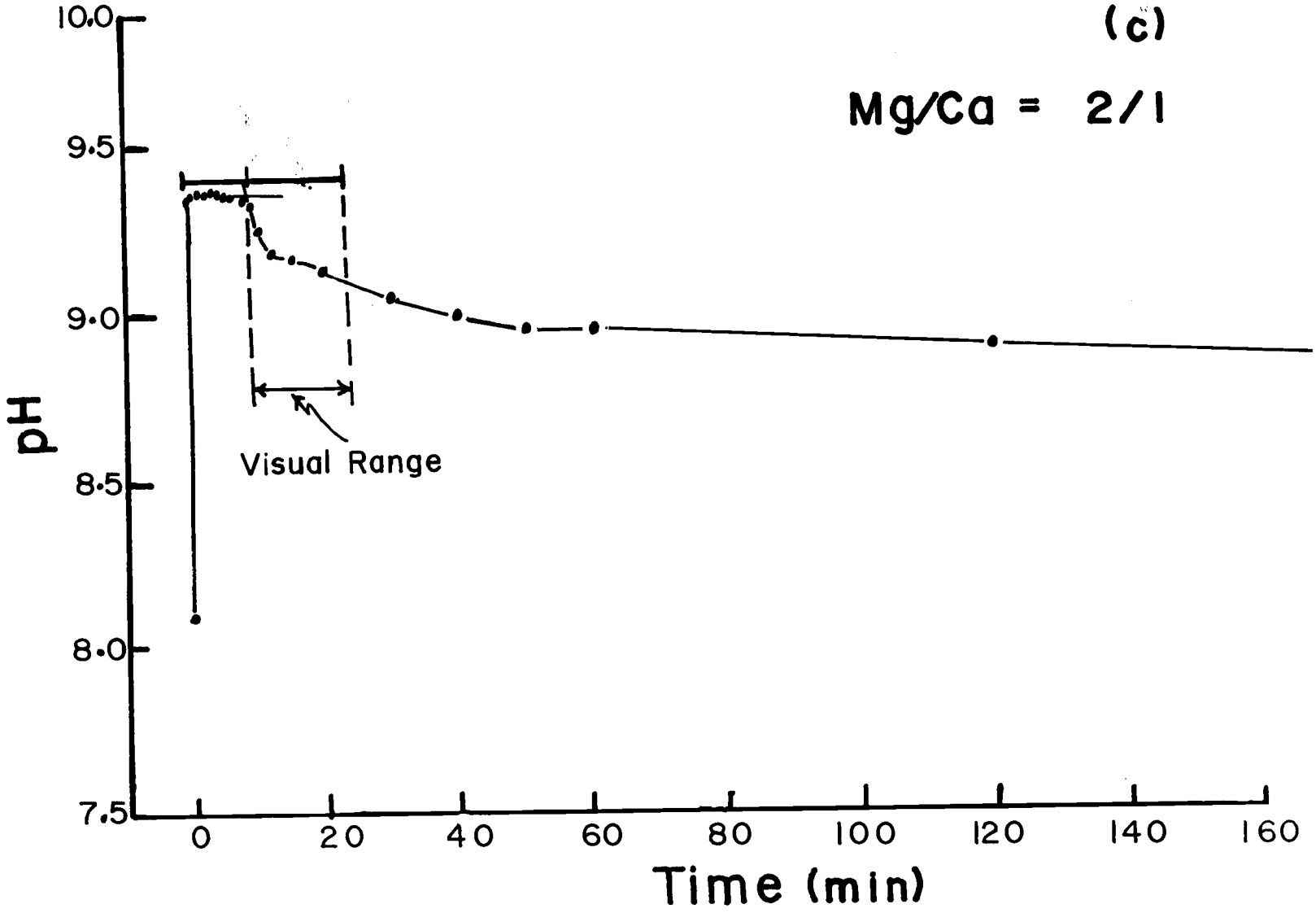

Figure 1.1 continued

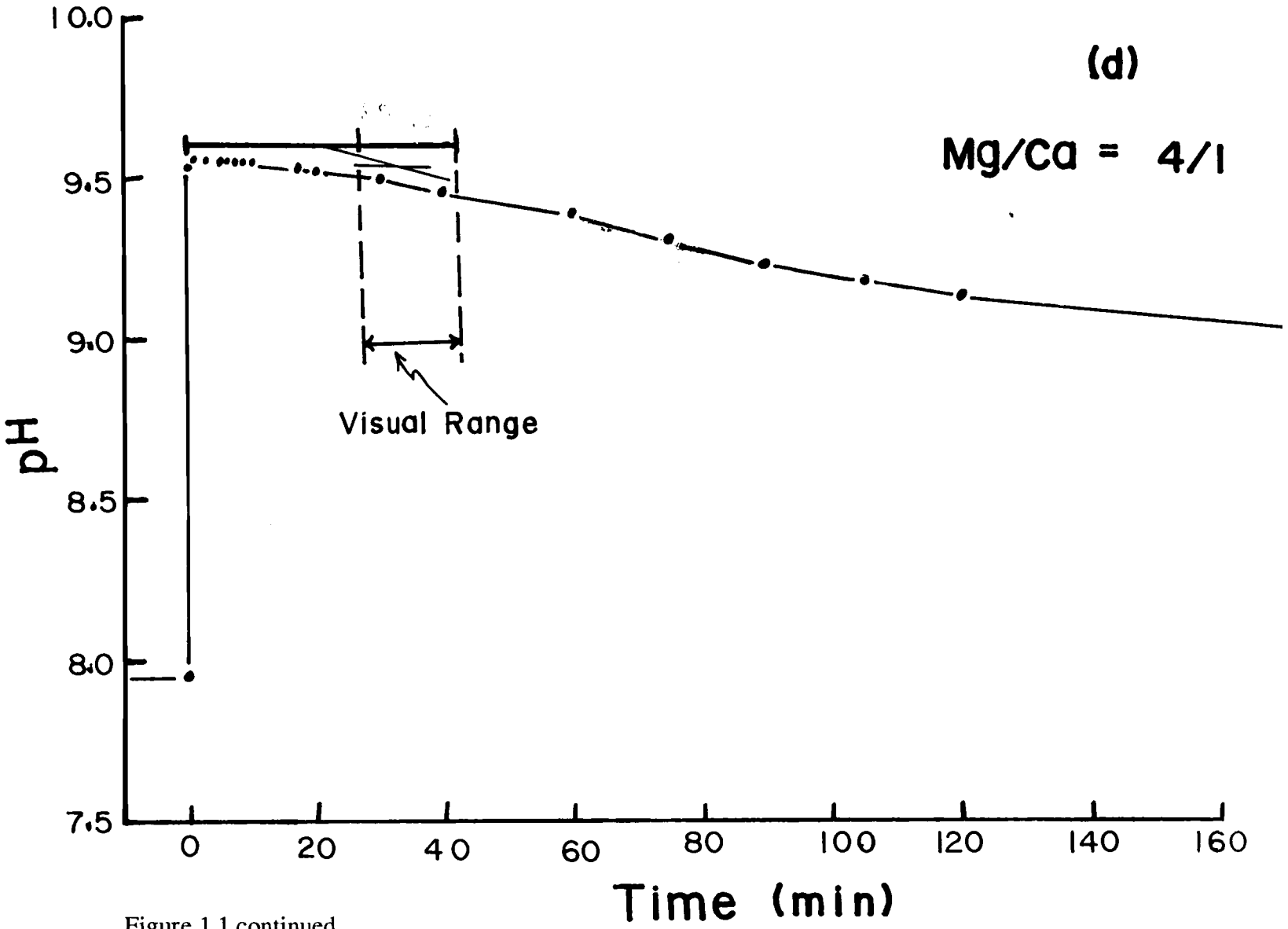

Figure 1.1 continued

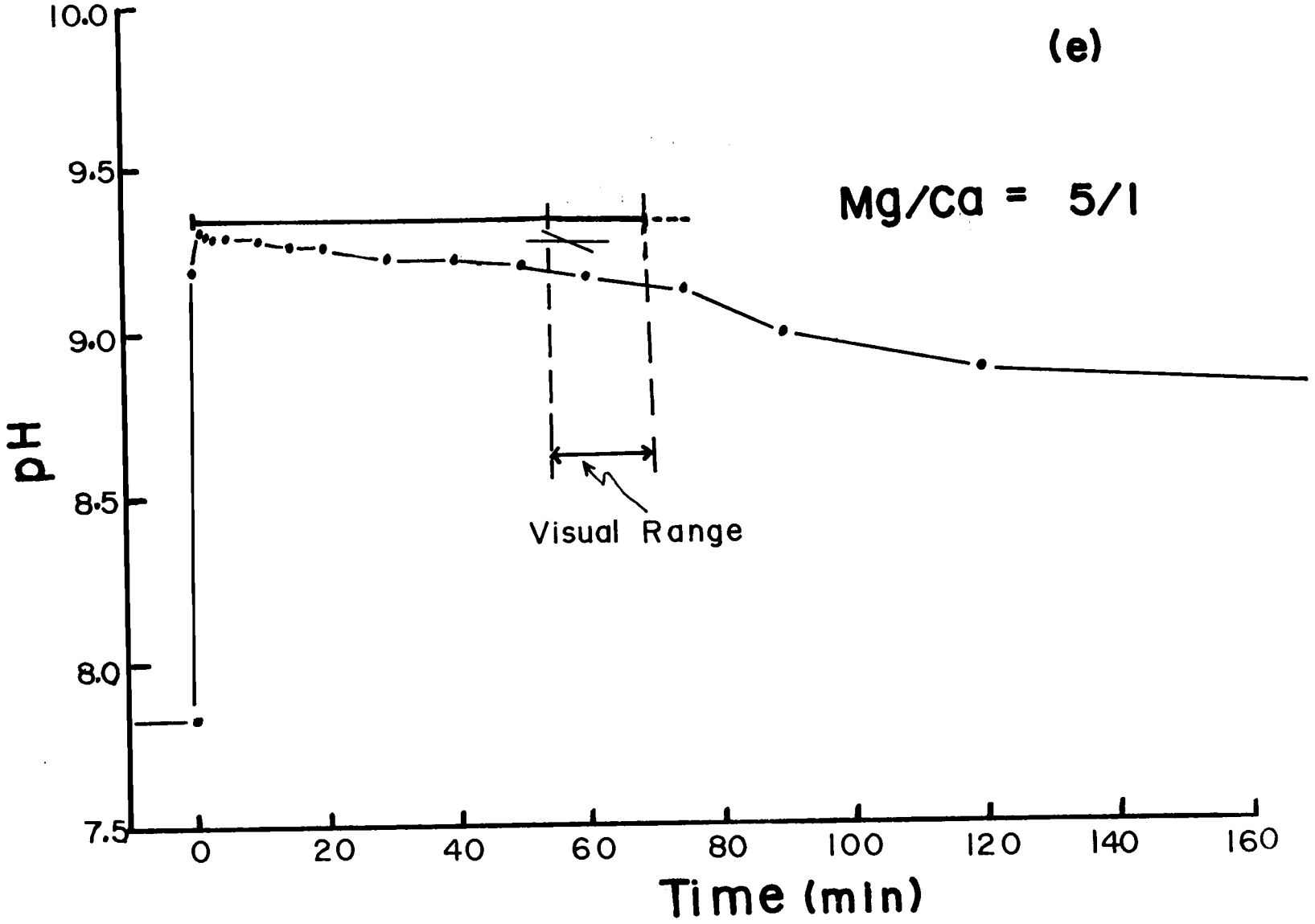

Figure 1.1 continued

1.4. Results and Discussion

1.4.1. Effects of Magnesium on Time of Nucleation and Type of Precipitate

Addition of Na_2CO_3 to solutions with varying amount of magnesium caused changes in the time of nucleation (TN) and lead to the formation of different mineralogies. The results are summarized in Table 1.2 and Figure 1.2. The amounts of magnesium added are shown as $(Mg^{2+})/(Ca^{2+})$ ratios, where the Ca^{2+} concentration was 0.00993 molar in all cases. The induction times are shown as a function of added amounts of carbonate ions from Na_2CO_3 solutions.

Table 1.2 shows the effect of magnesium on the time of nucleation, the kind of crystal formed, and the weight percent of calcite. It can be seen that magnesium ions inhibit the precipitation and delay it from minutes to weeks (Figure 1.2). This is most pronounced in going from zero magnesium to a magnesium concentration of 0.05 molar which is found in natural seawater. The data in Table 1.2 and Figure 1.2 show two features; the initial increase in the induction time with ion supersaturation and the minimum time of nucleation at higher addition of Na_2CO_3. These features will be discussed later.

X-ray diffraction results show three different mineralogies of the calcium carbonate formed: pure calcite (at zero magnesium ion in solution), mixtures of magnesian calcite (of increasing mole% $MgCO_3$ with increase magnesium in solution) with aragonite, and aragonite alone.

Chave et al.,(1962) showed that the solubility of calcium carbonate minerals increases in order from pure calcite, low-magnesian calcite, aragonite to high-magnesian calcite; i.e. high-magnesian calcite is the most soluble phase and pure calcite is the most

Table 1.2

The Effect of Magnesium Concentration and Degree of Supersaturation on the Time of Nucleation and the Mineralogy of Calcium Carbonate:

$(Mg^{2+}):(Ca^{2+})^*$ Ratio	Na_2CO_3 (mM)	TN (minutes)	wt% (calcite)	mole% $MgCO_3$
0:1	8.32	0.2	100	0
"	6.52	0.4	"	"
"	4.75	1.0	"	"
"	2.90	4.0	"	"
"	1.92	8.0	"	"
"	1.48	15.0	"	"
"	0.99	-	"	"
"	0.79	168.0	"	"
1:1	8.30	18.0	90	10.4
"	6.50	10.0	76	20.1
"	4.74	5.0	96	11.2
"	2.90	7.0	61	6.7
"	1.95	14.0	33	3.0
"	1.45	30.0	11	3.0
"	0.99	72.0	?	1.4
"	0.79	168.0	?	?
2:1	8.20	60.0	78	17.1
"	6.50	18.0	81	12.7
"	4.70	8.0	66	12.7
"	2.90	9.0	89	12.3
"	1.90	12.0	8	1.4
"	1.50	60.0	3	1.4
"	1.00	118.0	0	0
"	0.80	168.0	?	2.1
"	0.70	380.0	?	0

Table 1.2 continued

$(Mg^{2+}):(Ca^{2+})$ Ratio	Na_2CO_3 (mM)	TN (minutes)	wt% (calcite)	mole% $MgCO_3$
3:1	8.10	123.0	59	19.3
"	6.40	24.0	45	16.4
"	4.70	10.0	65	11.4
"	2.90	13.5	38	11.2
"	1.90	40.0	1	12.7
"	1.50	-	-	-
"	1.00	160.0	0	0
.."	0.80	480.0	?	?
4:1	8.09	180.0	60	22.2
"	6.40	48.0	44	19.3
"	4.82	27.0	46	14.7
"	2.82	39.5	3	12.7
"	1.90	72.0	0	0
"	1.45	96.0	"	"
"	0.97	450.0	"	"
"	0.78	1020.0	"	"
5:1	8.10	480.0	0	0
"	6.37	120.0	"	"
"	4.64	57.0	"	"
"	2.84	96.0	"	"
"	1.91	120.0	"	"
"	1.44	360.0	"	"
"	0.97	1440.0	"	"
"	0.78	3200.0	"	"

* In all cases, the concentration of Ca^{2+} was 0.00993 molar.

Figure 1.2.

Added Na_2CO_3 versus the time of nucleation for different $(Mg^{2+}):(Ca^{2+})$ ratios in artificial seawater.

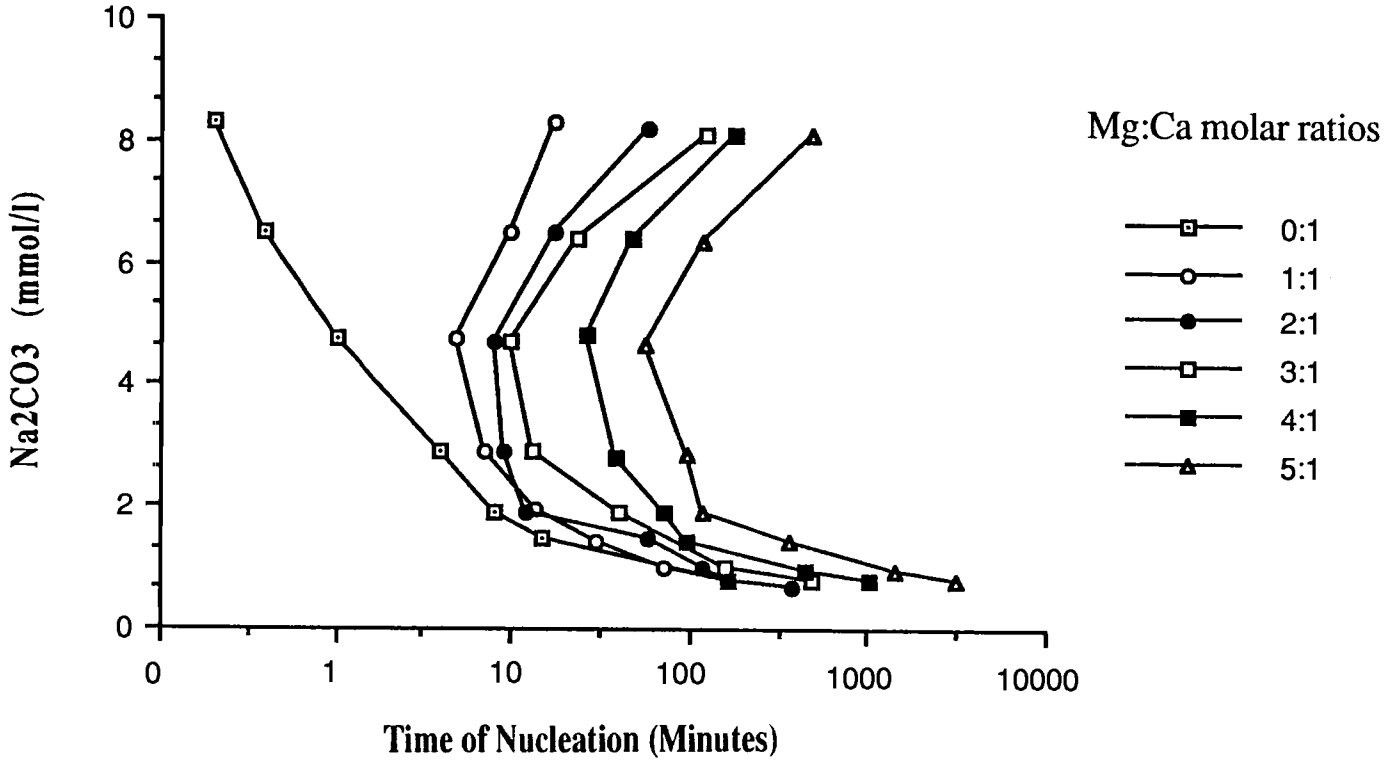
10
8
6
4
2
0
Na2CO3 (mmol/l)
0
1
10
100
1000
10000
Time of Nucleation (Minutes)
Mg:Ca molar ratios
0:1
1:1
2:1
3:1
4:1
5:1

Figure 1.2

stable one. *Plummer and Mackenzie, (1974)* showed that the solubility product of calcite increases with an increase in the $MgCO_3$ fraction in calcite. *Land, (1967)* showed that the carbonate produced by living organism which contains magnesium has a higher solubility than that of pure calcite.

The results demonstrate that two factors have a role in controlling the time of nucleation and the kind of crystal formed. They are the presence of magnesium ions in the solution and the initial degree of saturation. The increase in the degree of saturation, causes an increase in the number of collisions of ions so that the time to form nuclei of critical size of calcium carbonate is shorter, as illustrated in Figure 1.2. Magnesium ions, when present, are also involved in the formation of nuclei. Depending upon how much magnesium is in solution, the time of nucleation and the kind of crystal precipitated vary. An increase in magnesium ions in solution leads to nuclei with a high magnesium content, their solubilities increase and a longer time is required for precipitation. The formation of magnesian calcite nuclei of critical size, which serve as centers of growth, decreases. The effect of magnesium ion on the time of nucleation is also illustrated in Figure 1.3, where the ratio of $(Mg^{2+}):(Ca^{2+})$ is plotted against the time of nucleation for different degrees of supersaturation.

The data in Table 1.3 and Figure 1.4 show that high Na_2CO_3 added in the presence of magnesium slows precipitation and the high degree of saturation kinetically favors magnesian calcite minerals over aragonite. At low supersaturation aragonite is favored. High magnesium contents in solution favor the formation of aragonite over that of magnesian calcite. The tendency to form aragonite over magnesian calcite at magnesium concentration smaller than 0.03 molar and at a low supersaturation indicates that the nuclei of high $MgCO_3$ contents are formed but redissolve as they are more soluble and have a longer TN favoring the more stable aragonite to form. The more soluble nuclei are formed

Figure 1.3.

$(Mg^{2+}):(Ca^{2+})$ ratios versus the log time of nucleation for: 0.79, 4.73 and 8.19 mmole l^{-1} of added Na_2CO_3.

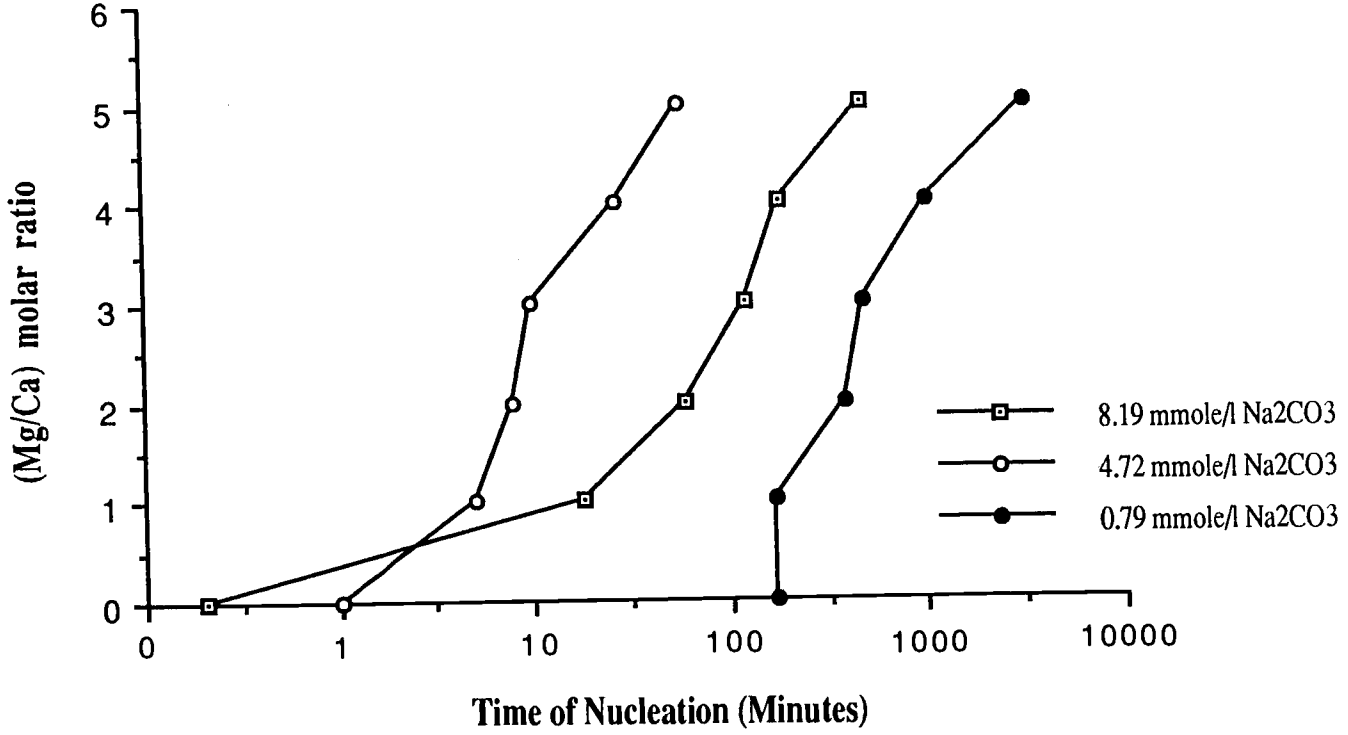
(Mg/Ca) molar ratio
6
5
4
3
2
1
0
0
1
10
100
1000
10000
Time of Nucleation (Minutes)
8.19 mmole/l Na2CO3
4.72 mmole/l Na2CO3
0.79 mmole/l Na2CO3

Figure 1.3

at higher Mg concentrations. By increasing the degree of saturation, the formation of high-magnesian calcite is enhanced. Decreasing the degree of saturation, tsaturation favors the most stable low-magnesian calcite to coexist with aragonite (see Table 1.2 and Figure 1.4).

It is concluded that the presence of magnesium ions in the solution favors the formation of metastable aragonite. Aragonite is formed when the ratio of (Mg2+):(Ca2+) is greater than 4. This agrees with observations of *Kitano et al., (1962), Pytkowicz, (1965), Moller and Rajagapolan (1975)* and others. Magnesian calcites are favored at low magnesium concentrations. It is surprising that the time of nucleation increases again with the addition of higher concentrations of Na_2CO_3. This observation was first attributed to the decrease in hydrogen ion that occurs with the addition of carbonate. It was believed that hydrogen ions were required in the reaction intermediate. Runs with added bicarbonate, which increases the hydrogen ion concentration in solution, however, disprove this hypothesis because the decrease in pH does not affect the time of nucleation *(Pytkowicz, 1965).*

The reason for the increase of the time of nucleation when more than 5.0 mmole/l Na_2CO_3 are added may be due to a decrease in the degree of saturation. This decrease may be caused by preferred magnesium uptake into the nuclei. The results show that at high (CO_3^{2-}) in solution, high-magnesian calcite is kinetically favored. In other words, nuclei with high $MgCO_3$ are formed. These nuclei are more soluble than those of pure $CaCO_3$, and it takes longer to reach the stable nuclei of critical radius. According to the Boltzman distribution, the number of critical nuclei, (N_c), is:

$$N_C = N_O \exp - \left(\frac{6\pi\sigma^3}{3\left(RT \ln \frac{IAP}{K_{so}} \right)^2} \right) \frac{1}{\kappa T} \qquad (1.4)$$

Table 1.3

Effect of magnesium concentration and degree of saturation upon the mineralogy of calcium carbonate; indicated by their induction times (A,B,C etc....).

	$(Mg^{2+}):(Ca^{2+})$																	
	0:1			1:1			2:1			3:1			4:1			5:1		
	a*	b*		a	b		a	b		a	b		a	b		a	b	
A1	0	100	A2	10.4	90	A3	17.1	78	A4	19.3	59	A5	22.2	60	A6	0	0	
B1	0	100	B2	20.1	76	B3	12.7	81	B4	16.4	45	B5	19.3	44	B6	0	0	
C1	0	100	C2	11.2	96	C3	12.7	66	C4	11.9	65	C5	14.9	46	C6	0	0	
D1	0	100	D2	06.7	61	D3	12.7	89	D4	11.2	38	D5	12.7	03	D6	0	0	
E1	0	100	E2	03.0	33	E3	01.4	08	E4	12.7	01	E5	00.0	00	E6	0	0	
F1	0	100	F2	03.0	11	F3	01.4	03	F4	-	-	F5	00.0	00	F6	0	0	
G1	0	100	G2	01.4	?	G3	00.0	00	G4	00.0	00	G5	00.0	00	G6	0	0	
H1	0	100	H2	?	?	H3	02.1	?	H4	00.0	?	H5	00.0	?	H6	0	0	

* where a = mole% $MgCO_3$ and b = weight percent of calcite, calculated from results of XRD and AA's analysis, so the weight percent of aragonite and vaterite is (100-b).

Figure 1.4.

The mineralogy of calcium carbonate precipitates at different $(Mg^{2+}):(Ca^{2+})$ ratios in artificial seawater, indicated by their induction time.

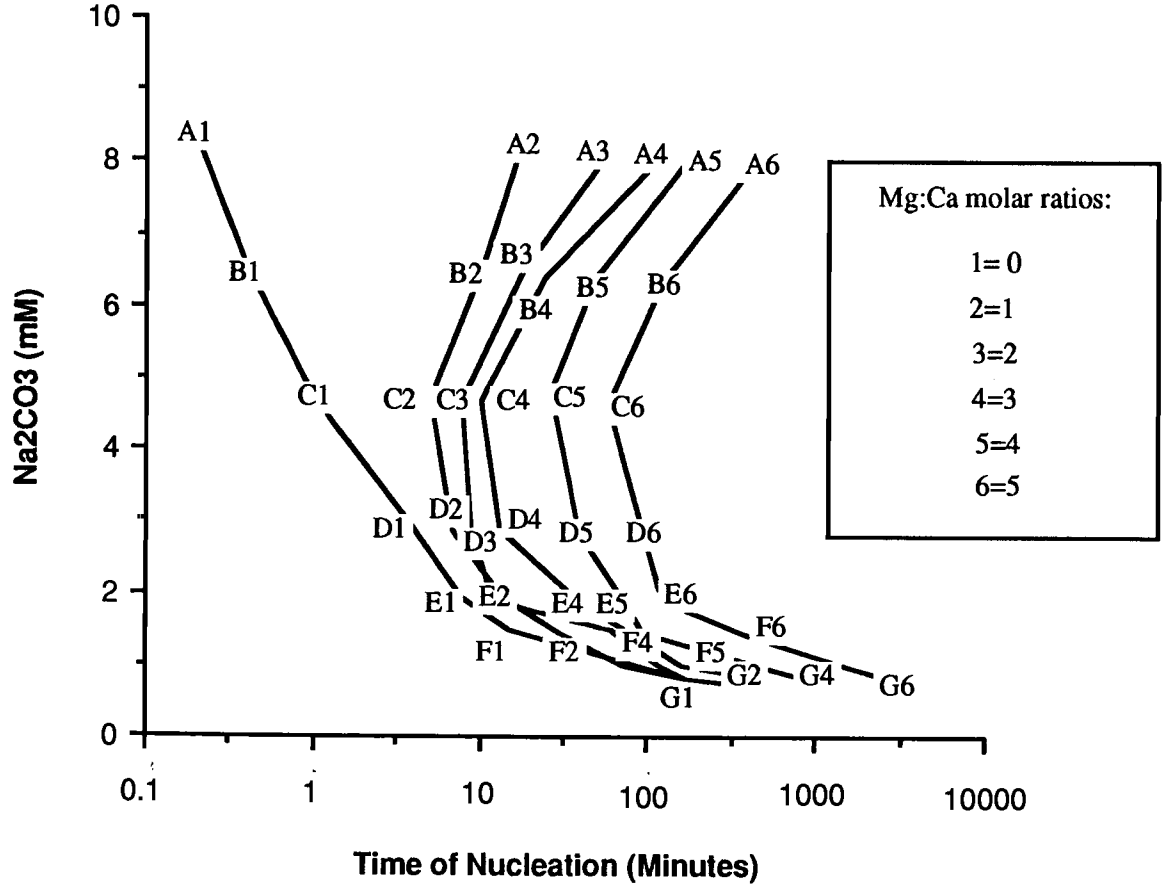
Na2CO3 (mM)
Time of Nucleation (Minutes)
Mg:Ca molar ratios:
1= 0
2=1
3=2
4=3
5=4
6=5
A1
A2
A3
A4
A5
A6
B1
B2
B3
B4
B5
B6
C1
C2
C3
C4
C5
C6
D1
D2
D3
D4
D5
D6
E1
E2
E4
E5
E6
F1
F2
F4
F5
F6
G1
G2
G4
G6
0
2
4
6
8
10
0.1
1
10
100
1000
10000

Figure 1.4

(from Fine, 1964; Wollast 1971;Stumm and Morgan, 1982). Thus, to increase the value of N_c we must increase the degree of saturation IAP/K_{SO}. Due to the incorporation of $MgCO_3$, the activity of the nucleus increases and IAP/K_{SO} (= degree of saturation) decreases. It takes a longer time to reach the steady-state of the reaction, at the point where critical sizes of nuclei are formed in the presence of magnesium. The equation:

$$xCa^{2+} + (1-x)\,Mg^{2+} + CO_3^{2-} \underset{b}{\overset{f}{\Longleftrightarrow}} Ca_xMg_{1-x}CO_3 \qquad (1.5)$$

shows the formation the mineral. f is the rate of the reaction for the formation of the nuclei of critical sizes and b is the rate of dissolution. Because of magnesium uptake by nuclei, one would expect b>f and an increase in K_{SO}, if we consider the nuclei as solid phase *(Dufour and Defay, 1963).* This leads to the decrease of the degree of saturation and to a slower formation of nuclei. The ionic products also increased in Figure 1.2 for a greater addition of CO_3^{2-}. It may be, however, that the ionic products are not large enough to overshadow the increase in the solubility products of high-magnesian calcites.

The curves in Figure 1.2 must approach the 100% saturation level asymptotically. Thus, extrapolation of the curves by lines which are tangent to the curves at about 0.79-0.69 mmole/l of added Na_2CO_3 will yield the minimum time for precipitation from seawater, when they intercept the 0.05 mmole/l of CO32- line. This may be a time when precipitation would occur in natural seawater if it stayed in the supersaturated near-surface layers because a 0.05 mmole/l of added Na_2CO_3 leads to seawater that is at least 300% supersaturated. The result of the intercept of the straight line extrapolation with the 0.05 mmole/l line in artificial seawater with varying amounts of magnesium is illustrated in Figure 1.5 and are shown in Table 1.4. The minimum time for artificial seawater which

Table 1.4

The estimated minimum times of onset of precipitation in different ratios of $(Mg^{2+}):(Ca^{2+})$ in artificial seawater:

$(Mg^{2+}):(Ca^{2+})$ Ratio	Time of nucleation (onset)
0:1	8.3±1.7 days
1:1	62.5±13.1 days
2:1	15±3.2 years
3:1	761±160 years
4:1	21,000±4,000 years
5:1	38,000±8,000 years

Figure 1.5.

Straight line extrapolation of the minimum time of spontaneous onsets at $(Mg^{2+}):(Ca^{2+})$ ratios of 0:1 in artificial seawater.

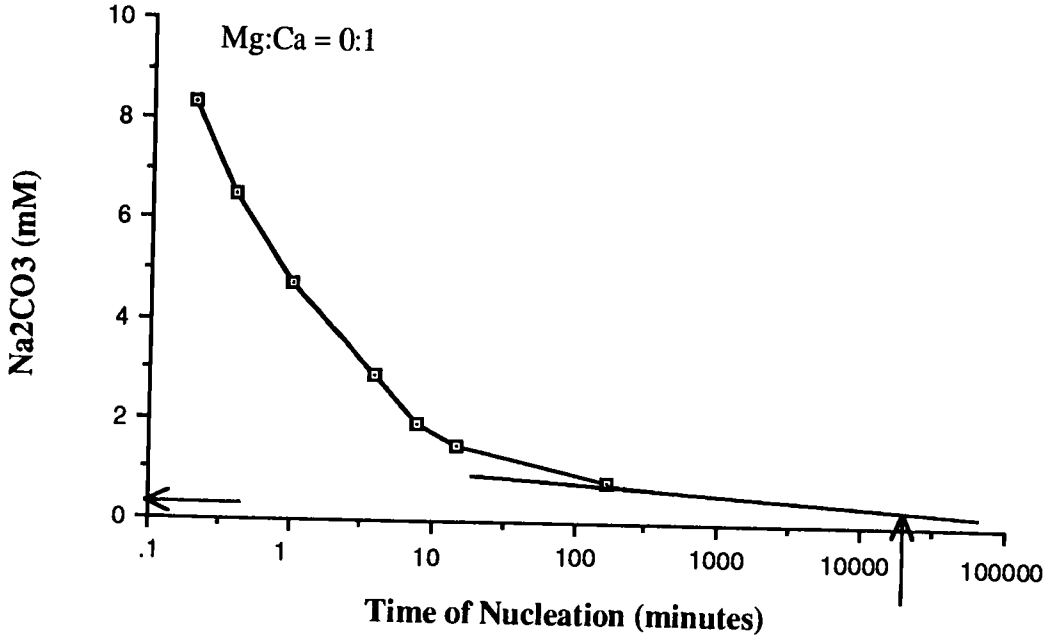
Mg:Ca = 0:1
Na2CO3 (mM)
10
8
6
4
2
0
.1
1
10
100
1000
10000
100000
Time of Nucleation (minutes)

Figure 1.5

has about the same amount of magnesium as natural seawater was found to be 38,000±8,000 years, in agreement with *Pytkowicz, (1973)*. That means the magnesium can inhibit the precipitation of calcium carbonate from supersaturated seawater to such an extent that spontaneous precipitation will not occur in the open ocean. In these experiments, artificial seawater was used in which there were no poisons such as dissolved organic matter *(Chave and Suess, 1970; Suess, 1970)* and polyphsphate *(Berner, 1968)* which may cause further inhibition.

Mucci and Morse, (1983b) concluded that the magnesian content of calcite is dominantly influenced by the magnesium-to-calcium ratio of water from which it precipitates. *Berner, (1975; 1978)* and *Thorstenson and Plummer (1977)* suggested that magnesian calcite composition is controlled by growth rates. The results (see Table 1.2) show that the composition of magnesian calcite, aragonite and maybe vaterite (see section 2) are controlled by $^{a}Mg^{2+}$:$^{a}Ca^{2+}$ ratio in the solution and by the growth rates. The growth rates are affected by magnesium concentration in the solution (see Figure 1.2).

1.4.2. Effects of Magnesium and the Degree of Saturation upon the Transformation of the Mineralogy of the Precipitate

Table 1.5 and Figures 1.6a,b,c,d,e and f show the transformation of precipitates during thirty-five days. The results indicate dissolution and reprecipitation of carbonate minerals. The mineralogy of the crystal was also found to depend upon the initial degree of saturation and upon the magnesium concentration in solution. Generally it was found that the mole% $MgCO_3$ in calcite decreases with time.

The results showed that the formation of calcium carbonate minerals was kinetically controlled. At high supersaturations precipitation of high-magnesian calcite was favored (see Table 1.5). Vaterite was found to be less stable than magnesian calcite and aragonite

Table 1.5

Effect of degree of supersaturation and Mg^{2+} concentration upon the transformation of calcium carbonate mineralogy.

$(Mg^{2+}):(Ca^{2+}) = 2:1$							
Na_2CO_3 added (mM)							
8.18				4.72			
Time days	Mole% $MgCO_3$	wt% calcite	$I_{Arag.}/I_{Vater.}$	Time days	Mole% $MgCO_3$	wt% calcite	$I_{Arag.}/I_{Vater.}$
1	16.4	89	.125	1	20.0	78	.083
7	14.9	66	2.1	7	10.4	50	.619
14	13.4	65	8.0	14	9.7	64	.910
21	13.4	65	7.2	21	8.9	62	.889
28	13.4	66	8.0	28	8.9	56	4.57
35	11.5	68		35	8.9	80	10.0

$(Mg^{2+}):(Ca^{2+}) = 3:1$							
Na_2CO_3 added (mM)							
8.10				4.70			
Time days	Mole% $MgCO_3$	wt% calcite	$I_{Arag.}/I_{Vater.}$	Time days	Mole% $MgCO_3$	wt% calcite	$I_{Arag.}/I_{Vater.}$
1	23.0	20	.111	1	00.0	00	-
7	17.9	36	.077	7	13.4	12	.065
14	17.9	56	.222	14	11.9	22	.171
21	20.8	61	.800	21	12.7	21	.500
28	18.6	56	4.667	28	12.7	28	3.75
35	19.3	54	6.000	35	12.7	29	4.40

Figure 1.6.

XRD results for homogeneous precipitates when $(Mg^{2+}):(Ca^{2+})$ ratio is 3:1 and 4.7 mM of Na_2CO_3 in artificial seawater during a period of 35 days.

a) Immediately after the massive solution,

b) after one week in solution

c) after two weeks in solution

d) after three weeks in solution

c) after four weeks in solution

c) after five weeks in solution

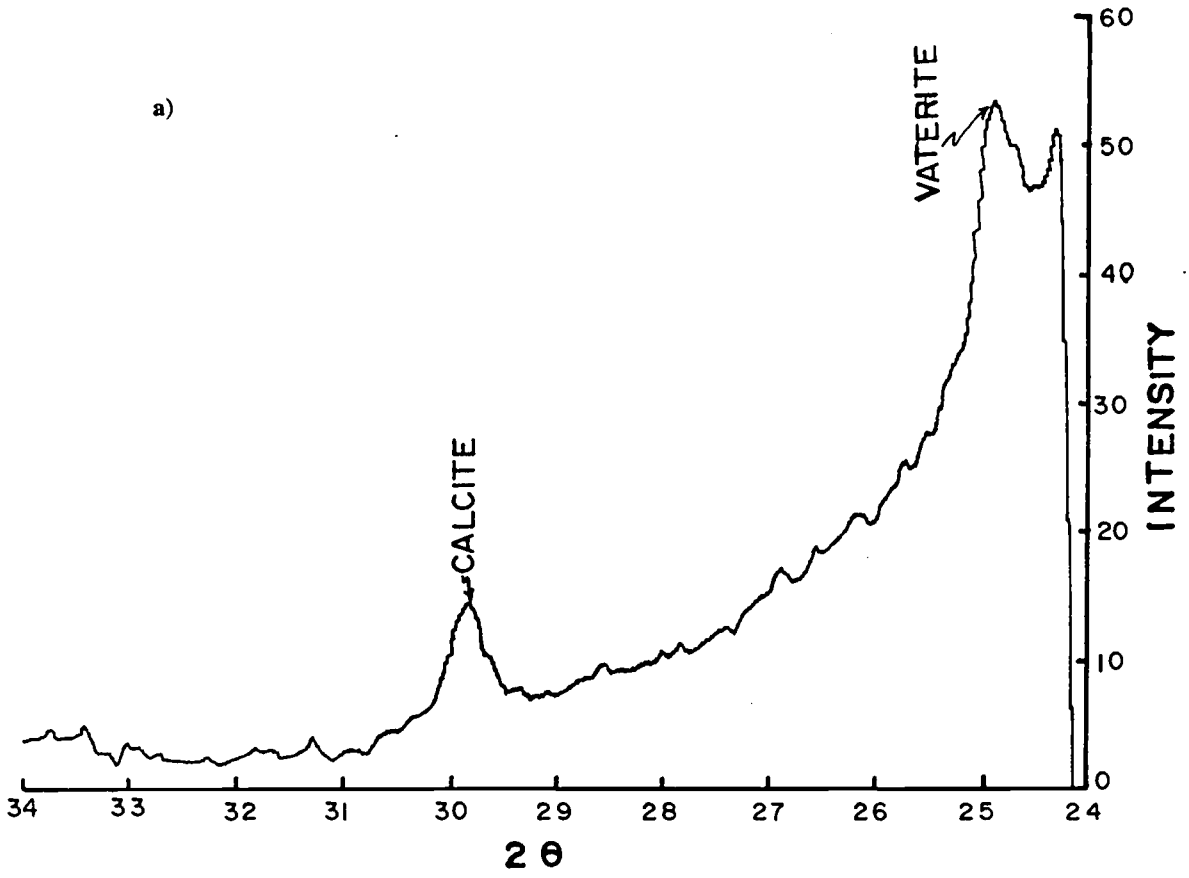
a)
VATERITE
CALCITE
60
50
40
30
20
10
0
INTENSITY
34
33
32
31
30
29
28
27
26
25
24
2θ

Figure 1.6

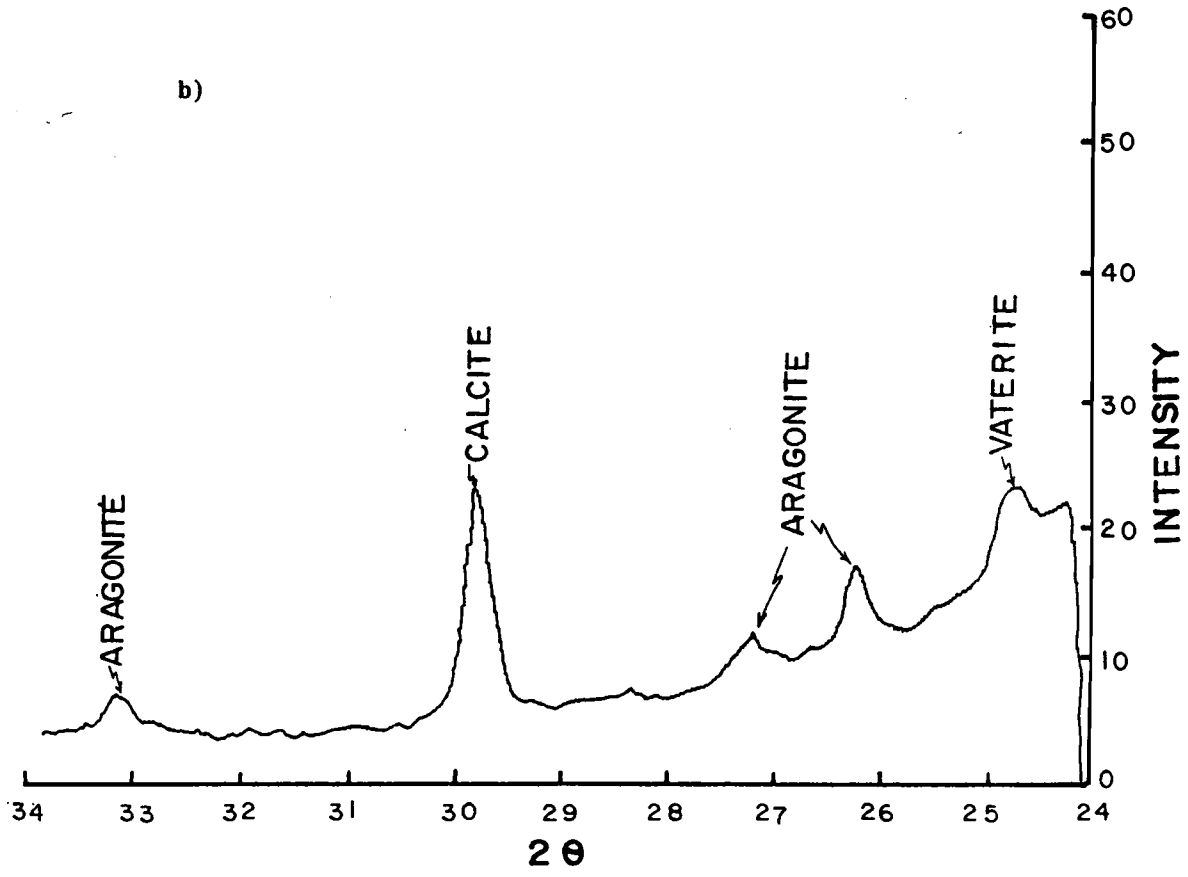

Figure 1.6 continued

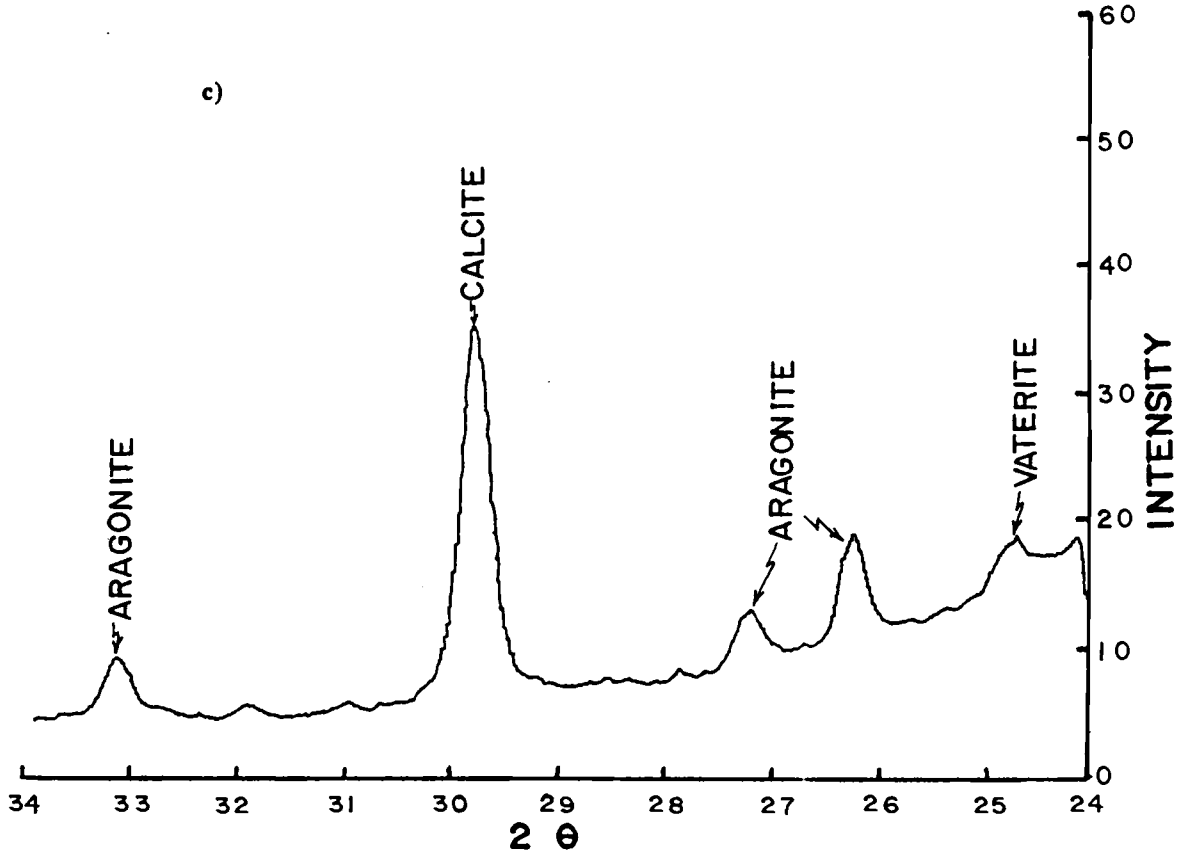

Figure 1.6 continued

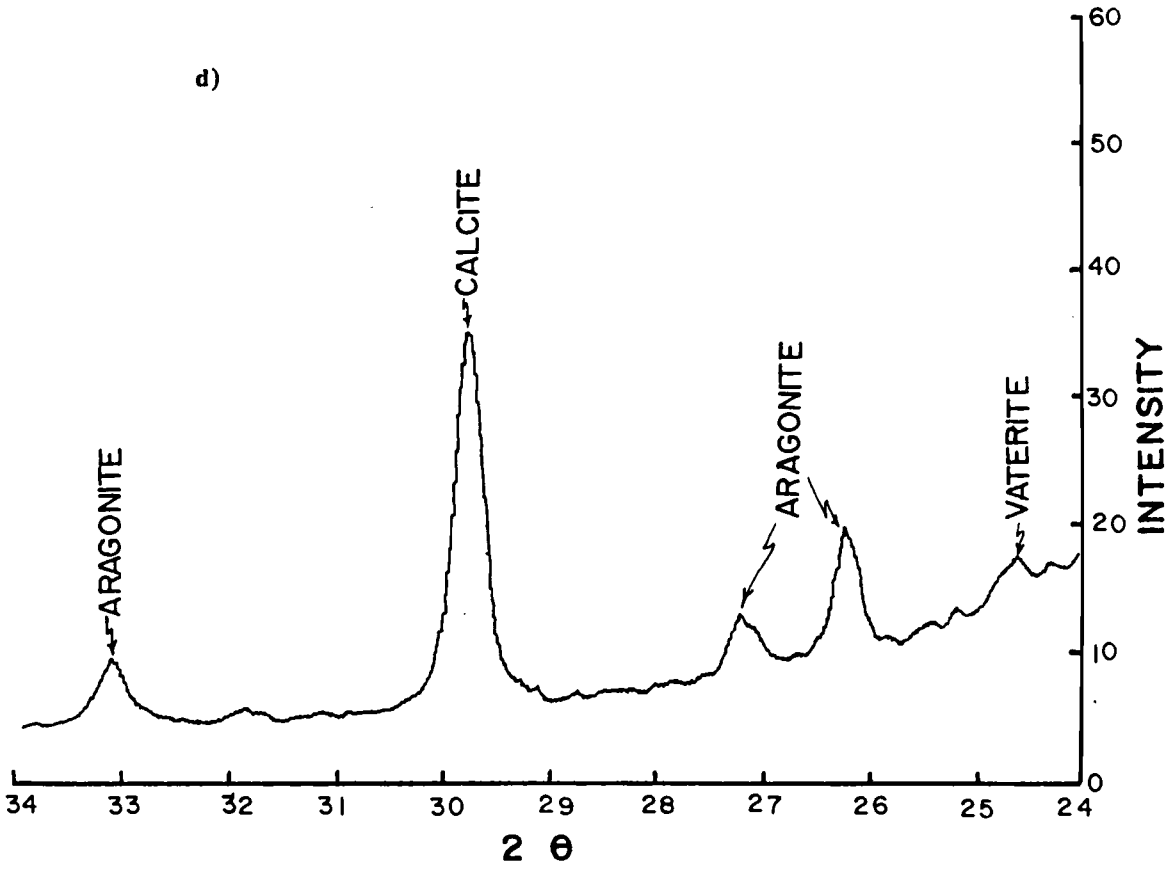

Figure 1.6 continued

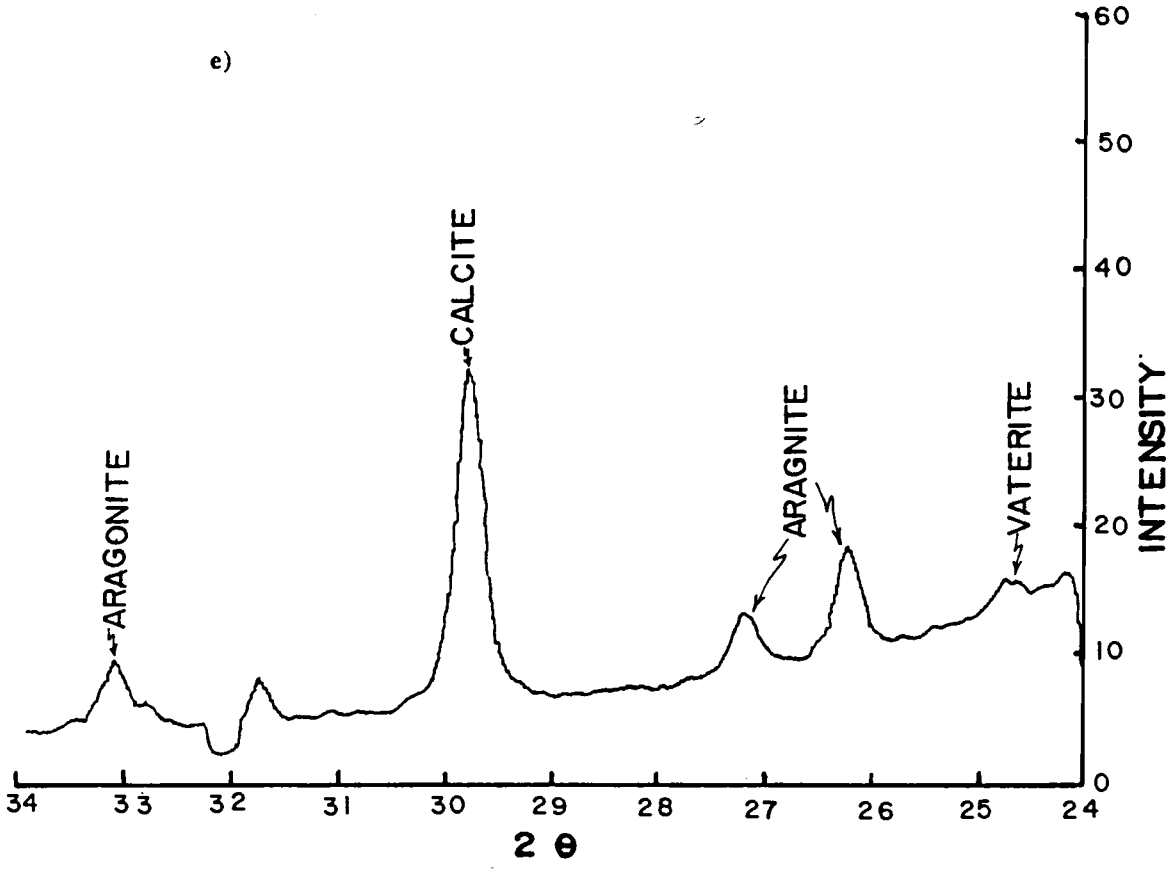

Figure 1.6 continued

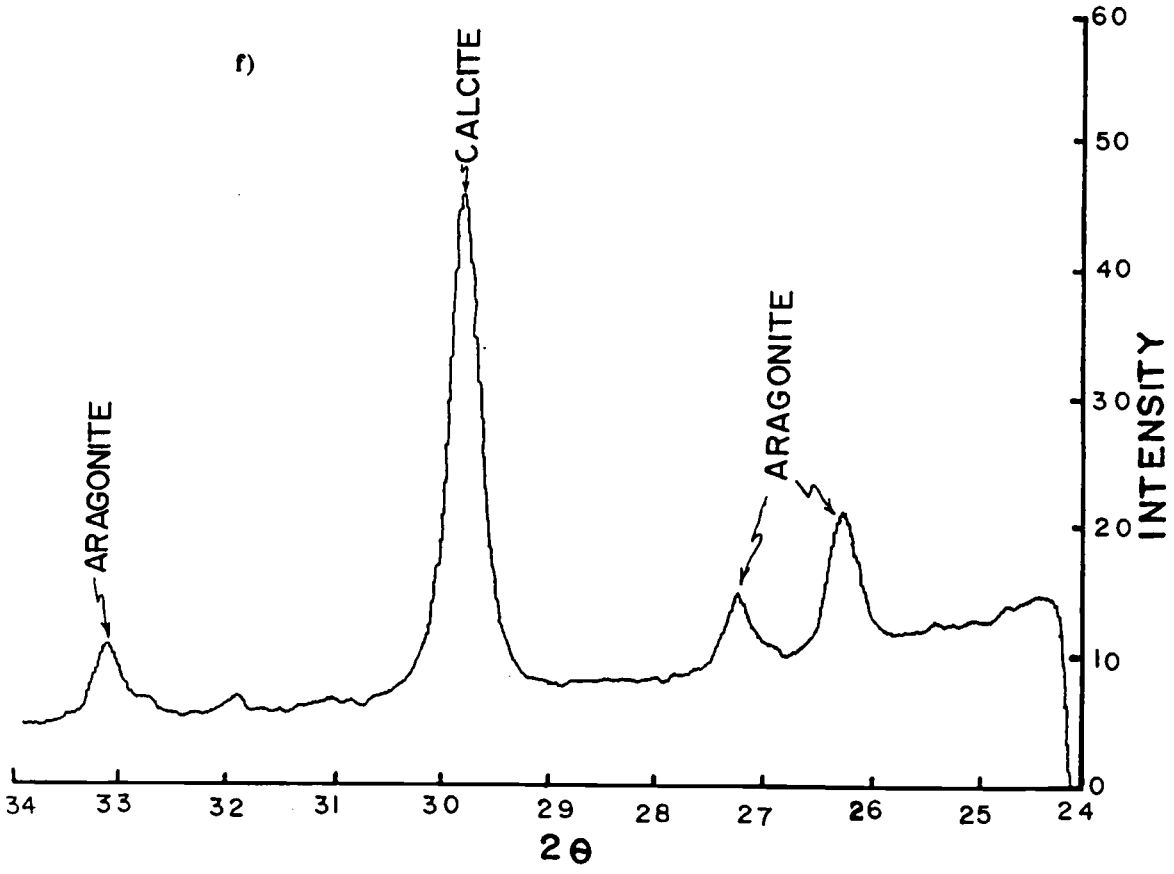

Figure 1.6 continued

and was the transition phase between them as they increased at the expense of vaterite. The results showed that the mineral compositions depend upon the initial supersaturation and the magnesium content and tended to approach a multistate equilibrium *(Wollast and Rienhard-Derrie, 1977; Pytkowicz and Cole, 1979;Pytkowicz, 1983b)*, which is described in chapter 4. The dissolution of high-magnesian calcite and the precipitation of calcite with a lower $MgCO_3$ content and aragonite obviously, had occurred. These precipitates have stabilities which depend upon the activities of the ions in solution and of the composition of the mineral itself. According to the phase rule, in the presence of two solids, a solution and vapor at equilibrium. $f = 2$, $f_m = 3$, and $f_c = 1$ if we use the molar degree of freedom *(Pytkowicz, 1983b)*. Then, one compositional variable such as the x fixes the system.

Based on the thermodynamic equilibria and experimental studies of *Goldsmith and Heard, (1961)*, dolomite and low-magnesian calcite are the more stable phases in sedimentary rocks. The formation of dolomite is kinetically very slow *(Goldsmith and Heard, 1961; Berner, 1971; Seperber et al., 1984)*. The result above showed that there was a transformation and drift toward the multistate equilibrium, indicated by the disappearance of vaterite. Change from this equilibrium requires a change in the solution composition and requires a long time. The multistate composition is the truly stable one for a given solution composition a solid-to-solution ratio.

Figure 1.7 shows that the composition and the weight percent of the first massive precipitation depends upon the magnesium concentration in the bulk of the solution and upon the degree of saturation. Different rates of precipitation can cause different amounts of magnesium to be incorporated into the solid. A high rate should cause a larger $MgCO_3$ uptake and an increase in the solubility of calcite. This solubility was caused by magnesium collisions during the rate controlled calcite crystal growth and reduced the chance for equilibration relative to slower runs. The resulting metastable solids may persist

Figure 1.7.

The mole% $MgCO_3$ versus the weight percent of calcite during 35 days. At $(Mg^{2+}):(Ca^{2+}) = 2:1$, (✕———✕), 8.18mM Na_2CO_3 was added; (⧈———⧈) 4.72 mM of Na_2CO_3 was added. At $(Mg^{2+}):(Ca^{2+}) = 3:1$. (◘———◘) 8.10 mM Na_2CO_3 was added; (■———■) 4.70 mM Na_2CO_3 was added.

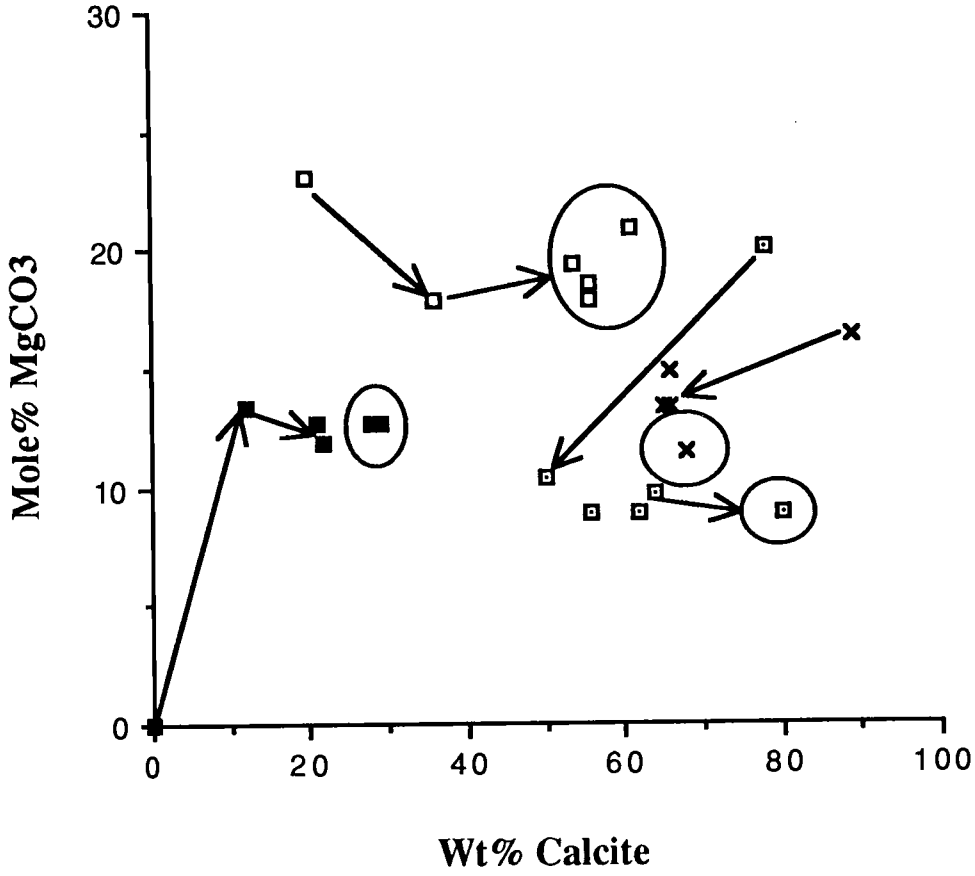

Figure 1.7

for long times. The principle is the same for coating effects when different amount of Na_2CO_3 are added *(Pytkowicz and Cole, 1979)* as it is for bulk changes.

1.4.3. The Effects of Magnesium ions and the Degree of Saturation in the Artificial Seawater upon the Morphology of Calcium Carbonate Phases

The different crystal forms which were precipitated at different (Mg^{2+})-to-(Ca^{2+}) ratios and different ionic products in artificial seawater are shown in Figures 1.8, 1.9, 1.10, 1.11 and 1.12. The images of all carbonate minerals are acicular except for Figure 1.8, which is equant. Some elongated precipitates are found at a (Mg^{2+})-to-(Ca^{2+}) ratio of 3-4. The terms micrite, fibrous, and elongated are defined by *Folk, (1974)* based upon their shapes and sizes. I prefer to use the term acicular (needle-like in form) to include any elongated shape other than equant (same diameter in all directions).

The sizes of the crystal forms are shown to be about 10μm or larger at zero magnesium ion in solution (see Figure 1.8). The sizes decreased with the increase of magnesium ions in the solution (≈ 2-1μm). Aragonite crystals were the smallest (≤ 1μm). The characteristics of the surfaces of the crystals also appeared to be affected by the degree of saturation and the magnesium-to-calcium ratio. In the presence of magnesium ions the crystals appeared in the forms of bundles of fibrous or needlelike aggregates.

Two major factors may explain the different carbonate mineralogies and morphologies. (1) magnesium content (and maybe of other ions, such as SO_4^{2-}) of the solution and (2) rate of crystallization *(Murray, 1967; Bischoff, 1968; Bischoff and Fyfe, 1968; Pytkowicz, 1965 and others).*

The experimental results showed that the presence of magnesium in solution was the most effective parameter that controlled the morphologies of calcium carbonate. At zero magnesium concentration in solution the crystal morphology was equant (see Figure 1.8)

both at high and low degree of supersaturation and thus at fast and slow rates of reaction. Therefore, one would expect that the reaction rate of precipitation was not the main control in determining the morphological feature of calcium carbonate crystals but, rather the presence of different ions in the solution, specially, of magnesium ions.

Folk, (1974) has shown an interesting example from the formation of the chicken egg, in as-much as 90% of the 5-gram weight of the shell is precipitated in 16 hours *(Romanoff and Romanoff, 1949)* and yet, despite this very rapid rate of precipitation, the egg-shell consists of calcite of reasonably coarse crystals. The egg-shell example and my results show that the precipitation rates actually exert an effect only in the presence of magnesium in solution and its incorporation in the growth process.

These observations of mineralogies and morphologies have been the subject of extensive geological and geochemical studies. The first qualitative explanation for the magnesium effect on calcium carbonate morphology was proposed by *Folk, (1974).* In his model he illustrated that magnesian calcite grows as fibres parallel to the c-axis. The calcite lattice consist of alternating layers of CO_3^{2-} groups and Ca^{2+} ions perpendicular to the c-axis (see Figure 1.14). If a Mg^{2+} ion is attached to the end of a growing crystal, it can easily be covered by alternate overlapping CO_3^{2-} sheets without any deformational effect (see Figure 1.14a). But, if the magnesium ion is attached at the side of the crystal, it will block growth, because of its smaller ionic radius which causes the over- and underlying CO_3^{2-} sheet to move closer together to accommodate it. Such a deformed structure will not accept the next larger Ca^{2+} (see Figure 1.14b). *Folk ,(1974)* has concluded that magnesium in solution promotes rapid growth in the direction of the c-axis, and that perpendicular to its growth is retarded by selective "Mg-poisoning."

Figure 1.8.

SEM images of equant pure calcite precipitated from artificial of Mg-free seawater and different rates of reactions (a) at addition of 1.48mM Na_2CO_3 and (b) at addition of 4.75 mM Na_2CO_3.

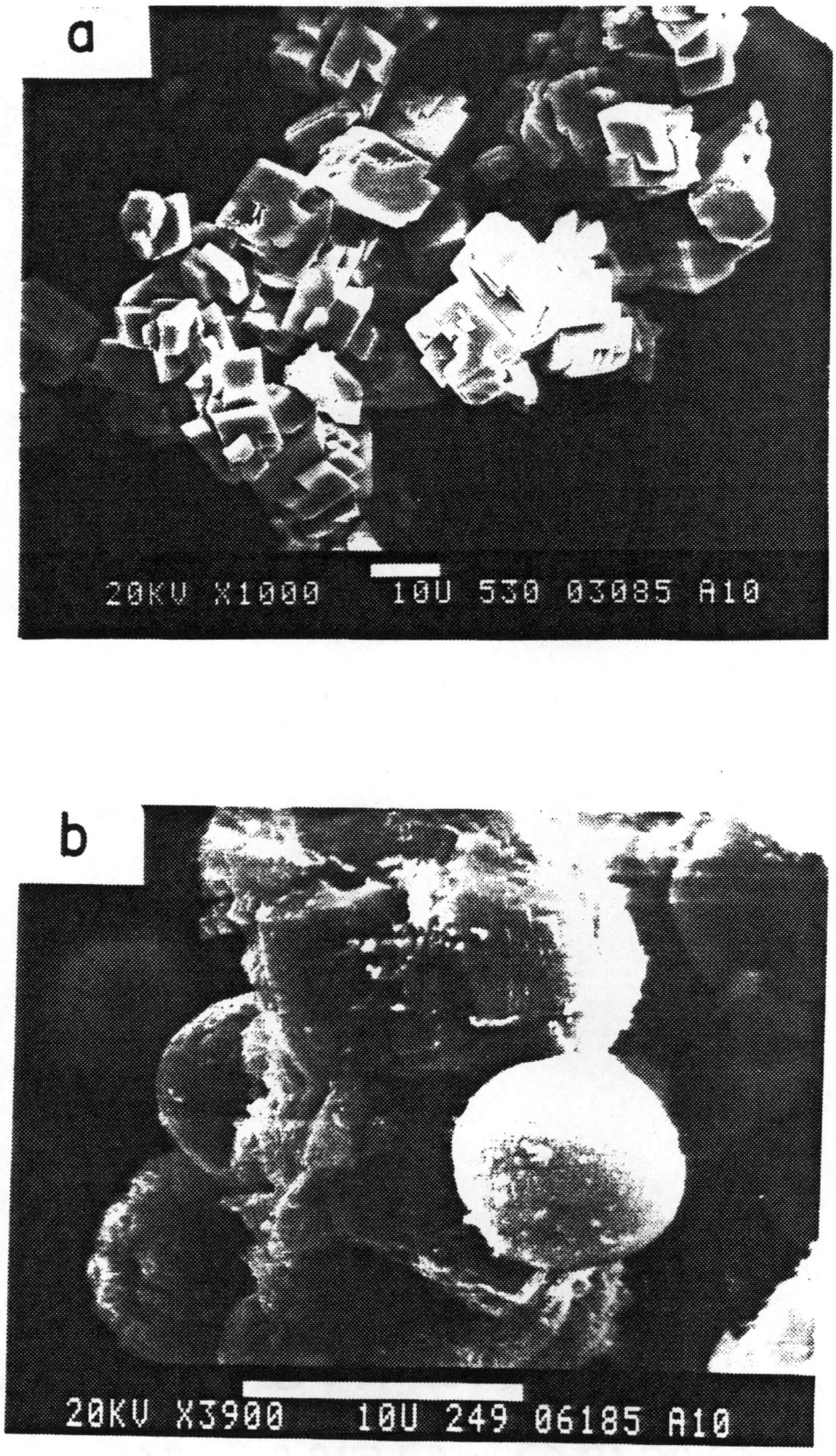

Figure 1.8

Figure 1.9.

SEM images of acicular magnesian calcite and aragonite mixture at $(Mg^{2+}):(Ca^{2+})$ ratio of 1:1 in artificial seawater (a) mixture of 11 weight percent calcite of 3 mole% $MgCO_3$ and 89 weight percent aragonite precipitated by adding 1.45 mM Na_2CO_3 and (b) Mixture of calcite of 96 weight percent of 11.2 mole% $MgCO_3$ and 4 weight percent aragonite precipitated by adding 4.74 mM Na_2CO_3.

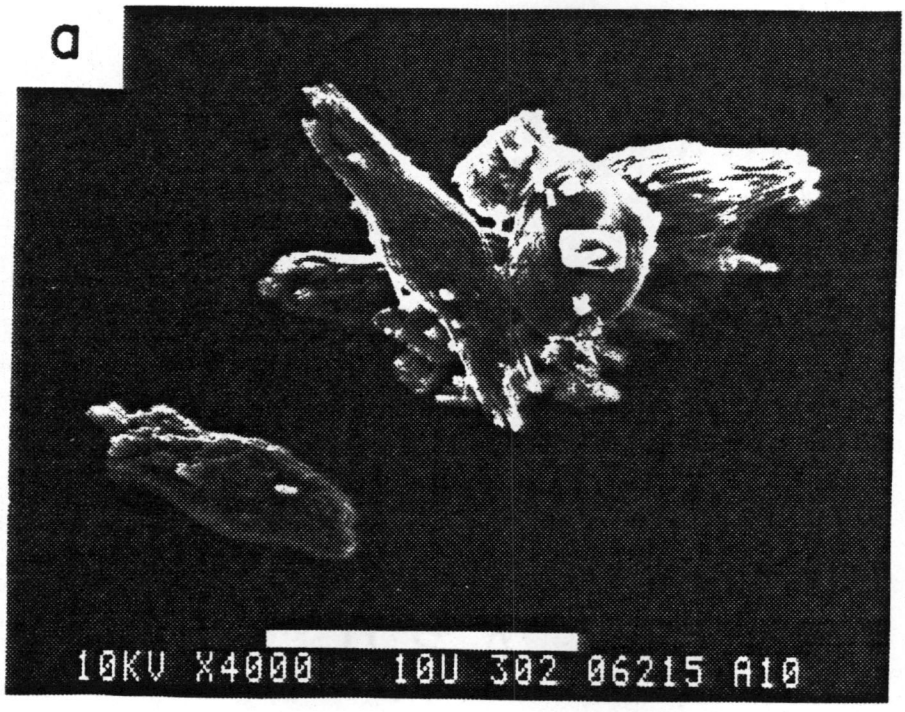

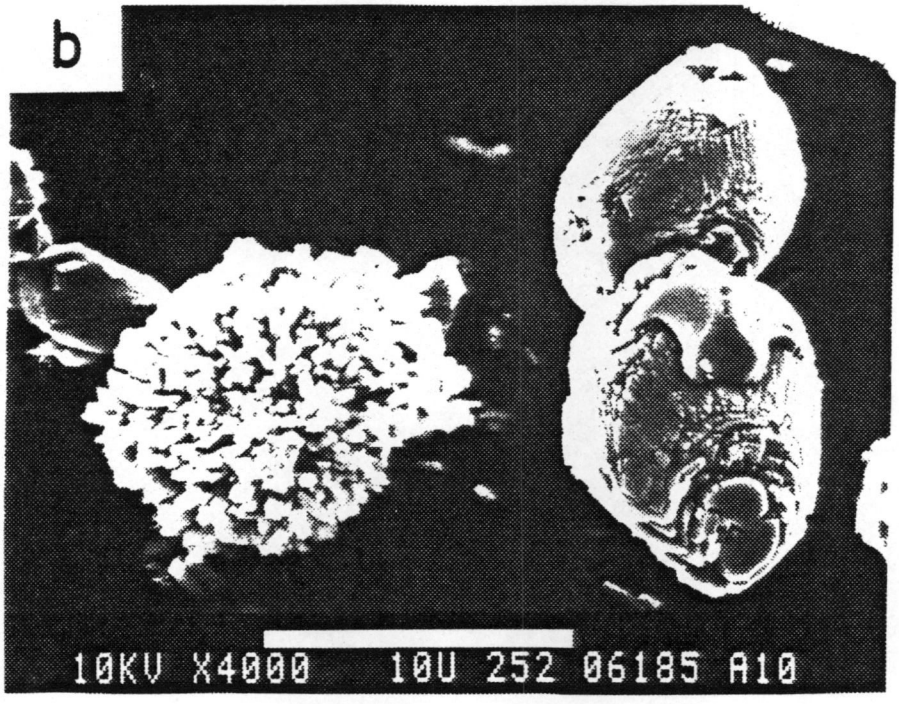

Figure 1.9

Figure 1.10.

SEM images of acicular magnesian calcite and aragonite mixture at $(Mg^{2+}):(Ca^{2+})$ ratio of 2:1 in artificial seawater (a) mixture of 3 weight percent calcite of 1.4 mole% $MgCO_3$ and 97 weight percent aragonite precipitated by adding 1.4 mM Na_2CO_3 and (b) Mixture of calcite of 66 weight percent of 12.7 mole% $MgCO_3$ by adding 4.74 mM Na_2CO_3.

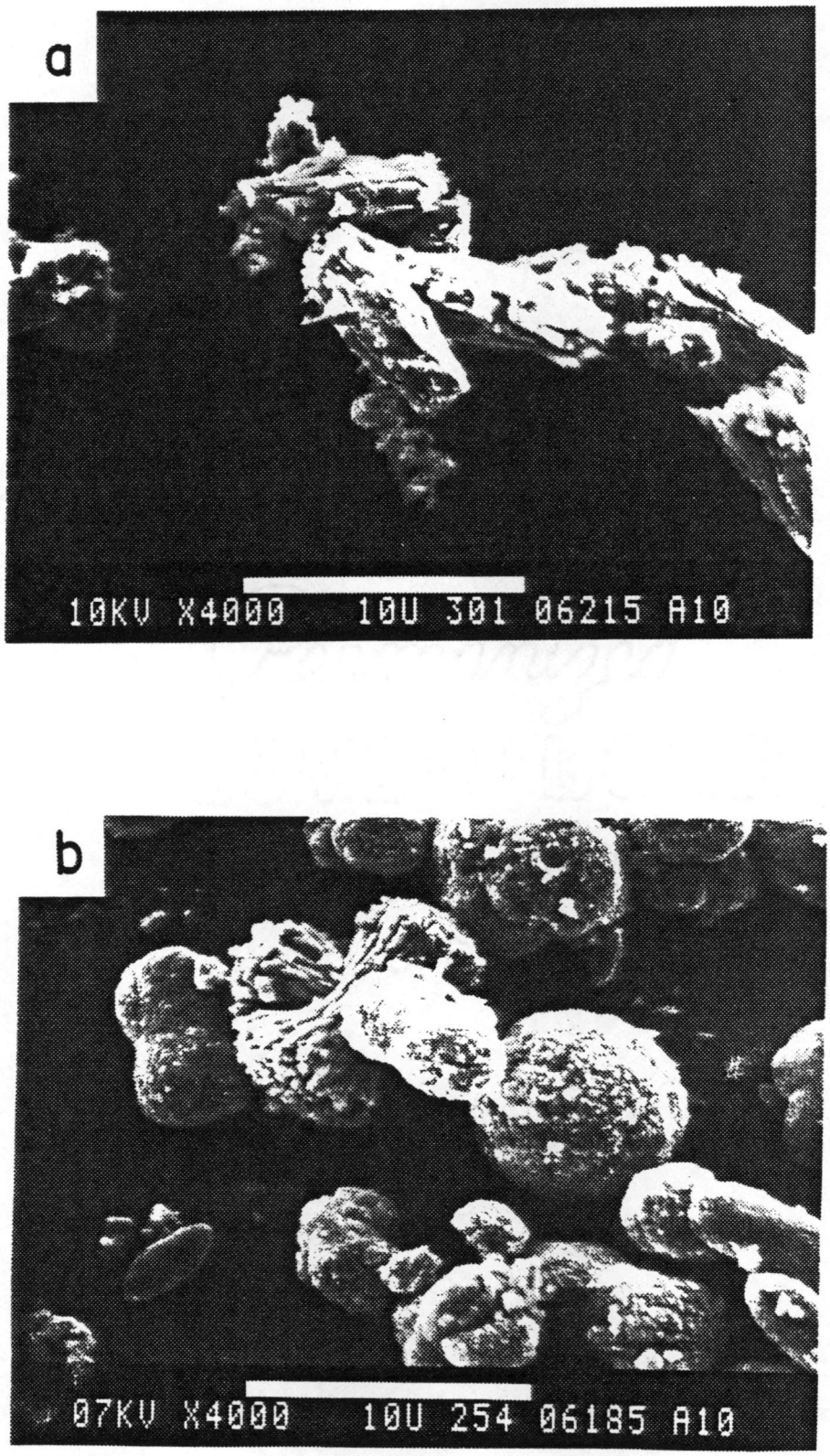

Figure 1.10

Figure 1.11.

SEM images of acicular magnesian calcite and aragonite mixture at $(Mg^{2+}):(Ca^{2+})$ ratio of 3:1 in artificial seawater (a) pure aragonite precipitated by adding 1.0 mM Na_2CO_3 and (b) mixture of 66 weight percent calcite of 11.4 mole% $MgCO_3$ and 35 weight percent aragonite precipitated by adding 4.7 mM Na_2CO_3.

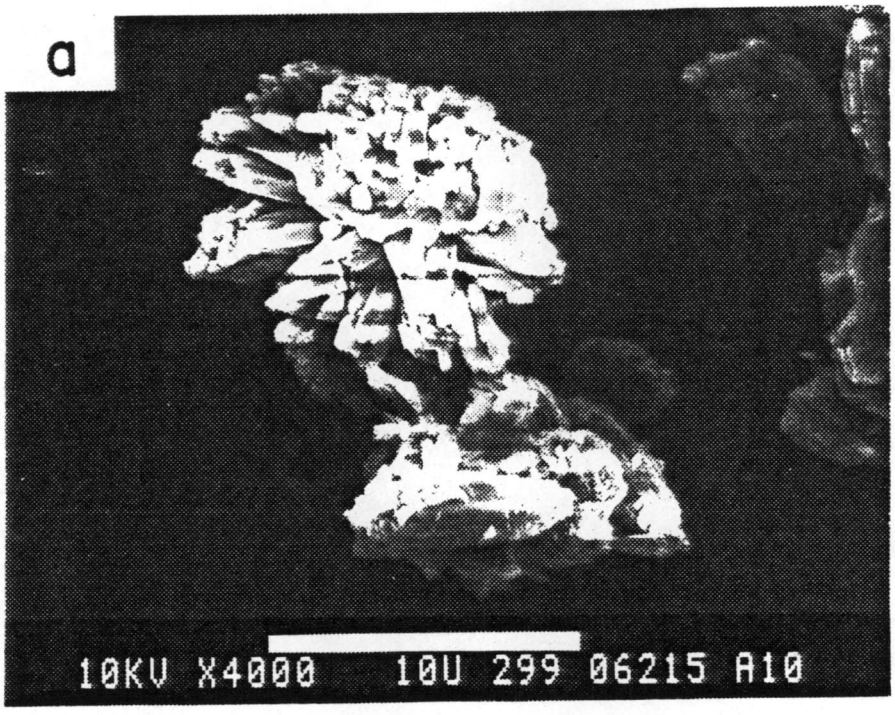

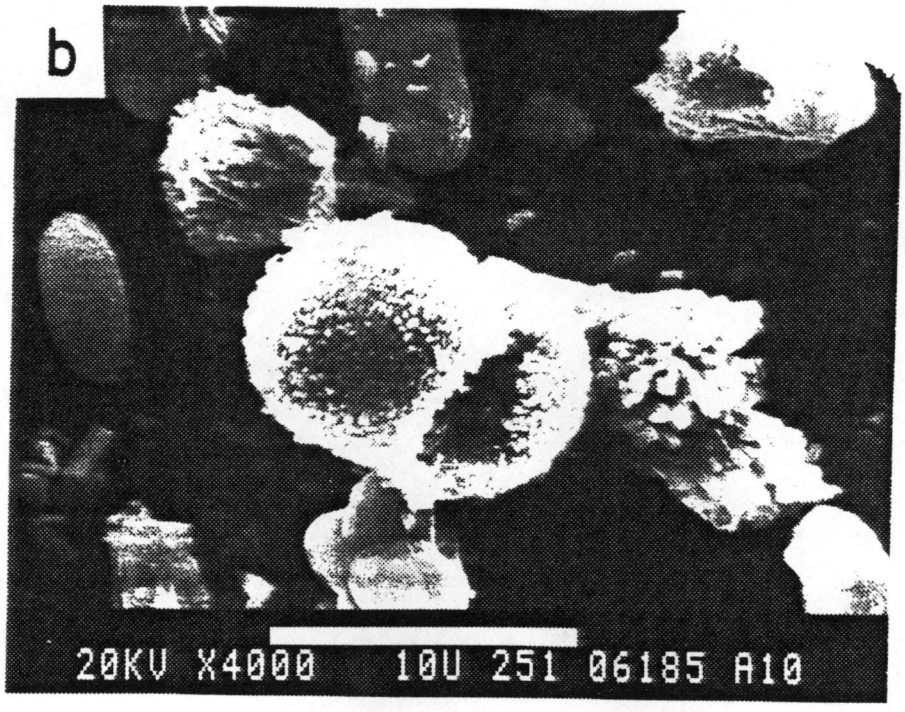

Figure 1.11

Figure 1.12.

SEM images of acicular magnesian calcite and aragonite mixture at $(Mg^{2+}):(Ca^{2+})$ ratio of 4:1 in artificial seawater (a) pure aragonite precipitated by adding 1.45 mM Na_2CO_3 and (b) mixture of 46 weight percent calcite of 14.7 mole% $MgCO_3$ precipitated by adding 4.82 mM Na_2CO_3.

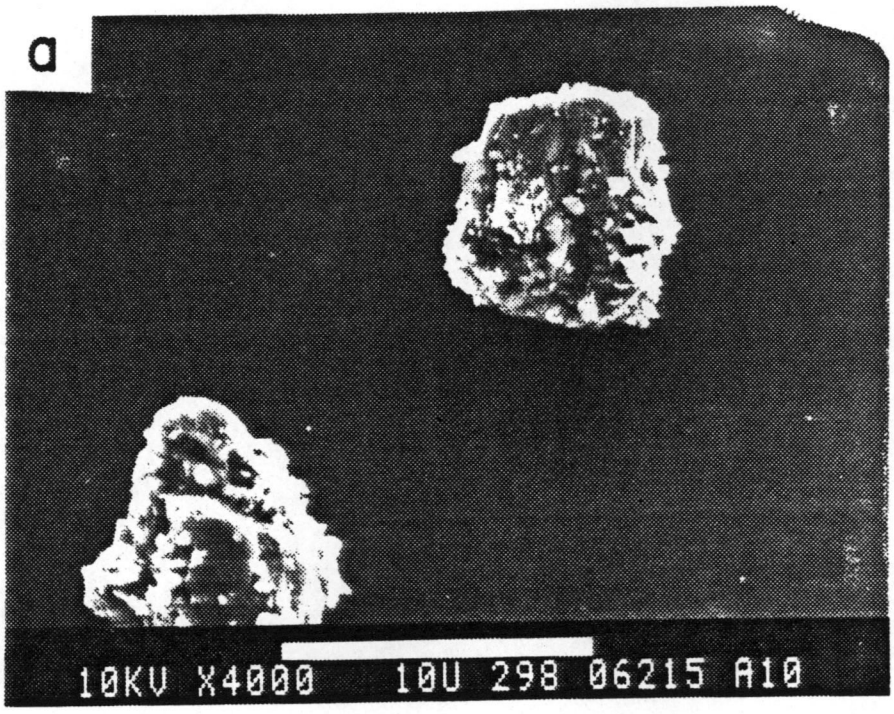

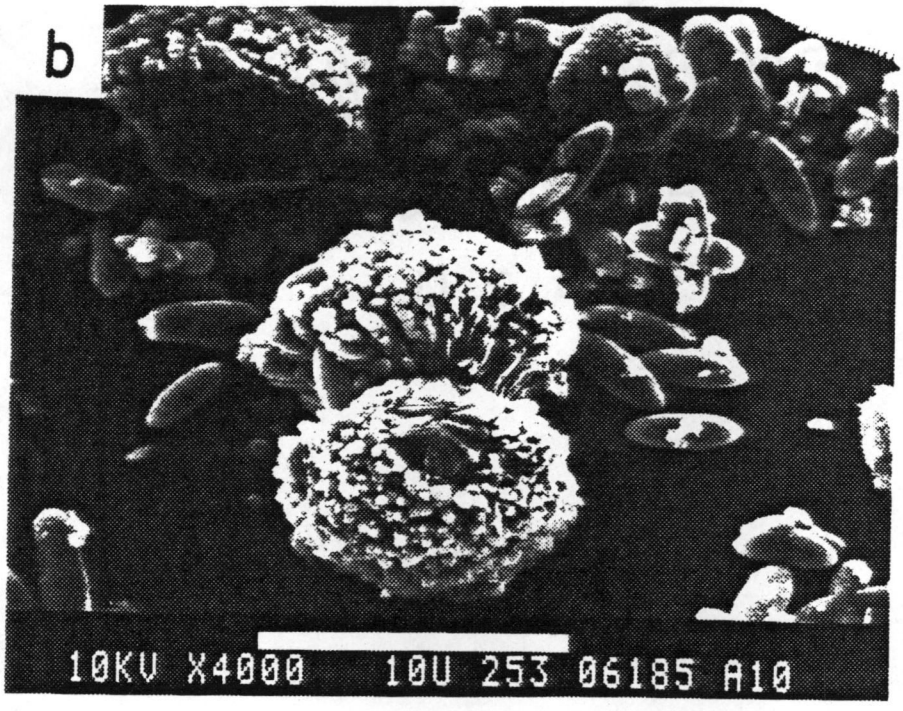

Figure 1.12

Figure 1.13.

SEM images of acicular magnesian calcite and aragonite mixture at $(Mg^{2+}):(Ca^{2+})$ ratio of 5:1 in artificial seawater (a) pure aragonite precipitated by adding 1.44 mM Na_2CO_3 and (b) pure aragonite precipitated by adding 4.64 mM Na_2CO_3.

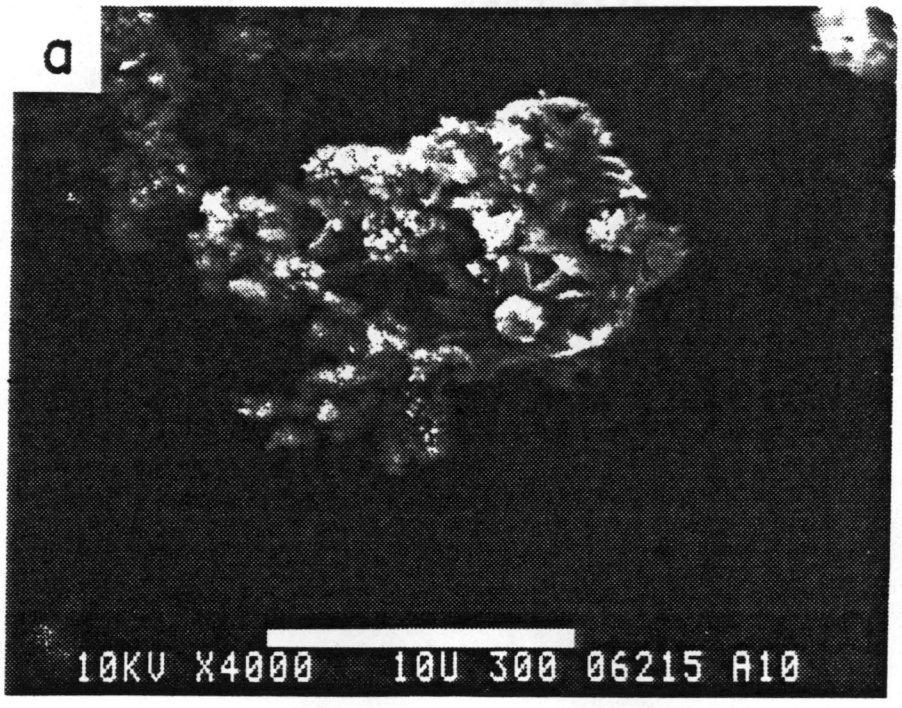

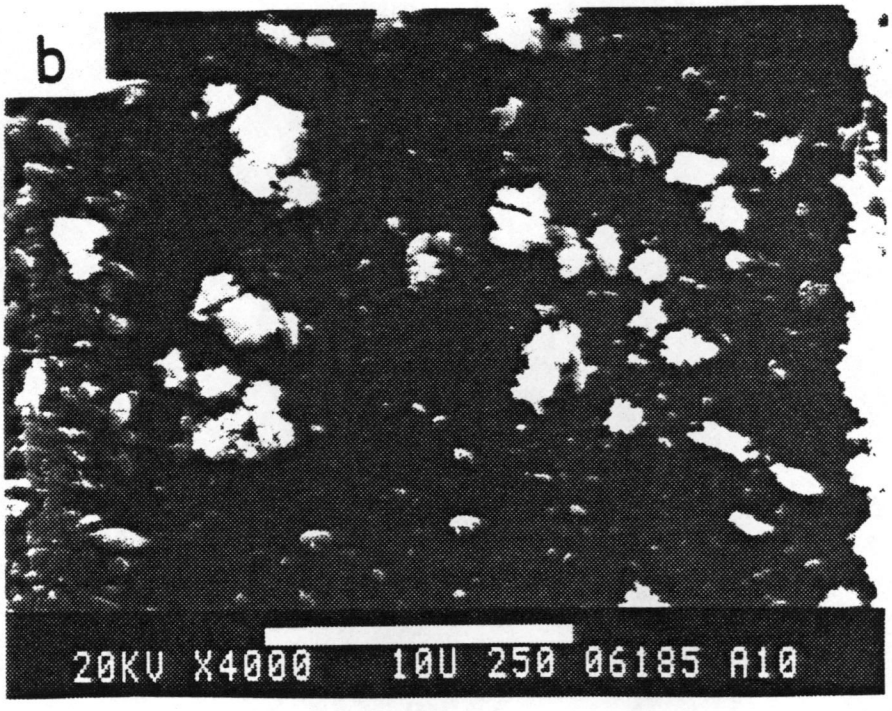

Figure 1.13

The model of *Folk, (1974)* was criticized by *Lahann (1978b).* He disagreed with the morphological variation explained by Folk. *Lahann, (1978a,b)* stated that the experimental evidence on the kinetics of calcite crystal growth indicates that dehydration of surface adsorbed Ca^{2+} ion may be the rate-determining step in calcite growth. He showed that the ionic radii of Ca^{2+} and Mg^{2+} are 0.99 and 0.64 Angstrom respectively *(from Evan, 1966)* and that the effective radii of the ions in aqueous solution are 3.21 and 4.65 Angstrom, respectively *(from Stern and Amis, 1959).* The substitution of magnesium ions for calcium ions on growing calcite surface would markedly, slow the rate of the crystal growth because of the greater energy required for dehydration. The free energy of hydration for magnesium is 17% greater than calcium *(from Lippman, 1960).* Based on the Guoy-Chapman double-layer theory, he concluded that the crystallization of calcite was dependent upon the availability of carbonate or bicarbonate ions which become more significant if the presence of a carbonate ion is required to dehydrate surface adsorbed Ca^{2+} ions. The crystallography of calcite allows differences in surface potentials to develop on different crystal faces. These differences in surface potentials lead to formation of needle-like crystal habits. For example, the excess of surface active cations over surface-active anions, however, that the normal circumstance for a c-axis face will be saturated of the surface with cations. In contrast to the edge faces, where rows of carbonate ions will be exposed to solution. The absence of exposed carbonate groups, and saturation of the surface with Ca^{2+} and Mg^{2+} ions should create a strong positive potential along the c-axis. The final conclusion is that the potential on a c-axis face will be higher than on edge faces where both $CO3^{2-}$ and Ca^{2+} ions must be exposed to solution. According to Lahann's model one may conclude that the calcite growth is favored along a c-axis face even in the absence of magnesium. The presence of magnesium will increase the retardation of growth on the edges of calcite.

Thus, both models show that the presence of magnesium in solution favors the c-axis face, and preferential growth of the crystal in c-direction will occur. *Folk, (1978)* re-evaluated his model and explained that the increase of magnesium and other ions in solution produce these acicular crystals.

The model I proposed is based on my results (section 1.4.1 and 1.4.3) and based on the increase of calcite solubility with the increase of mole% $MgCO_3$ *(Chave et al., 1962)*. I agree with *Folk, (1974;1978)* and *Lahann, (1978)* that the crystal growth is favored along the c-axis face, as a result of magnesium ion interaction. The retardation of magnesium ions to the growth of the edges faces is due to the magnesium incorporation in calcite between rows by increasing the $MgCO_3$ fraction, the solubility of calcite increases as a result of the distortion of the over- and underlying CO_3^{2-} sheets. This increase in lattice distortion will, eventually, lead to the fragmentation of CO_3^{2-} sheets. On the other hand, suppose a few magnesium ions are placed at c-axis face. If the reaction is fast enough the CO_3^{2-} sheet will spread as normal with little distortion that does not affect the over- and underlying sheets (see Figure 1.15a). At low magnesium concentration in solution and high rates of reaction the overlapping CO_3^{2-} will cover the Mg^{2+}, because the rate of reaction > rate of dissolution as a result of distortion.

Edge face growth will be slower because there is no overlapping which may overshadow the dissolution rate, and depending upon the rate of dissolution (i.e. $MgCO_3$ content) the edge growth is the result. At low magnesium ions the edges may grow and form equant crystal.

Because of high magnesium concentration in solution, the formation of $MgCO_3$ will be enhanced, and if the rate of the reaction is about equal to the rate of dissolution or less the overlapping sheet will dissolve as well as some the underlying sheet, which may result in the formation of smaller elongated crystal of aragonite. If the rate of the reaction is

rapid the overlapping sheet will cover some of these Mg^{2+} ions and the resulting distortion will block edge growth. This results in needle-like crystal of high-magnesian calcite. Eventually due to the reduction in reaction rate and higher solubility of high-magnesian calcite, the Mg^{2+} ions in solution will increase and will lead to the formation of aragonite (see Figure 1.13b, and Table 1.5). Therefore, the presence of magnesium will cause the instability of CO_3^{2-} due to their attractions to the smaller Mg^{2+} ion, and results in dissolution of $MgCO_3$ molecules.

One should raise the question why is dolomite $CaMg(CO_3)_2$ more stable in solution? The formation of dolomite is very slow and the mechanism is not well understood. The crystallography shows that it is composed of alternating sheets of Ca^{2+}, CO_3^{2-} and Mg^{2+} ions. This arrangement will not cause any distortion of CO_3^{2-} sheets. Over geological times dolomite could arrange these alternating sheets and not disturb the normal growth of equant crystal (see Figure 1.16).

The different morphologies of calcium carbonate, their various sizes and their surface edges and corners will have different activities in solution and may control the interaction of carbonate crystal with the surrounding waters. Because the surface energy of a crystalline solid is a part of the total energy of the particle, the surface energy of the particle will increase with the increase of the surface-to-volume ratio of the particle. *Chave and Schmalz, (1966)* and *Pytkowicz, (1969)* have shown that the activity of calcite increases with decreasing particle size of calcite and no longer is equal to unity (Table 1.7, base on *Chave and Schmalz, 1966*). The activity of the particle increase with the decreases of its radius according to equation:

$$a_{CaCO3} = a^{o}_{CaCO3} \exp\left(\frac{2\,t\,v}{RT\,r}\right) \qquad (1.6)$$

Figure 1.14.

The model proposed by Folk (1974) showing the effect of magnesium ions in solution upon the morphology of calcium carbonate crystals (a) Mg^{2+} ions have small effects on the c-axis face (b) growth on the edges is inhibited by Mg^{2+} ion due to bending of over- and underlying CO_3^{2-} sheets.

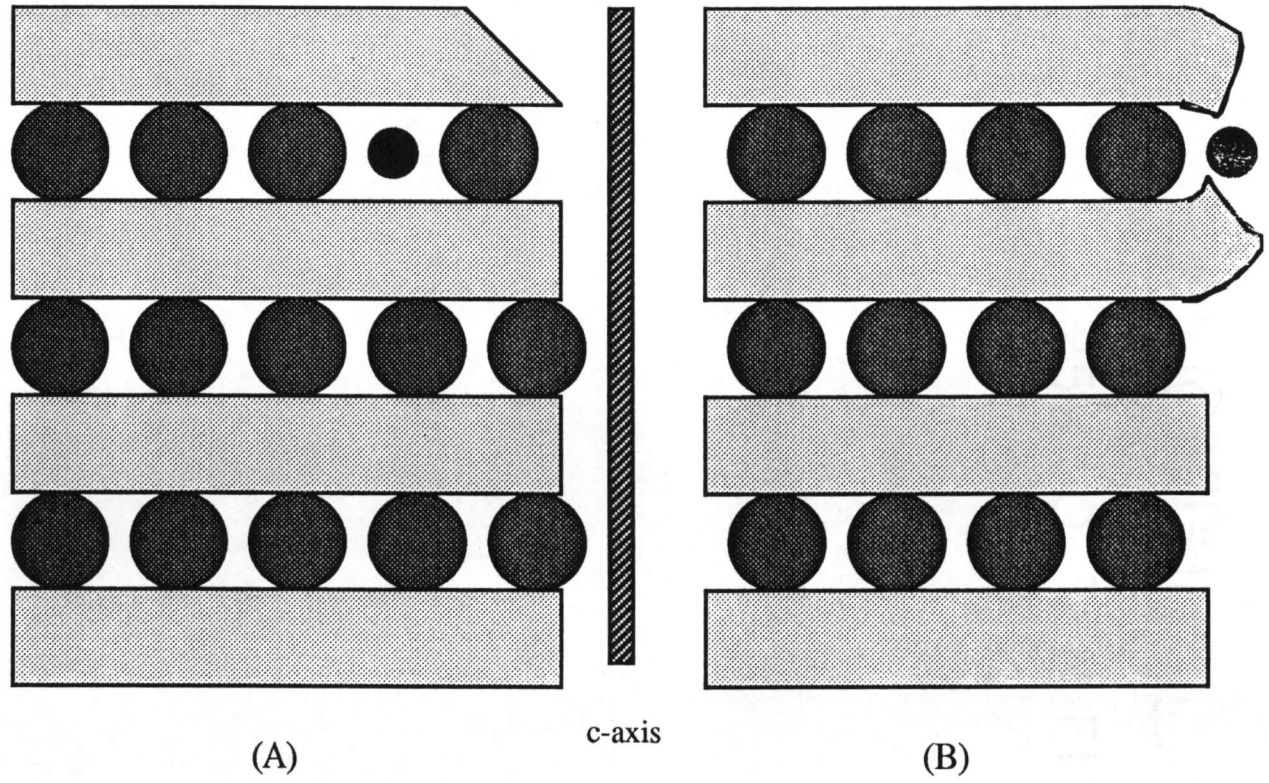

Figure 1.14

Figure 1.15.

The model I proposed based on my results and those of Chave et al., (1962) shows growth (a) along the c-axis, small amounts of Mg^{2+} ions will not affect the growth too much, because distortion is small (b) on the edge where high probability of Mg^{2+} interaction the distortion will be effective and causes separation of $MgCO_3$ molecules, and inhibits the edges' growth of calcites and (c) if the Mg^{2+} ions are high in solution collision and incorporation with Ca^{2+} along c-axis face will increase, then distortion increases and leads to dissolution of high-magnesian crystallites. So the growth on c-axis may also be affected and leads to smaller crystals of aragonite.

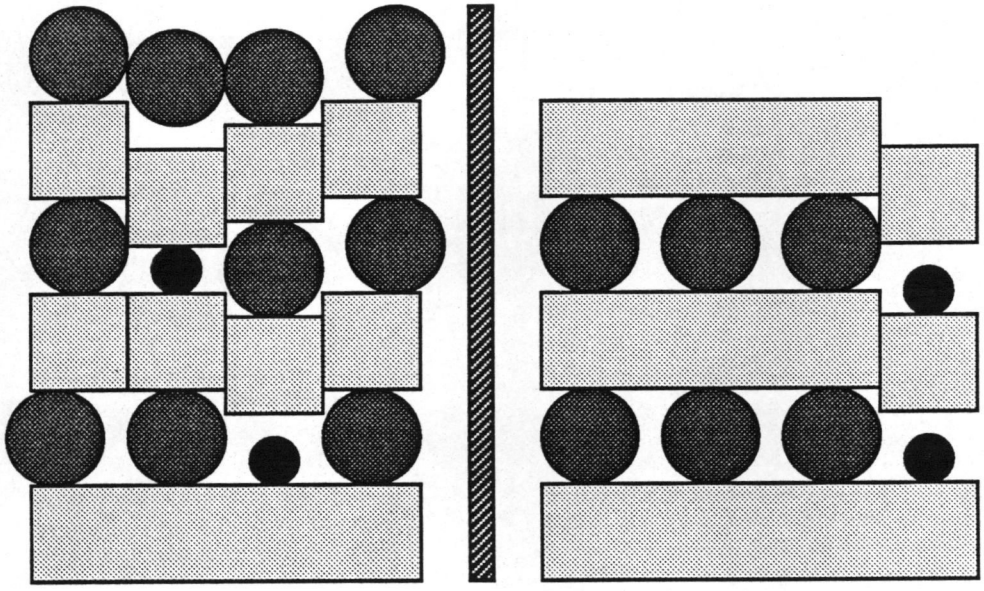

c-axis

(A) (B)

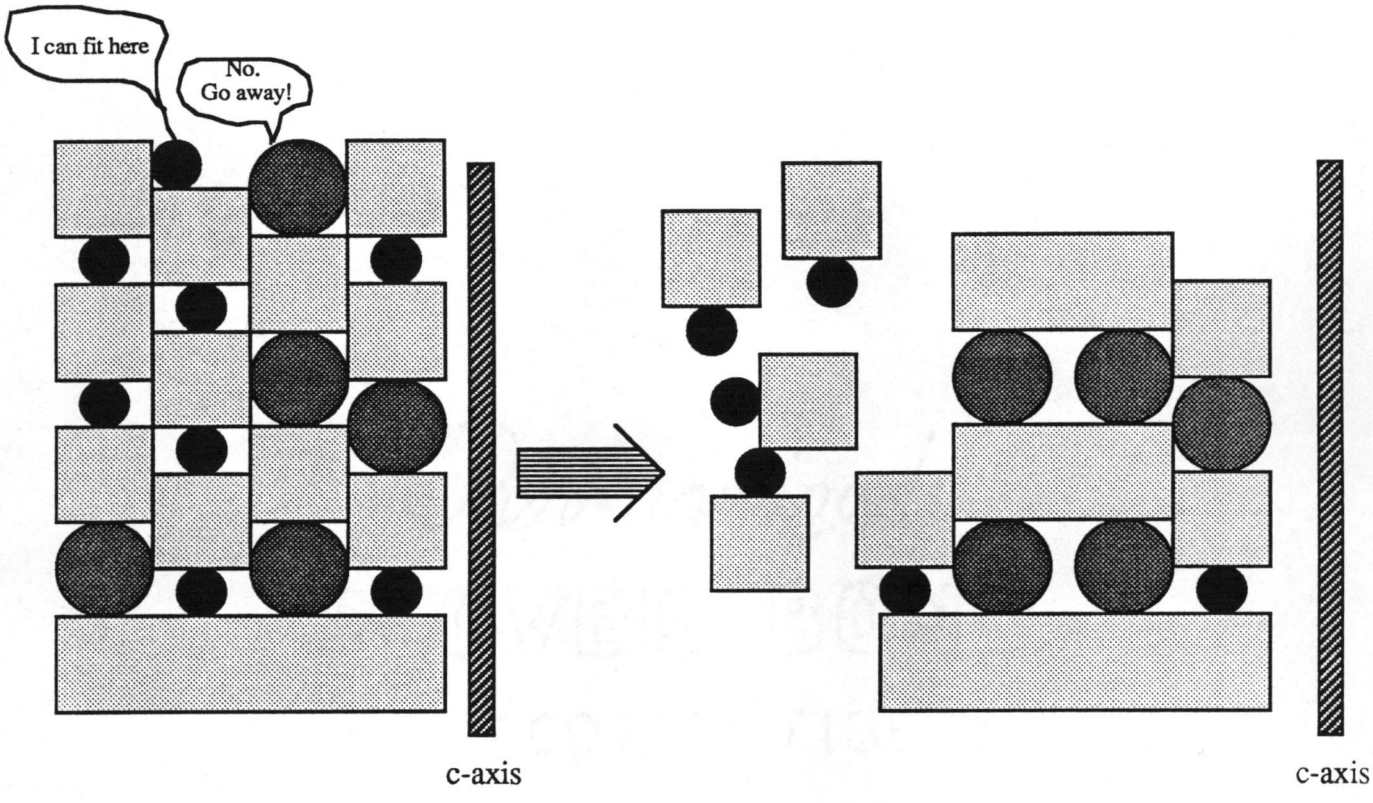

(C)

Figure 1.15

Figure 1.16.

A diagram shows the possible mechanism of dolomite crystal growth.

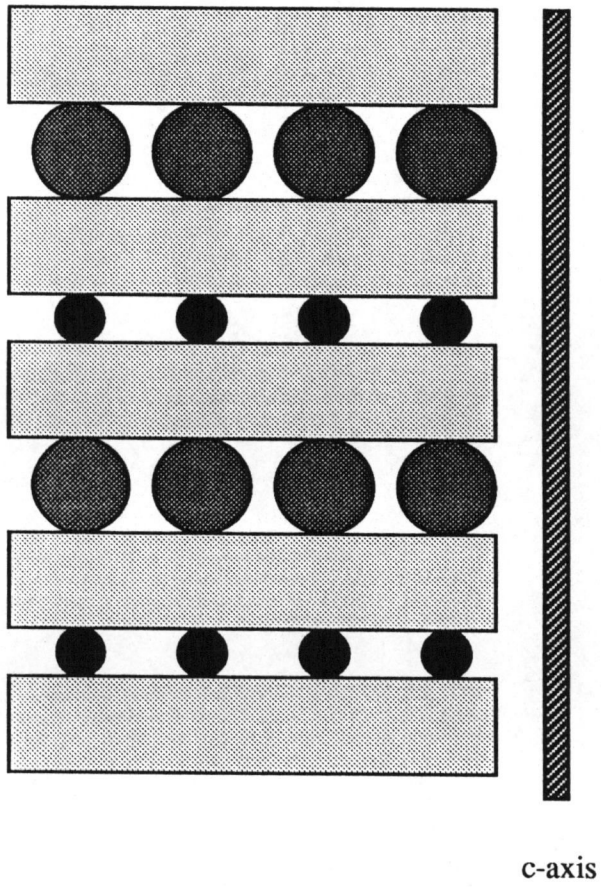

Figure 1.16

(from Pytkowicz, 1969). Wherer $a^{o}CaCO3$ is the activity for planer surface with $r = \infty$, t is the interfacial tension, v is the molar volume, R is the gas constant, T is the absolute temperature and r is the particle size.

The solubility products should increase with decreasing radius according to

$$Kso = \frac{a_{Ca^{2+}} a_{CO3^{2-}}}{a_{CaCO3}} \qquad (1.7)$$

1.5 Summary and Conclusion

It has been shown that the magnesium ions can prevent the inorganic homogeneous precipitation of calcium carbonate from supersaturated seawater to such an extent that the removal of carbonate ions from the ocean is strictly biological, except in special environments when abundant nucleating surfaces are present. Then inorganic precipitation and abiotic cementation can occur. Results suggested that homogeneous inorganic precipitation does not play a significant role in an average marine environment. However, times for the onset of precipitation would be expected in seawater containing recycling calcium carbonate seeds. Thus oolites thrown into suspension in the Bahamas could act as seeds for the precipitation of calcium carbonate.

Rates of the reaction have significant effects on the kinetics of calcium carbonate formation in the presence of magnesium ions in solutions. There is an interaction between these two parameters, and one will be dominant over the other, depending upon its respective concentration and the conditions of the reaction.

Table 1.6

Effect of particle size on the activity of calcite (from Chave and Schmalz, 1966).

Size (cm)	$^{a}CaCO_3$
1	1
10^{-4}	1.02
$2 X10^{-5}$	1.15
10^{-6}	8.92

The mineralogy of inorganic homogeneous precipitation is a result of these two parameters (e.g. Mg^{2+} ion concentration and degree of saturation) at constant temperature and pressure conditions. Pure calcite is favored in Mg-free solution; low-magnesian calcite is favored at magnesium-to-calcium less than 2 and low degree of saturation, pure aragonite is favored at magnesium-to-calcium more than 4, magnesian calcite is favored at high degrees of saturation and vaterite is found to be the least stable phase, and could be a transition phase between aragonite-calcite transformation. These different mineralogies may affect the equilibrium conditions of calcium carbonate, especially on the surface coatings. These surface coatings of the minerals are known to be interface where they are in contact with seawater.

The morphologies of calcium carbonates are also influenced by the concentration of magnesium (and maybe other ions such as SO_4^{2-}) in the solution, and the rate of the reaction. Thermodynamic equilibrium is affected by the morphologies as well as mineralogies of calcium carbonates.

The increase in the solubility of the precipitation products, as a result of mole% $MgCO_3$ increase in calcite, can lead to a rate controlled composition or to a multistate equilibrium. The different morphologies of calcium carbonate, their sizes and their surface edges and corners will have different activities in solution. So both mineralogies and morphologies may control the interaction of carbonate crystals with surrounding solution.

Chapter 2.

DETERMINATION OF THE APPARENT DISSOCIATION CONSTANTS OF CARBONIC ACID IN ARTIFICIAL SEAWATER OF DIFFERENT (Mg^{2+})-TO-(Ca^{2+}) RATIOS AND IONIC STRENGTH OF 0.718 AT 25°C.

2.1 Introduction

Equilibrium constants are important to calculate the concentration of ions that result from the dissociation of weak acids and their salts. There are three choices: thermodynamic constants that are determined in dilute solution, thermodynamic constants defined for a standard state of seawater and apparent constants measured directly in seawater (*Pytkowicz et al 1974*, and *Pytkowicz 1983b)*. Estimation of single ion activity coefficient which is of unknown accuracy, is required to use the thermodynamic constants defined in distilled water. The apparent constants are quasi-stoichiometric constants which relate the hydrogen ion activity to the concentrations of other species involved in the dissociation reaction. They are more preferable over thermodynamic constants defined in seawater because the single ion activities of ions can not be determined from electrode measurements without non-thermodynamic assumptions (*Pytkowicz 1983b*), and because the anionic concentrations are not extrapolated to the infinite dilution of anions of interest in standard seawater (*Pytkowicz et al., 1974*).

The dissociation constants of carbonic acid in seawater do not depend on the pH but they depend on the major ion composition of seawater within the pH range of oceanographic interest *(Pytkowicz et al., 1974)*. The apparent equilibrium constants of carbonic acid (*Lyman, 1956; Mehrbach, 1973; Pytkowicz et al.,1974*) do not require estimations of activity coefficients. They are of practical value as long as they remain constant for the processes of interest, such as photosynthesis, precipitation and dissolution, which have small effects on the major ion composition of seawater.

In sediment reservoirs where there are physico-chemical processes that cause notable changes in the major ion composition such as magnesium, there will be a variation of apparent dissociation constants. These processes include diagenesis of Mg-calcite and

dolomite (*Keltz and Mckenzie, 1982; Kulm et al., 1984*). Consumption of magnesium from interstitial water is caused by dolomitization (*Suess et al., 1987*) and basalt-sediment reaction (*McDuff and Gieskes, 1976*). It is suggested that marine organic matter is a significant sink for magnesium from seawater (*Von Breymann, 1988*).

Therefore, it should be noted that reactions in pore water can affect the composition of the major ions and, generally, the apparent constants used for open ocean water can not be applied (*Ben-Yaakov and Goldhaber, 1973; Pytkowicz et al., 1974; Pytkowicz,1983b*).

The variation of apparent dissociation constants of carbonic acid which depends upon the major ion composition of the solution at constant ionic strength (*Lyman,1956*) is attributed to the formation of ion-pairs and the true complexes (*Kester and Pytkowicz, 1969; Pytkowicz and Hawley, 1974*). Therefore, the purpose of this phase of work was to measure the variation of apparent dissociation constants of carbonic acid in artificial seawater having different (Mg^{2+})-to-(Ca^{2+}) ratios and constant total ionic strength of 0.718M at 25°C. These apparent dissociation constants have been used to calculate the concentrations of carbonic acid species in the following chapters.

2.2 Theory:

The system H_2CO_3-H_2O is defined by the following equations in absence of vapor pressure:

$$H_2CO_3 = H^+ + HCO_3^- \quad ; K_1'' = \frac{(H^+)_T(HCO_3^-)_T}{(H_2CO_3^*)} \qquad (2.1)$$

$$HCO_3^- = H^+ + CO_3^{2-} \quad ; K_2'' = \frac{(H^+)_T(CO_3^{2-})_T}{(HCO_3^-)} \qquad (2.2)$$

$$H_2O = H^+ + OH^- \quad ; KW'' = \frac{(H^+)_T(OH^-)_T}{(H_2O)_T} \qquad (2.3)$$

where ($H_2CO_3^*$) is the sum of (H_2CO_3)+(CO_2) in solution and K_1'' and K_2'' are the first and second stoichiometric dissociation constants of carbonic acid and the subscript T refers to total concentrations.

In this work, the method of *Weyl, (1961)* was modified to determine the values of apparent dissociation constants of carbonic acid (K_1' and K_2') in synthetic seawater, having different (Mg^{2+})-to-(Ca^{2+}) ratios, and an ionic strength of 0.718M at 25°C. The product of the constants $K_1'K_2'$, was determined first following the method developed by *Weyl, (1961)* and used by *Kester and Pytkowicz, (1967); Mehrbach, (1973); Hawley, (1973)* and *Pytkowicz and Hawley, (1974).* Then K_1' was determined from the modified function:

$$F(x) = \frac{(K_1'K_2' - x^2)}{(x^2 + xK_1' + K_1'K_2')} \qquad (2.4)$$

which was introduced by *Weyl (1961),* and also by the method used by *Hawley, (1973)* and *Pytkowicz and Hawley, (1974).* The theory of these methods will be discussed following the introduction and definitions of the equations that are used in this work. The definitions of these equations are:

$$TA = (HCO_3^-)_T + 2(CO_3^{2-})_T + (OH^-)_T - (H^+)_T \qquad (2.5)$$

where TA is the total alkalinity in equivalents per kg of artificial seawater. Because borate is not included in our artificial seawater, and the carbonate alkalinity in equivalents per kg artificial seawater is:

$$CA = TA - (OH^-)_T + (H^+)_T = (HCO_3^-)_T + 2(CO_3^{2-})_T \qquad (2.6)$$

Total carbon dioxide, ΣCO_2, in moles per kg of artificial seawater is defined as:

$$\Sigma CO_2 = (H_2CO_3^*) + (HCO_3^-)_T + (CO_3^{2-})_T \qquad (2.7)$$

The measured pH of these electrolyte solutions is actually defined as :

$$pH = - \log x_H \qquad (2.8)$$

where x_H is akin to the thermodynamic activity of hydrogen, a_H, but differs from it because the liquid junction and asymmetry potentials change with pH electrodes when transferred from dilute buffers to seawater (*Hawley, 1973* ; *Pytkowicz, 1983b*). A further diference, which has a small effect and will be neglected, occurs because an assumption was made about the activity of chloride ions when a pH was assigned to buffer solutions. (*Bates, 1973*). Then:

$$x_H = k' a_H \qquad (2.9)$$

where k' is constant within the reproducibility of pH measurements. The reproducibility is high if the same types glass electrodes are used (*Johnson et al., 1977*).

The theory behind measuring the value of $K_1'K_2'$ originates from the fact, that when the solution of interest is at equilibrium and the increase of (HCO_3^-) does not affect the equilibrium pH, the ratio of CA/ΣCO2 is one, and:

$$\frac{(HCO_3^-)+2(CO_3^{2-})}{(H_2CO_3^*)+(HCO_3^-)+(CO_3^{2-})} = 1 \qquad (2.10)$$

$$\frac{\Sigma CO2(xK_1'+2K_1'K_2')}{\Sigma CO2(x^2+xK_1'+2K_1'K_2')} = 1 \qquad (2.11)$$

Again borate is neglected in equation (2.10). Then

$$x^2 = K_1'K_2 \qquad (2.12)$$

and, in terms of pH,

$$pH = -\log x = 0.5(pK_1'+pK_2') \qquad (2.13)$$

This pH value is defined as pH_e in this phase of work, and is equivalent to point b in Figure 2.1A (appendix 2.1).

At this pH_e, the reference level of the solution is HCO_3^- and H_2O and the proton condition is:

$$(H_2CO_3^*)+(H^+)=(CO_3^{2-}) + (OH^-) \qquad (2.14)$$

(*Stumm and Morgan, 1982*). The titration alkalinity, TA_e, to this reference level is defined as:

$$TA_e=(CO_3^{2-})+(OH^-) - (H_2CO_3^*) - (H^+) \qquad (2.15)$$

and

$$CA_e=(CO_3^{2-})-(H_2CO_3^*)=TA_e-(OH^-)+(H^+) \qquad (2.16)$$

$$CA_e = \frac{\Sigma CO_2(K_1'K_2'-x^2)}{(x^2+xK_1'+2K_1'K_2')} \qquad (2.17)$$

and the function F(x) introduced by *Weyl, (1961)* is

$$F(x) = \frac{CA_e}{\Sigma CO_2} = \frac{(K_1'K_2'-x^2)}{(x^2+xK_1'+K_1'K_2')} = 0 \qquad (2.18)$$

In other words

$$F(x) = \frac{CA}{\Sigma CO2} - 1 \qquad (2.19)$$

so both equations (2.18) and (2.19) show that $F_{(x)} = 0$ at pH_e.

A graphical plot of $x[1+1/F_{(x)}]$ against $[1/F_{(x)} -1]/x$ is straight line. The intercept at $[1/F_{(x)} -1]/x = 0$ gives the value of K_1' and the slope of the line gives the value of $K_1'K_2'$. This method was also successfully used for K_1' and K_2' measurements in natural seawater by *Pytkowicz et al., (1974).*

$F_{(x)}$ was modified in this work to calculate K_1' directly, after measuring $K_1'K_2'$, by the following equation:

$$K_1' = \frac{K_1'K_2' [1/F_{(x)} -1]}{x} - x[1+1/F_{(x)}] \qquad (2.20)$$

K_1' was also determined from the graphical plot of x versus 1/CA, following the approach developed by *Hawley, (1973).* This approach can only be applied to low pH, where one deals only with CO_2(aqueous), H_2CO_3 and HCO_3- species, and CO_3^{2-} is negligible. Since the concentration of CO_3^{2-} is almost zero, one can treat carbonic acid as a monoprotic acid, and the following modification and definitions are applicable:

$$\Sigma CO_2 = (H_2CO_3^*) + (HCO_3^-)_T \qquad (2.21)$$

and

$$TA = (HCO_3^-) + (OH^-) - (H^+) \qquad (2.22)$$

so that the carbonate alkalinity is:

$$CA = TA - (OH^-) + (H^+) = (HCO_3^-) \qquad (2.23)$$

Equation (2.21) and (2.23) yield:

$$(H^+) = \frac{\Sigma CO2\ K_1'}{CA} - K_1' = x \qquad (2.24)$$

(for more details see appendix 2.2). Plotting x versus 1/CA gives a straight line, the intercept at 1/CA=0 is the negative value of K_1', and the slope of the line is $\Sigma CO_2\ K_1'$.

2.3 Experimental Procedure

(Mg^{2+}),(Ca^{2+}) and (H_3BO_4)-free artificial seawater (ASW) was prepared following the formula of *Kester et al., (1966)*. The formula of the ASW is illustrated in appendix 2.3. This ASW with ionic strength of 0.498M was equilibrated with laboratory pCO_2 by bubbling air through the solution for about two days. Bubbling was stopped when the measured pH was at steady-state and did not change by further bubbling. From this ASW and pre-standardized $MgCl_2$ and $CaCl_2$ stock solutions by the Mohr titration *(Blaedel and Meloche, 1957)* five test solutions were prepared to obtain (Mg^{2+})-to-(Ca^{2+}) molar concentration ratios of ; 00-to-00,00-to-.01,.01-to-.01,.03-to-.01 and .05-to-.01, for the determination of the dissociation constants of carbonic acids. These solutions had different ionic strength, so amounts of reagent grade NaCl were added to maintain the ionic strength of 0.718.

A titration cell was constructed from a beaker fitted into a water jacket for carbonic acid equilibrium constants determination. The cell included a pH electrode (Radiometer #K401), a reference electrode (Radiometer #G202c), a cut-off glass syringe that was displaced as the titrant was added, a glass tube with stopcock to serve as a passage for flushing out excess volume, and a hole for a micrometer syringe burette (Gilmont S1200).

Figure 2.1

The Titration Cell.

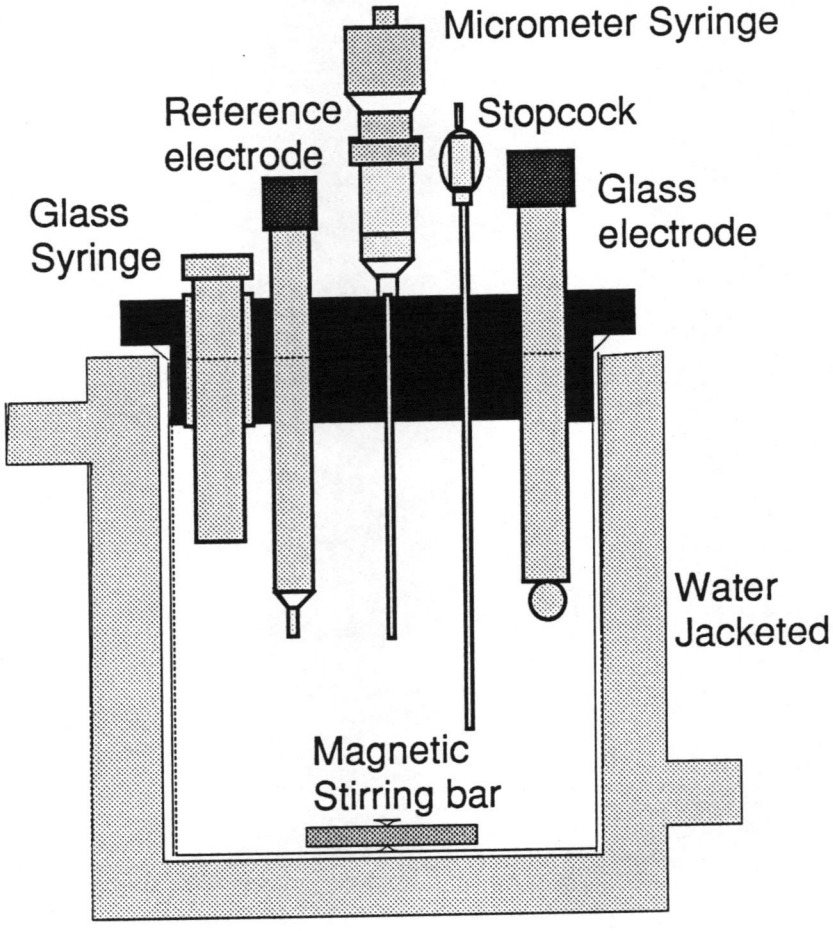
Micrometer Syringe
Reference electrode
Stopcock
Glass electrode
Glass Syringe
Water Jacketed
Magnetic Stirring bar

Figure 2.1

Table 2.1

The practical slope, S, of the electrode pair from five different measurements using NBS pH buffers 4.006 and 7.415 at 25°C.

Measurement #	S	% error
1	58.756	-.667
2	58.786	-.624
3	58.844	-.526
4	58.815	-.575
5	58.874	-.475

The cell is shown in Figure 2.1. It's volume was 82.894+ 0.031ml. The water jacket beaker was connected to a water bath (VWR1140) to maintain the temperature at 25±0.05°C. The electrode pair was connected to a Radiometer-pHmeter (PHM84 Research pHMeter.)

Before proceeding with any titration, the electrodes were standardized in two buffer solutions (NBS buffer 180f having an assigned pH of 4.006 at 25°C and Buffers 186-I-C and 186-II-C having an assigned pH of 7.415 at 25°C.) The slope, S, of the electrode pair expressed in mV/pH was determined. The measured slope was compared with the theoretical one (eg S=59.155mV/pH at 25°C) and if it was more than 99%, the theoretical one was usually used. The practical slope for five different measurement are shown in Table 2.1.

The measured pH, pH_m, was usually calculated from the equation:

$$pH_m = pH_b + \frac{(E_m - E_b)}{S} \qquad (2.25)$$

where pH_b is the pH of the standard buffer solution, E_m and E_b are the electrode potential in the test solution and in the standard buffer solution respectively and S is the slope of the electrode pair.

For the $K_1'K_2'$ determination, the titration cell, described previously, was completely filled with solution to avoid exchange of CO_2. The pH of the test solution was dropped to a pH approximately -0.05 pH unit lower than $0.5(pK_1'+pK_2')$ by addition of a few tenth of ml of 0.1N HCl. Then about 5-8 mg reagent grade $NaHCO_3$ was placed in dry 2.5ml Hamilton syringe and about 0.5ml of CO_2-free distilled water was pulled into the syringe to dissolve the salt. The solution in the syringe was injected slowly into the test

solution through the hole in stopcock while stirring. After stirring for about 2-3 minutes, the electrode potential was recorded for 2-3 minutes, without stirring. Usually about 5-7 additions of $NaHCO_3$ were done to achieve constant pH. The final total alkalinity of the test solution ranged from 3.49 to 5.75 meg./kgASW.

The purity of reagent grade $NaHCO_3$ is represented by the sample's value of $CA/\Sigma CO_2$. Pure bicarbonate has a value of one, while a sample contaminated with carbonate has a value of more than one. Since by definition, the primary standard's $CA/\Sigma CO_2$ is exactly one, its steady-state pH is equal to $0.5(pK_1'+pK_2')$. The steady-state pH is some value greater than $0.5(pK_1'+pK_2')$ due to contamination with carbonate. The values of $K_1'K_2'$, and K_1' in 0.72m NaCl *(Hawley and Pytkowicz, 1973)* were substituted in the following equation:

$$\frac{CA}{\Sigma CO_2} = \frac{(K_1'10^{-pHe}+2K_1'K_2')}{(10^{-2pHe}+K_1'10^{-pHe}+K_1'K_2')} \qquad (2.26)$$

The value of $CA/\Sigma CO_2$ for $NaHCO_3$ used in this work as calculated from eqn (2.26) was 1.0057. This was equivalent to a value of $0.0117\pm.001$pH unit between pH_e and $0.5(pK1'+pK2')$

The same cell was also used for the determination of K_1'. The cell was completely filled with the test solution and the electrodes were allowed to equilibrate until the potential changed by less than 0.1mV/hour. Then the solution was titrated with standard HCl (0.1001N) from a calibrated syringe burette (Gilmont #S1200) The equivalents of titration alkalinity initially present in the titration cell were calculated from the weight of the test solution. The titration alkalinity at each point in the titration was obtained from the equivalents of alkalinity initially present minus the equivalents of HCl added.

x versus 1/CA indicated by equation (2.24) is shown in Figure 2.2. The departure from linearity is tested by least squares from the first three titration points, by using the slope of x versus 1/CA. Then the fourth data point was combined with the first three and the slope was computed. If the variation of the slope from the successive calculation was less than 0.5 percent, the value of the slope, $\Sigma CO2K1'$,obtained was used to calculate K_1'. K_1' was calculated at each point on the titration curve from the expression $K_1'=(\Sigma CO2K_1'/CA-x)$ and K_1' was taken as the mean of the individual values.

From each test solution, at least two aliquots were brought to different pHs with HCl and pre-weighed amounts of sodium bicarbonate were added to the test solution. The change in pH produced was recorded, and the amount of acid or base, z, required to produce the same change in pH was obtained from the titration curve of the same test solution, which had been done before. $1/F_{(x)}$ was calculated from the moles of (HCO_3^-) and (H^+) added per kg ASW, where $F_{(x)}$=moles of (H^+)/moles of (HCO_3^-) (acid-base comparison) *Weyl, (1961)*. The $K_1'K_2'$ values of the test solution obtained from pH steady-state is used to calculate K_1', which was calculated from the expression:

$$K_1' = \frac{K_1'K_2'[1/F(x)-1]}{x} - x[1+1/F(x)] \qquad (2.27)$$

The K_1' value obtained from equation (2.27) was introduced into the expression:

$$\frac{F(x) - K_1'K_2'-x^2}{(x^2+xK_1'+K_1'K_2')} = \Delta \qquad (2.28)$$

and modified to obtain $\Delta \cong 0$.

Figure 2.2

Plot of x versus 1/CA for (Mg^{2+})-to-(Ca^{2+}) concentration ratio equals 0-to-0.

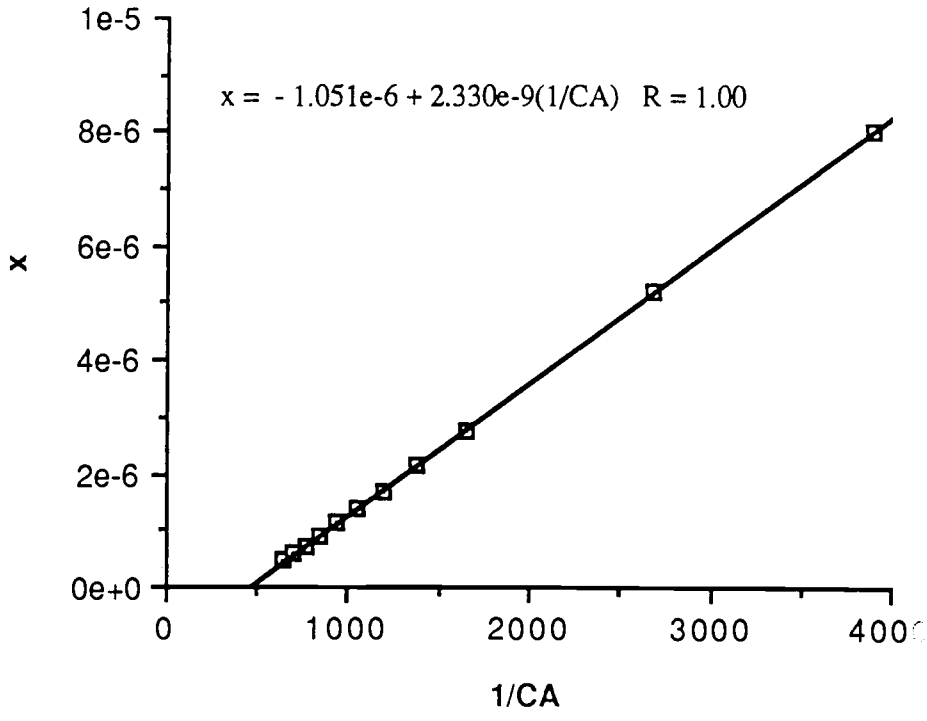
x = - 1.051e-6 + 2.330e-9(1/CA) R = 1.00
1e-5
8e-6
6e-6
4e-6
2e-6
0e+0
x
0
1000
2000
3000
1/CA

Figure 2.2

2.4 Results

The results of the determination of pH_e and $K_1'K_2'$ values are shown in Table 2.2. The values for the first apparent dissociation constants were determined by the modified *Weyl's (1961)* F(x) function (equation 2.20), after taking the mean of $K_1'K_2'$ values in Table 2.2 and also by the graphical plot of x versus 1/CA, are shown in Table 2.3.

2.5 Discussion

The data in Table 2.3 shows that there is a linear increase of K_1' with the increase of (Mg^{2+})-to-(Ca^{2+}) in solution. The results of $K_1'K_2'$ in Table 2.2 indicate a linear relation with curvature. Both K_1' and $K_1'K_2'$ showed a positive function with total cation concentration in solution. This is usually attributed to the formation of ion-pairs (outer sphere interaction due to electrostatic attraction) which decrease activity coefficients and increase solubility products in the same electrolyte solution (*Kester and Pytkowicz, 1969;* and *Pytkowicz and Hawley, 1974*). These features support the concept of ion-pairs formation, such as $CaHCO_3^+$,$CaCO_3^o$,Ca_2CO3^{2+},$MgHCO_3^+$,$MgCO_3^o$ and $Mg_2CO_3^{2+}$ and also support the validity of the ion association model as an adequate formal representation of the behavior of activity coefficients and equilibrium constants *(Pytkowicz and Kester, 1969; Pytkowicz and Hawley, 1974 ; Pytkowicz 1983b).* Ionic interactions affect the charge distribution of solutes and may influence some important properties such as electrical conductivity, osmotic pressure, solubility of minerals and sound attenuation.

Two successful approaches have been used to account for the effect of interaction on activity coefficients; the ionic-pair concept which was introduced to mixed electrolyte solution by *Garrels and Thompson, (1962)* in which association constants are determined and applied to seawater and the specific interaction model of *Bronsted, (1922);*

Table 2.2
Determination of pH_e and $K_1'K'_2$ of carbonic acid in ASW of different (Ca^{2+}) and (Mg^{2+}) concentrations and ionic strength of 0.718 at 25°C.

Solution #	(Ca^{2+}) mmole/kgASW	(Mg^{2+})	pH_e	$K_1'K'_2$ X 10^{+16}
1	0	0	7.808	2.4118
			7.811	2.3845
			7.814	2.3518
			7.810	2.3955
2	9.706	0	7.682	4.3192
			7.686	4.2403
			7.683	4.2993
			7.682	4.3192
3	9.7117	9.6847	7.672	4.5227
			7.668	4.6068
			7.661	4.7577
			7.663	4.6068
4	9.7262	29.5603	7.650	5.0050
			7.647	5.0740
			7.648	5.0513
			7.639	5.2650
5	9.7249	48.9854	7.541	8.2794
			7.548	8.0279
			7.538	8.4062
			7.539	8.3445

Table 2.3

The values of $K_1'K'_2$ of carbonic acid in ASW of various (Ca^{2+}) and (Mg^{2+}) concentrations and ionic strength of 0.718 at 25°C.

Solution #	(Ca2+)	(Mg2+)	$K_1'K'_2(10+16)$	$K_1'(10^{+6})$	
	mmole/kgASW		(*)	(**)	(***)
1	0	0	2.3859±0.027	1.039	1.051
				1.0339	1.041
				1.0533	1.037
2	9.706	0	4.2945±0.036	1.0882	1.075
				1.0686	1.0843
3	9.7117	9.6847	4.6235±0.096	1.1213	1.104
				1.0970	1.103
					1.093
4	9.7262	29.5603	5.0988±0.123	1.1181	1.119
					1.113
5	9.7249	48.9854	8.2645±0.166	1.1689	1.1686
				1.1621	1.157
					1.1443

(*) $K_1'K'_2$ are the means of the values in Table 2.5.
(**) K_1' values were determined from the equations (2.27) and (2.28).
(***) K_1' values were determined from the plot of x versus 1/CA.

Guggenhiem, (1935); and *Pitzer, (1971)* in which interaction terms of an unspecific nature are measured in binary solution and applied to complex solutions such as seawater *(Leyendekkers, 1972; Robinson and Wood, 1972; Whitfield, 1973*). Although, apparent association constants can be measured in simple binary solution and applied to seawater, the resulting total activity coefficients and species distributions are function of medium composition *(Pytkowicz, 1969; Kester, 1969; Pytkowicz and Hawley, 1974; Pytkowicz, 1983).* This is also shown by the increase of K_1' and $K_1'K_2'$ values with metal concentration in electrolyte solution of the same ionic strength shown in Figure 2.3 and 2.4. The apparent curvature in Figure 2.3 may be due to the formation of a triple ion *(Hawley, 1973).*

The total concentrations appeared in equations (2.1),(2.2) and (2.3) are:

$$(HCO_3^-)_T = (HCO_3^-)_F + (CaHCO_3^+) + (MgHCO_3^+) \qquad (2.29)$$

and

$$(CO_3^{2-})_T = (CO_3^{2-})_F + (CaCO_3^o) + (Ca_2CO_3^{2+}) + (MgCO_3^o) + (Mg_2CO_3^{2+}) \qquad (2.30)$$

Pytkowicz and Hawley, (1974) showed that K_1' and K_2' can be expressed by the equations:

$$K_1' = k\,\gamma_{CO2}\,a_W\,K_1^o\{1 + K^*_{NaHCO3}(Na^+)_F + K^*_{MgHCO3}(Mg^{2+})_F + K^*_{CaHCO3}(Ca^{2+})_F\}/(\gamma_{HCO3^-})_F \qquad (2.31)$$

and

Figure 2.3

The measured values of $K_1'K_2'$ of carbonic acid in ASW having different (Mg^{2+}) concentrations and 9.71 mmole(Ca^{2+}) kg^{-1}ASW and total ionic strength of 0.718 at 25°C.

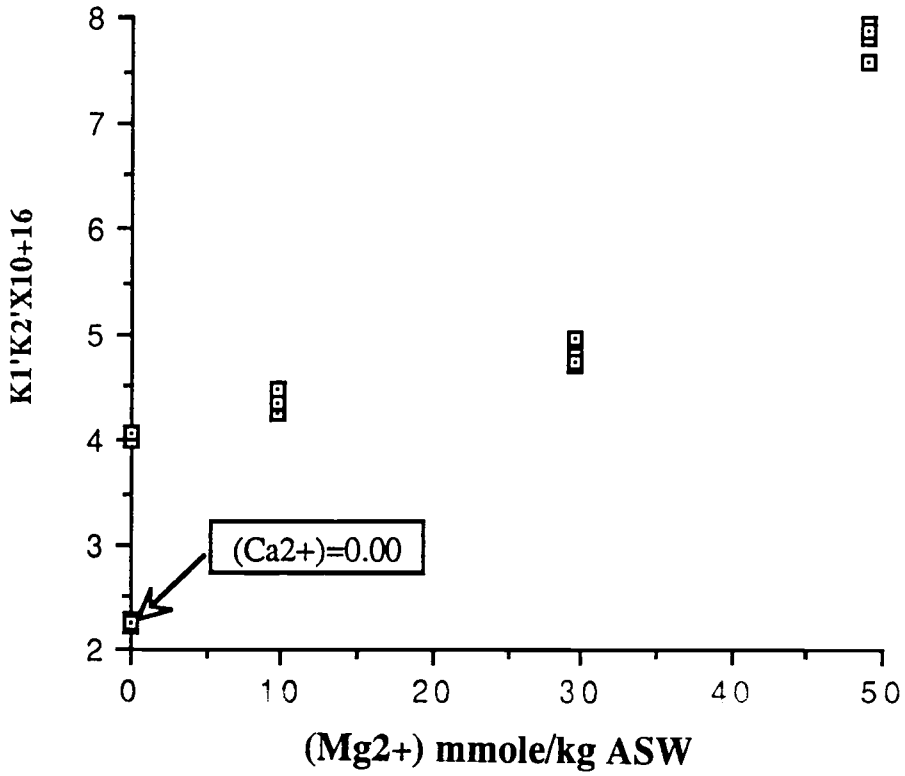

Figure 2.3

Figure 2.4

The measured first dissociation constants, K_1', in ASW having different (Mg^{2+}) concentrations and 9.71 mmole (Ca^{2+})kg^{-1} ASW and total ionic strength of 0.718 at 25°C.

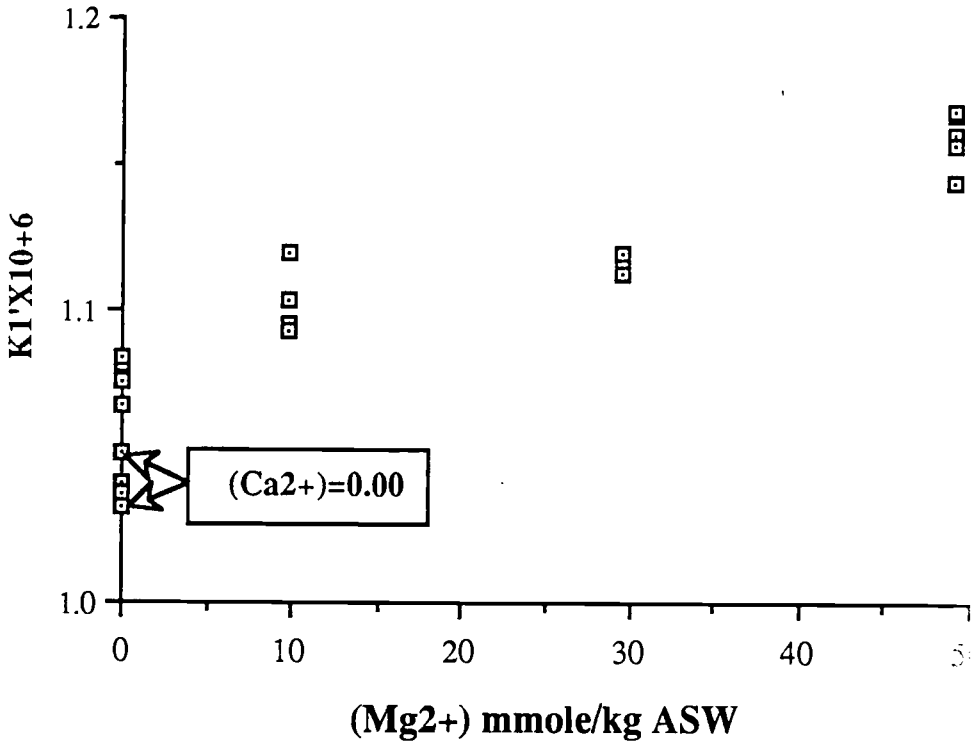

Figure 2.4

$$K_1'K_2' = k^2\,\gamma_{CO2}\,a_W\,K_1^oK_2^o[1+K^*_{NaCO3}(Na^+)_F+K^*_{MgCO3}(Mg^{2+})_F$$
$$+K^*_{CaCO3}(Ca^{2+})_F+K^*_{CaMgCO3}(Ca^{2+})_F(Mg^{2+})_F$$
$$+K^*_{Mg2CO3}(Mg^{2+})_F^2]/(\gamma_{CO3^{2-}})_F \qquad (2.32)$$

where γ_{CO2} is the activity coefficient of CO2, a_W is the activity of water, K_1^o and K_2^o are the thermodynamic dissociation constants of carbonic acid, $(\gamma_i)_F$ is the free activity coefficient of the subscribed species, K^* is the apparent association constants of ion association MA, and the terms in parentheses are the free ion concentrations. It is stated, that the changes in composition at a given ionic strength do not affect f_{CO2}, a_{H2O}, $(\gamma_i)_F$ and K^*_{MA} *(Pytkowicz and Hawley, 1974).* K_1^o and K_2^o depend only on temperature and pressure. Thus, equations (2.31) and (2.32) explain that K_1' and K_2' will remain constant if the free ion concentrations of cations are not altered by any processes. The results of this work (Table 2.2) showed that (Ca^{2+}) had more effect on the dissociation constant than (Mg^{2+}), which suggests that Ca^{2+} associats with bicarbonate and carbonate more strongly than Mg^{2+}. This was illustrated by the higher shift of the first and second ionization fraction α_1 and α_2 of carbonic acid in Figure 2.5, when only (Ca^{2+}) = 9.75mM added to the test solution compared to the shift that produced when (Mg^{2+}) =29.8mM was added in presence of (Ca^{2+}). The shift was increased and became significant when the concentration of (Mg^{2+}) was five times the concentrations of (Ca^{2+}).

The concentrations of HCO_3- and CO_3^{2-} in seawater are very small compared to those of major ions, Thus the change of their concentrations caused by pH change do not alter the extent of ion-pairing and therefore, the free concentrations of Na^+, Ca^{2+}, Mg^{2+} remain realy the same. *Pytkowicz et al., (1974)* showed that the changes in K_1' and K_2' were small (within the experimental uncertainty) for a change in alkalinity from 2.537 to 5.074 megkg^{-1} SW. They also showed that the variation in K_1' with pH at high alkalinity

amount to only 1% even at 16 times normal seawater concentration of HCO_3^- and CO_3^{2-}. Changes of K_2' with pH about 12% at 16 times the normal alkalinity.

The total activity coefficient of bicarbonate and carbonate, $(\gamma HCO_3)_T$ and $(\gamma CO_3)_T$ at different magnesium-to-calcium ratios were calculated following the method of *Pytkowicz, (1975)*:

$$(\gamma HCO_3)_T = \frac{K_1^o}{K_1'} (\gamma CO_2)\, a_W\, k \qquad (2.33)$$

and

$$(\gamma CO_3)_T = \frac{K_1^o K_2^o}{K_1' K_2'} (\gamma CO_2)\, a_W\, k^2 \qquad (2.34)$$

The thermodynamic dissociation constants used here were from *Harned and Davies, (1943)* and from *Haned and Scholes, (1941)*. The activity coefficient of CO2 was obtained from the expression :

$$(\gamma CO_2) = \frac{s_{DW}}{s_{SW}} \qquad (2.35)$$

where ^sDW and ^sSW are the Bunsen Coefficient in distilled water and seawater, determined by *Murry and Riley, (1971)*, and the solutions were treated as seawater with different salinities. The computed activity coefficients of CO_2 of the solutions and the values of θ, the factors which were used to convert the concentrations from $molekg^{-1}SW$

Table 2.4

The salinity, the factor θ, and the activity coefficient of CO_2 for various (Mg^{2+})-to-(Ca^{2+}) concentration ratios in the test solutions of I=0.718 and 25°C.

$(Mg:Ca)_{soln}$	S‰	θ	(γCO_2)
0:0	41.26	0.9587	1.209
0:1	40.64	0.9594	1.205
1:1	39.27	0.9603	1.200
3:1	38.27	0.9617	1.191
5:1	36.72	0.9633	1.182

Table 2.5

Total activity coefficients of bicarbonate and carbonate ions in the test solutions of various (Mg^{2+})-to-(Ca^{2+}) concentration ratios at 25°C and I_T=0.718.

(Mg:Ca)soln	$(\gamma HCO_3)_T$	$(\gamma CO_3)_T$
0:0	0.6005	0.1221
0:1	0.5782	0.0678
1:1	0.5629	0.0624
3:1	0.5512	0.0568
5:1	0.5012	0.0343

into mole/kg H_2O are shown in Table 2.4. The activity of water, a_W, as function of salinity, S‰, in the solutions was determined from the equation of *Robinson, (1954)* by:

$$a_W = 1 - 5.096\,X10^{-4}\,S‰ - 1.31\,X\,10^{-6}\,(S‰)^2 \qquad (2.36)$$

The factor k was estimated from the following equation:

$$K1' = \frac{(H^+)_T(HCO_3^{2-})_T}{(H_2CO_3^*)}\,k\,(\gamma_{H+})_F = K1''\,k\,(\gamma_{H+})_F \qquad (2.37)$$

The value of K_1" was found to be 1.105×10^{-6} at ionic strength of 0.718 from *Harned and Bonner, (1945)* and $(\gamma_{H+})_F$ was 0.866. The average value of k was 1.140 for the test solutions in agreement with k = 1.134 determined by *Hawley, (1973).* The estimated activity coefficients of carbonate system are reported in Table 2.5, which indicate the decrease in total activity coefficients with the increase of the major ions in solutions as a result of the formation of ion pairs in electrolyte solution.

The data in Table 2.2 and 2.3 can be expressed by the following polynomial equations:

$$\log K1 = \beta_{01}+\beta_{11}(Ca^{2+})+\beta_{21}(Ca^{2+}:Mg^{2+}) \qquad (2.38)$$

and

$$\log K1'K2' = \beta_{02}+\beta_{12}(Ca^{2+})+\beta_{22}(Ca^{2+}:Mg^{2+})-\beta_{23}(Ca^{2+}:Mg^{2+})^2 \qquad (2.39)$$

Figure 2.5

The ionization fraction of carbonic acid of different (Mg^{2+})-to-(Ca^{2+}) concentration ratios in ASW versus pH.

Ionization fraction of carbonic acid

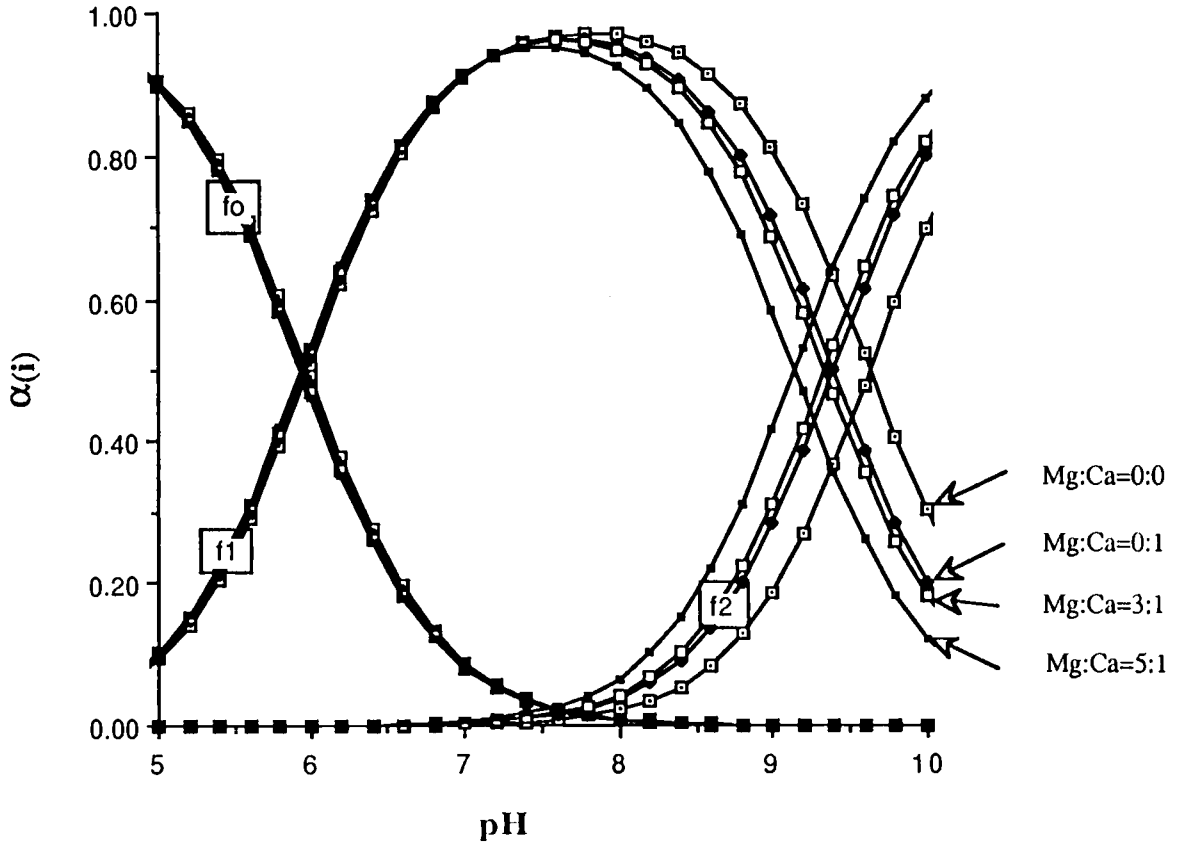

Figure 2.5

where the coefficients are: β_{01}= -5.9818, β_{11}= .0015, β_{21}=0.006, β_{02}= −15.6228, β_{12}=0.0263, β_{22}=− 0.0168, β_{23}= 0.0139, and the concentration of Ca^{2+} is in mmolekg^{-1}ASW.

Chapter 3.

KINETICS OF CALCITE OVERGROWTH PRECIPITATION AS A FUNCTION OF MAGNESIUM CONCENTRATIONS AND DEGREE OF SUPERSATURATION IN ARTIFICIAL SEAWATER.

3.1 Introduction

Precipitation and dissolution reactions of carbonate minerals are the processes that control their composition and behavior. The unique characteristics of carbonates, such as retention of supersaturation, metastablility of solid phases, and slow transformation of one phase to another, are indications of the special importantce of kinetics during the processes of precipitation and dissolution. So, thermodynamics and kinetics are equally important to fully, understand the chemical behavior of carbonate minerals in natural water. While geochemists have made a fairly good progress in developing and applying thermodynamic principles to carbonate system, the kinetics of the reactions remains poorly defined *(Lasaga, 1981; Morse, 1983; Reddy, 1983).* The major methods that have been applied to describe reaction rates includes theoretical and experimental laboratory studies of calcite dissolution and precipitation *(for example, Sjoberg, 1976; Plummer et al., 1978; Reddy et al., 1981),* but the laboratory rate laws are still to be tested in field situations *(Plummer and Back, 1980).* Most of the investigations of reaction kinetics have been focused on calcite and aragonite in simple or mixed electrolyte and in seawater solutions *(for example, Reddy and Nancollas, 1971; Nancollas and Reddy, 1971; Plummer et al ., 1979; Morse and Berner, 1979)* because they are the most common carbonate minerals in sediments and soils. However, the majority of studies have been focused on the dissolution kinetics in the ocean, because of the interest on dissolution processes of calcite and aragonite during particle settling from the surface to the bottom of the water column. Still, the precipitation is also important because there are overgrowth processes that occur in the water column, on foreign surfaces and, most commonly, in sediments.

The first major study of calcite precipitation in simple solutions was done by *Nancollas and Reddy, (1971)* and Reddy and *Nancollas, (1971).* The precipitation rate was interpreted as a second order surface controlled process expressed by:

$$\frac{\partial TCa^{2+}}{\partial t} = -k_n A \left[(Ca^{2+})(CO_3^{2-}) - \frac{K_{sp}}{f_{(2)}^2} \right] \qquad (3.1)$$

where TCa^{2+} is the total concentration, t is the time, and k_n is the rate constant, A is the surface area, and $f_{(2)}$ is the divalent ion activity coefficient. They found that precipitation rate was independent of stirring rate. It was also suggested that the *Plummer et al (1978)*, model could be used for calcite precipitation *(Plummer et al., 1979)*. The observation of the degree of saturation on the rate of the reaction suggested that the standard empirical equations could not be used *(Reddy et al., 1981; House, 1981)*. *House (1981)*, tested the equation of *Davies and Jones (1955)*, *Nanocollas and Reddy (1971)* and the spiral growth mechanism model, he concluded none of them was adequate. The rates of calcite precipitation measured in the field were compared with the rates predicted from laboratory derived studies*(Plummer et al., 1978)* and the agreement in the rates was within a factor of 3 *(Herman and Lorah, 1988)*.

Inskeep and Bloom, (1985) tested, almost, all the rate equations for calcite precipitation and concluded that, the rate equations which were described by *Plummer et al., (1978)* and *Nancollas and Reddy (1971)* were more successful. They also concluded that, the best successful model which described calcite precipitation at high pH (e.g. pH > 8) is the Nancollas and Reddy model.

The purpose of this work was to conduct a laboratory investigation of calcite precipitation rates at different (Mg^{2+})-to-(Ca^{2+}) concentration ratios in artificial seawater in order to test the effect of magnesium on the reaction rates, and on the total order of the

reaction. The equation of the reaction rate, developed by *Nancollas and Reddy, (1971)*, will be used, with slight modification to represent the calcite overgrowth.

3.2 General Principles

The law of mass action at equilibrium between solid and solution is achieved when the dissolution rates, k_d, and the precipitation rates, k_p, are equal and there is no net change in the reaction. This definition for $CaCO_{3(s)}$ solid is represented by:

$$CaCO_{3(s)} \underset{k_b}{\overset{k_d}{\Longleftrightarrow}} Ca^{2+} + CO_3^{2-} \qquad (3.2)$$

and

$$\frac{k_d}{k_p} = K_{eq} = \frac{(Ca^{2+})_{T,e}(CO_3^{2-})_{T,e}}{(CaCO_{3(s)})} \qquad (3.3)$$

where the parenthesis represents the concentration and the subscripts T and e refer to total and equilibrium state respectively. The thermodynamic equilibrium equation is:

$$K_{eq} = \frac{a_{Ca^{2+}}\, a_{CO_3^{2-}}}{a_{CaCO_{3(s)}}} \qquad (3.4)$$

where a_i is the activity of the component i. Usually the activity of pure solid is assigned a value of one. The saturation state, Ω, of the solution is determined from the ratio of the measured activity ionic products to the equilibrium constants by:

$$\Omega = \frac{a_{Ca^{2+}} a_{CO_3^{2-}}}{K^{o}_{eq}} \qquad (3.5)$$

When $\Omega > 1$, the precipitation reaction is favored because the solution is supersaturated with respect to $CaCO_{3(s)}$. The dissolution of $CaCO_{3(s)}$ is favored when $\Omega < 1$.

3.3 Theory of Crystal Growth

3.3.1 Mechanisms of Crystal Overgrowth

Crystal growth occurs by the following mechanisms, either individually or concurrently, *(Stumm and Morgan, 1982; Pytkowicz, 1983b)*:-

a) Formation of a nucleus on a crystal seed, with growth spreading from this nucleus as a monolayer of ion pairs or molecules.

b) Nuclei are formed over the whole surface of the crystal, which lead to successive two-dimensional layer formation. This is known as a roughening.

c) Screw dislocation growth where the nuclei are always present.

The growth of the crystal, however, takes successive steps: transportation of solutes through the crystal-solution interface, adsorption of solute at the crystal surface, and the incorporation of the crystal constituents into the lattice. The dissolution process of the crystal as a back-reaction and as a ripening process, which leads to a larger crystal, are to be considered.

3.3.2 Derivation of the Precipitation Equation

The net precipitation equation was, originally, derived by *Nancollas and Purdie, (1964).* For deposition flux, J_p, or crystal overgrowth:

$$J_p = k_n A (c)_t^n \qquad (3.6)$$

where k_n is the rate constant, C is the ionic concentration and n is the order of the reaction. J_p is regulated by the surface reactions. The dissolution flux J_d, is :-

$$J_d = k' A \qquad (3.7)$$

At saturation state:

$$J_p = J_d \qquad (3.8)$$

and

$$k' A = k_n A (C)_e^n \qquad (3.9)$$

For a supersaturated solution, the following equation is obtained:

$$\frac{-\partial C}{\partial t} = J_p - J_d = k_n A (C)_t^n - k' A \qquad (3.10)$$

substitution of equation (3.9) into equation (3.10) yields:

$$\frac{-\partial C}{\partial t} = k_n A (C)_t^n - k_n A (C)_e^n \qquad (3.11)$$

and

$$\frac{-\partial C}{\partial t} = k_n A [(C)_t^n - (C)_e^n] \qquad (3.12)$$

where $\partial C/\partial t$ is the number of moles that leaves or enters the bulk solution per unit time and is expressed in mole sec^{-1}. It could be expressed as moles $sec^{-1}cm^{-2}$ if equation (3.12) is expressed by:

$$\frac{-\partial C}{A \ \partial t} = J_p - J_d = k_n [(C)_t^n - (C)_e^n] \qquad (3.13)$$

Generally, there are two limiting theories on growth kinetics that have been established. These are the diffusion controlled growth and the interface reaction controlled growth (*Nancollas and Purdie, 1964; Nancollas and Reddy, 1971; Stumm and Morgan, 1982; Pytkowicz, 1983.)* The slowest mechanism is known to be the rate controlling mechanism. If the value of n in equation (3.13) equals one, then the mechanism is known as a diffusion controlled growth and k_n depends upon the diffusion coefficients and the extent of the turbulence in solution. But if n value is more than one, the mechanism is considered to be an interface reaction controlled growth, and the mechanism does not depend upon the turbulence. The growth of the crystal can also be controlled by interfacial processes such as adsorption and dislocation steps as mentioned earlier.

The following reactions are expected during growth or dissolution of $CaCO_{3(s)}$ in simple solutions:

$$CO_{2(g)} \overset{H_2O}{\Longleftrightarrow} CO_{2(l)} \qquad (3.14)$$

$$H_2CO_3 + H_2O \Longleftrightarrow H^+ + HCO_3^- \qquad (3.15)$$

$$HCO_3^- \Longleftrightarrow H^+ + CO_3^{2-} \qquad (3.16)$$

$$H_2O \quad \Longleftrightarrow \quad H^+ + OH^- \qquad (3.17)$$

$$CaCO_{3(s)} \quad \Longleftrightarrow \quad Ca^{2+} + CO_3^{2-} \qquad (3.18)$$

$$Ca^{2+} + HCO_3^- \quad \Longleftrightarrow \quad CaHCO_3^+ \qquad (3.19)$$

$$Ca^{2+} + CO_3^{2-} \quad \Longleftrightarrow \quad CaCO_3^o \qquad (4.20)$$

$$Ca^{2+} + OH^- \quad \Longleftrightarrow \quad CaOH^+ \qquad (3.21)$$

The H^+ ion has an important effect on the growth or the dissolution of $CaCO_{3(s)}$ and its speciation. The presence of excess H^+ in solution will convert $Ca^{2+} + CO_3^{2-}$ into highly soluble Ca^{2+} and H_2CO_3 from equation 3.15. Equations 3.16 and 3.17 represent growth or dissolution depending on the conditions of the processes. According to the above equilibrium and mass balance equations, the pH decreases and pCO_2 increases in the solution during the growth of calcium carbonate. One can trace the rate of growth or the rate of dissolution by following the change in the pH of the solution. This pH-drift method has been used by many investigators *(for example Chave et al., 1962; Land, 1967; Plummer and Mackenzie, 1978; Wollast and Reinh-Derie, 1979; and many others).* In a solution with (Ca^{2+}) and (CO_3^{2-}) concentrations similar to that in natural seawater, the change in Ca^{2+} during growth or dissolution is very small and depends on the degree of saturation, but the change in (H^+) is about 100- times the change of (Ca^{2+}). Therefore, the pH, which influences the carbonate alkalinity, is a sensitive indicator to follow the rate of growth or the rate of dissolution. The following equation :

$$\frac{\partial CO_3}{\partial t} = -k_n A [(Ca^{2+})_t (CO_3^{2-})_t - (Ca^{2+})_e (CO_3^{2-})_e]^n \qquad (3.22)$$

can be used to study the kinetics of $CaCO3_{(s)}$ overgrowth mechanism. Later, equation (3.22) will be modified and expressed in terms of the change of carbonate alkalinity with time as a result of calcite overgrowth.

3.4 Experimental Procedure

3.4.1. Experiment

(Mg^{2+}),(Sr^{2+}) and (H_3BO_4)-free artificial seawater, ASW, was prepared following the procedure of *Kester et al (1967).* The composition of ASW is shown in Table 3.1. This ASW, which had ionic strength of 0.526M was equilibrated with the laboratory pCO_2 for about two days by bubbling air through the solution. The bubbling was stopped when the measured pH was stable and did not change by further bubbling. The concentration of (Ca^{2+}) in this solution was 9.754 mmole/kg ASW. Various amounts of magnesium were added from pre-standardized stock solution, by Mohr titration *(Blaedel and Meloche, 1957)*, to prepare (Mg^{2+})-to-(Ca^{2+}) ratios of; 1, 2 and 5. Different amounts of pre-dried reagent grade NaCl were added to these prepared solutions to maintain the ionic strength of 0.718M. Each solution was kept in a closed bottle and its pH was measured every 24 hours, it only changed by $\pm$0.005pH unit. It was noticed that the pHs of the solutions were decreasing with increasing magnesium concentrations.

A reaction cell was constructed from a glass beaker fitted with a water jacket for the determination of the reaction rates of overgrowth on different surface areas of calcite in ASW of different (Mg^{2+})-to-(Ca^{2+}) concentration ratios and constant ionic strength of 0.718 at 25°C. The cell involved a combination electrode (Radiometer GK2401C), a stopcock for flushing excess solutions, a ground glass syringe piston for displacement of

Table 3.1

The composition of Artificial Seawater prepared according to the formula of *Kester et al., (1967).*

Salt	Molarity
NaCl	0.40173
Na_2SO_4	0.02754
KCl	0.00891
KBr	0.00081
NaF	0.00007
$NaHCO_3$	0.00229
$CaCl_2$[1]	0.00996
Total ion strength	0.52647
Density	1.02160 $g.ml^{-1}$

1 was added from stock solution, which pre-standardized by Mohr Titration *(Blaedel and Meloche 1959).*

Figure 3.1

The Reaction Cell.

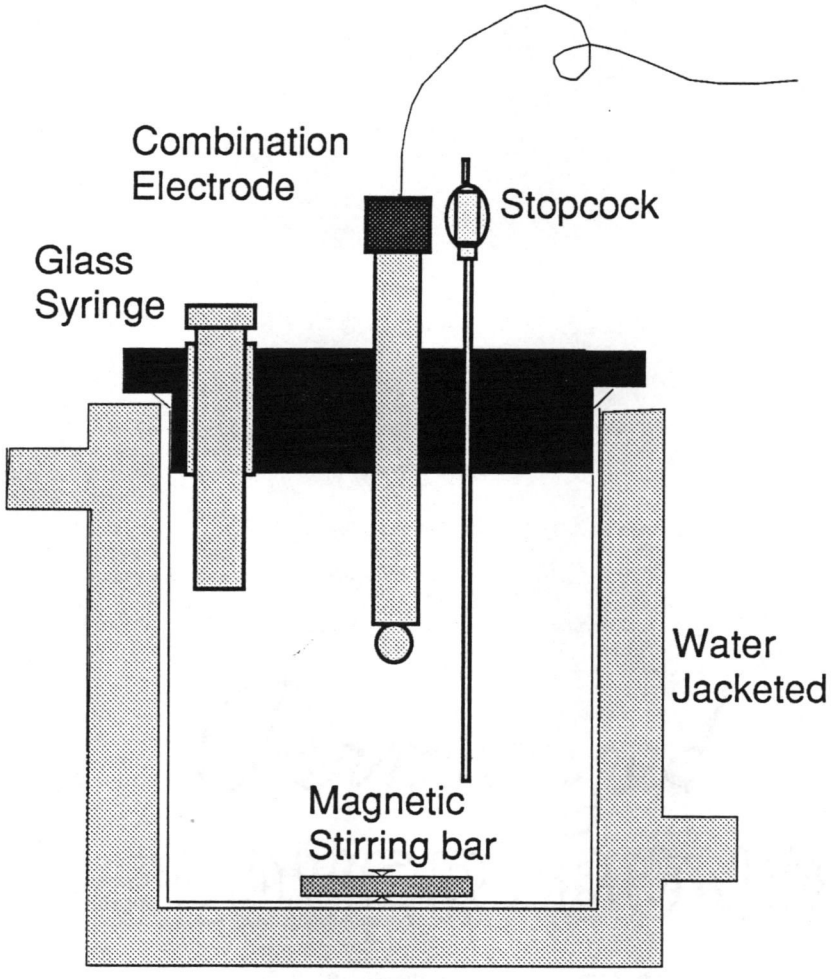
Combination
Electrode
Stopcock
Glass
Syringe
Water
Jacketed
Magnetic
Stirring bar

Figure 3.1

the excess solution and an stirring bar. The closed system reaction cell is shown in Figure 3.1. The volume of the cell was 103.761±0.027ml.

The seeds used this experiment were reagent grade synthetic calcite (J.T. Baker). The synthetic calcite was washed with double deionized distilled water, DDW, three times, filtered and dried at 110-130°C for about four hours, then they were kept in vacuum desiccator after cooling down, before being exposed to ASW. The x-ray diffraction showed that they were pure calcite by $2\theta = 29.4^{o}$. The specific surface area of calcite seeds was estimated from its density and the seed mean volume, which was determined by SEM images. It was estimated that the specific area was 0.589 $m^3\ g^{-1}$. The procedure is discussed in Appendix 3.1.

The combination electrode was calibrated with NBS buffers, 185f (pH=4.006 at 25°C) and 186-I-C and 186-II-C (pH=7.415 at 25°C.) The slope of the electrode was determined following the instruction in the PHM64 Research pHmeter Operating Instructions. Usually the slope was 99.00±0.21%.

Before each experiment, the initial total alkalinity of each test solution was measured using the Gran titration method *(Gran , 1952; Dyrssen and Sillen, 1967, Mehrbach et al., 1973; Pytkowicz, 1983)* and by single-acid addition *(Anderson and Robinson, 1946)* developed by *Culberson et al., (1970)* to a pH of 4.15±0.10. The standard deviation of the total alkalinity determined by both methods was ±5.8 μequivalent kg^{-1}ASW. Also the initial pH was measured for each test solution. The initial total carbon dioxide, $\Sigma CO_{2(i)}$ was calculated from these two known parameters and the values of first and second dissociation constants of carbonic acid which were determined at different magnesium concentration as described in the chapter 2.

The reaction cell was, completely, filled with the test solution and the combination electrode was allowed to equilibrate until the measured pH changed by less than 0.002pH unit per hour at 25°C. Two different degree of saturations were obtained by selecting two pH values. They were pH=8.1 and pH=8.6, and were achieved by adding drops of 0.1N NaOH to the test solution from a syringe of a long needle through the hole in the stopcock while stirring. Then the piston was pushed half-way into the solution to flush some of the excess solution. The pH was recorded every five minutes until three successive reading were the same then the calcite was added. The required weight of synthetic calcite was placed in a 2.5 ml Hamilton syringe with a long needle, then stirring was stopped and through the hole of the stopcock about 1.5 ml of ASW of the test solution was withdrawn into the syringe to form a slurry of calcite, which was then injected slowly into the solution without stirring. This step was done carefully to avoid any bubble trapping in the cell, and it was done at least three times to insure that all the amount of calcite was delivered into the solution and settled to the bottom of the reaction cell. Then the piston was pushed all-the-way down to displace the excess volume of ASW through the stopcock hole. The stopcock was immediately closed to prevent CO_2 exchange and the solution was stirred. The pH was recorded with time until it was at steady-state. The steady-state pH value was assumed when the change in pH was again less than 0.002pH unit per hour.

3.4.2. Calculation

From the initial pH and initial TA of the test solution, the initial total carbon dioxide of each test solution was calculated using the following equation:

$$\Sigma CO_{2(i)} = CA_{(i)} \left(\frac{1}{\alpha_1 + 2\alpha_2} \right)_i = CA_{(i)} \left[\frac{(x)^2 + (x)K_1' + K_1'K_2'}{(x)K_1' + 2K_1'K_2'} \right]_i \qquad (3.23)$$

The values of K_1' and K_2' of different magnesium-to-calcium concentratrion ratios were experimentally determined as described in the chapter 2. Because each test solution was kept in a closed bottle, the total carbon dioxide was, actually, constant before the introduction of calcite. This was also confirmed by the steady state pH measurements of the test solution.

The initial carbonate alkalinity of each experiment at the two pH values was calculated from the initial pH and the initial total carbon dioxide :

$$CA_{(i)} = \Sigma CO_{2(i)} \left[\frac{(x)K_1'+2K_1'K_2'}{(x)^2+(x)K_1'+K_1'K_2'} \right]_i \qquad (3.24)$$

The number of moles of (CO_3^{2-}), Δ, which was involved in $CaCO_{3(s)}$ overgrowth at time t was calculated from :-

$$\Delta = CA_{(i)} \frac{\left\{ \left[\frac{(x)^2+(x)K_1'+K_1'K_2'}{(x)K_1'+2K_1'K_2'} \right]_i - \left[\frac{(x)^2+(x)K_1'+K_1'K_2'}{(x)K_1'+2K_1'K_2'} \right]_t \right\}}{\left\{ \left[\frac{(x)^2+(x)K_1'+K_1'K_2'}{(x)K_1'+2K_1'K_2'} \right]_t - 1 \right\}} \qquad (3.25)$$

or

$$\Delta = \Sigma CO_{2(i)} \frac{\left\{ \left[\frac{(x)K_1'+2K_1'K_2'}{(x)^2+(x)K_1'+K_1'K_2'} \right]_i - \left[\frac{(x)^2+(x)K_1'+K_1'K_2'}{(x)K_1'+2K_1'K_2'} \right]_t \right\}}{\left\{ \left[\frac{(x)^2+(x)K_1'+K_1'K_2'}{(x)K_1'+2K_1'K_2'} \right]_t + 2 \right\}} \qquad (3.26)$$

The concentration of (CO_3^{2-}) at time t, $(CO_3^{2-})_t$, was calculated accordingly:

$$(CO3^{2-})_t = (\Sigma CO_{2(i)} + \Delta) \left[\frac{K_1'K_2'}{(x)^2+(x)K_1'+K_1'K_2'} \right]_t \quad (3.27)$$

It could also be calculated from:

$$(CO_3^{2-})_t = (CA_{(i)} + 2\Delta) \left[\frac{K_2'}{(x)+ 2K_2'} \right]_t \quad (3.28)$$

The rate of the reaction could be expressed, in terms of the driving force between equilibrium and ionic products, by the following equation:

$$\frac{\partial CA}{\partial t} = -2k_n A \left[(Ca^{2+})_t \, (CO_3^{2-})_t - (Ca^{2-})_e \cdot (CO_3^{2+})_e \right]^n \quad (3.29)$$

where $\partial CA/\partial t$ is the change in carbonate alkalinity with time. Since the change in (Ca^{2+}) is very small, which was found to be less than 3% of the total (Ca^{2+}) concentration in solution, while the change in (CO_3^{2-}) was more than 80% of the total (CO_3^{2-}) concentration in solution, hence, the following equation could be used:

$$\frac{\partial CA}{\partial t} = -2k_n A \left[\frac{(CO_3^{2-})_t}{(CO_3^{2-})_e} - 1 \right]^n \quad (3.30)$$

In terms of logarithmic formula equation (3.30) is written as:

$$\log\left[\frac{\partial CA}{\partial t}\right] = \log\left[-2k_n A\right] + n \log\left[\frac{(CO_3^{2-})_t}{(CO_3^{2-})_e} - 1\right] \qquad (3.31)$$

By fitting $\log[-\partial CA/\partial t]$ versus $\log\{[(CO_3^{2-})_t/(CO_3^{2-})_e]-1\}$, one obtains the rate constant of the reaction, k_n, from the intercept and the order of the reaction, n, from the slope.

3.5 Results and Discussion

The effects of (Mg^{2+}) ions and the amount of calcite seeds upon the change of the pH with time as a result of the overgrowth is shown in Figure 3.2. It is obvious that both magnesium and surface area influence the reaction process. Generally, the plots of log ∂CA/∂t versus log (CO3t/CO3e - 1) shows two types of slopes, as is illustrated in Figure 3.3. Each of these values of the slopes is, usually, referred to the total order of the reaction, n. Therefore, two values of n's for each reaction are reported in Table 3.2. The first n, n_1, which is the value of the slope at the beginning of the reaction, and second n_2, is the value of the second slope. The results showed that the n_1 value was larger than 4, and became larger with the increase of (Mg^{2+}) concentration in solution. The n_2 showed a value of about 2 for Mg-free solution and a value of about 3 in presence of Mg ions in solution. The n_1 value was observed to decrease with the increase of the surface area of calcite seeds as is shown in Figure 3.4. The effect of the availability of surface area was also demonstrated by the fast decrease in pH as a function of the increase of the amount of seed in solution in Figure 3.2. In Mg-free artificial seawater and high initial pH, e.g. high ionic products, it was noticed that n_1 disappeared and only n_2 was obtained.

The reactions showed two types of orders (>1) which indicated surface-controlled mechanisms of two types. This phenomenon was also observed by *Nancollas and Reddy, (1971)*. They suggested that the first one might be caused by the surface and

Figure 3.2

Change of pH as a result of calcite overgrowth, (a) about 0.5 g of calcite was added per kg of ASW, (b) about 5.0 g of calcite per kg ASW was added.

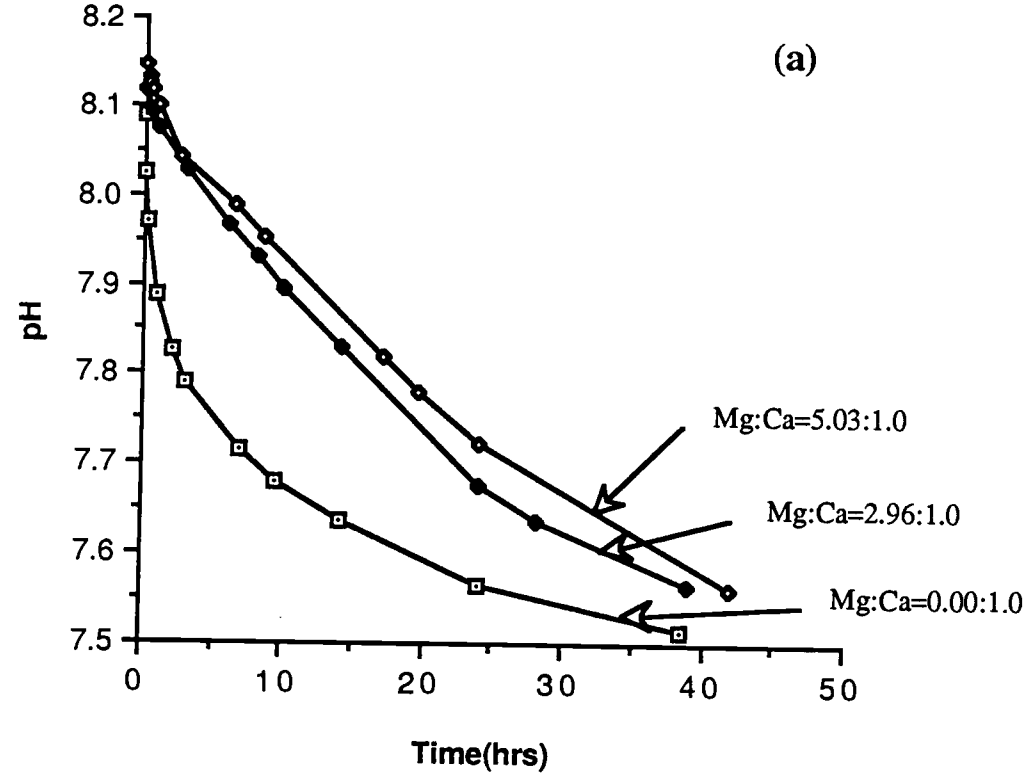
(a)
8.2
8.1
8.0
7.9
7.8
7.7
7.6
7.5
pH
0
10
20
30
40
50
Time(hrs)
Mg:Ca=5.03:1.0
Mg:Ca=2.96:1.0
Mg:Ca=0.00:1.0

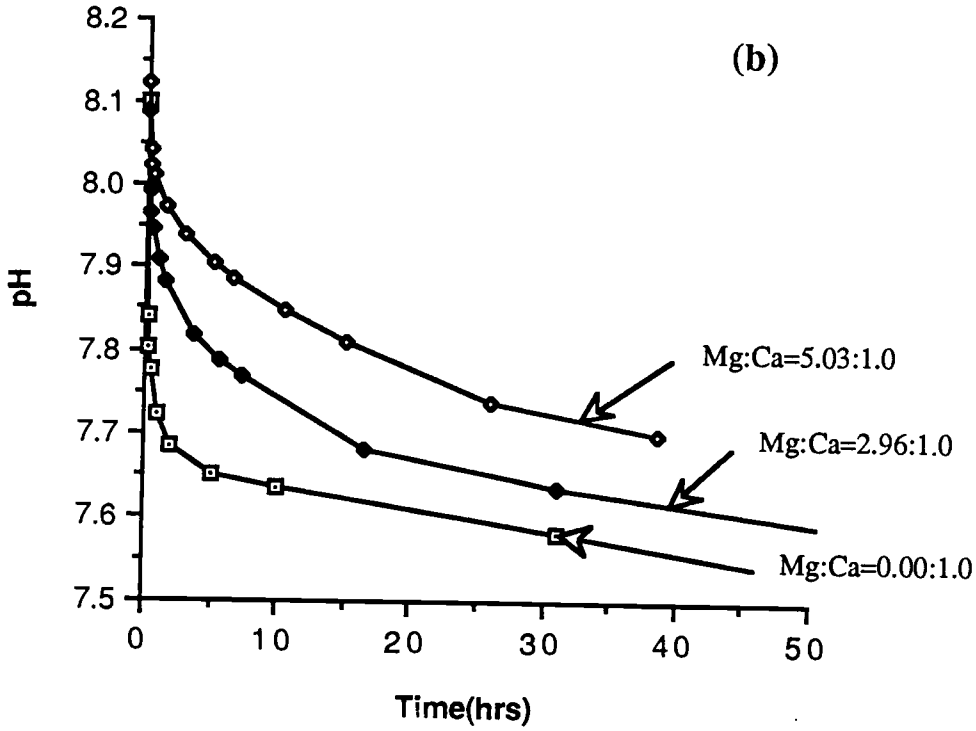
(b)
8.2
8.1
8.0
7.9
7.8
7.7
7.6
7.5
pH
0
10
20
30
40
50
Time(hrs)
Mg:Ca=5.03:1.0
Mg:Ca=2.96:1.0
Mg:Ca=0.00:1.0

Figure 3.2

Figure 3.3

Log $\partial CA/\partial t$ versus log [(CO32-)t/(CO32-)e - 1] for various Mg:Ca concentration ratios in ASW of pH_i = 8.1, (a) about 0.5 g of calcite was added per kg ASW; (b) 1.0 g of calcite was added per kg ASW.

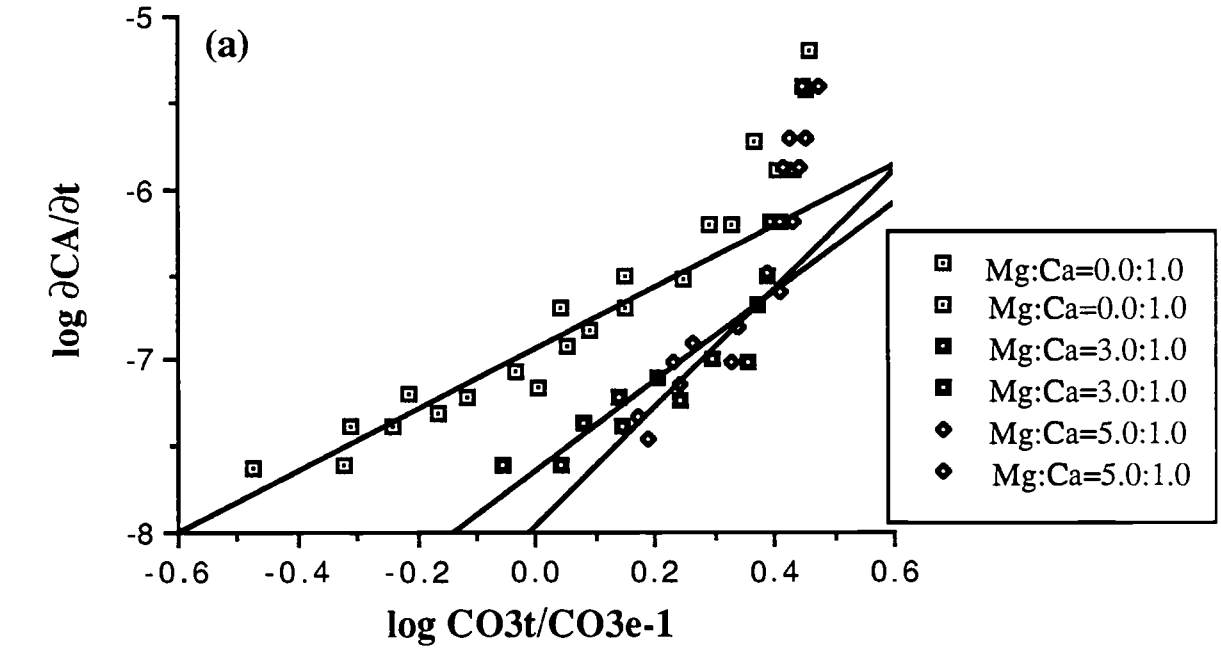
(a)
log ∂CA/∂t
-5
-6
-7
-8
-0.6
-0.4
-0.2
0.0
0.2
0.4
0.6
log CO3t/CO3e-1
Mg:Ca=0.0:1.0
Mg:Ca=0.0:1.0
Mg:Ca=3.0:1.0
Mg:Ca=3.0:1.0
Mg:Ca=5.0:1.0
Mg:Ca=5.0:1.0

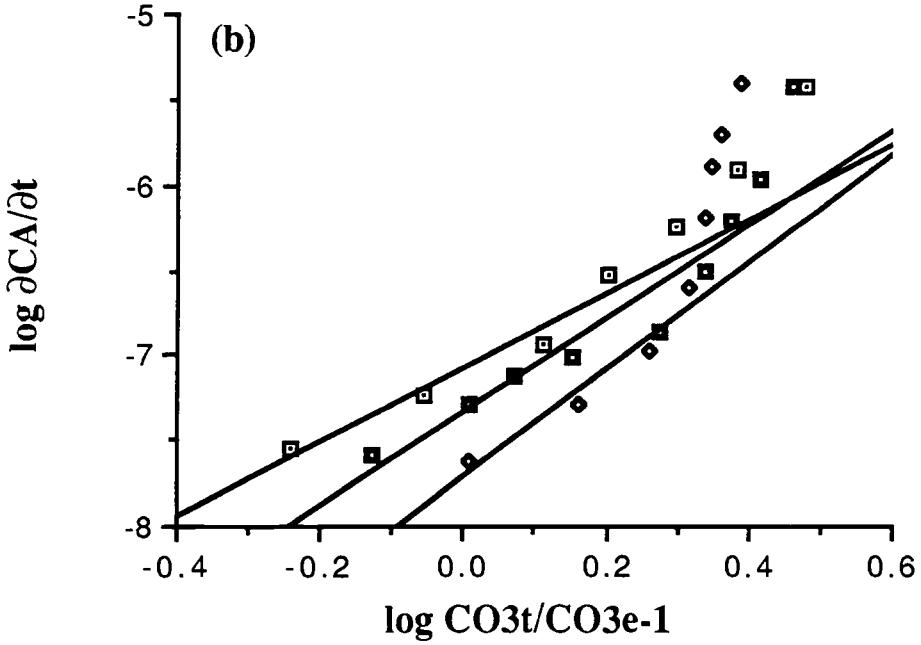
(b)
log ∂CA/∂t
-5
-6
-7
-8
-0.4
-0.2
0.0
0.2
0.4
0.6
log CO3t/CO3e-1

Figure 3.3

Table 3.2

The results of log ∂CA/∂t versus log (CO3t/CO3e - 1) fitting of calcite overgrowth in ASW with various Mg-to-Ca concentration ratios at 25°C and total ionic strength of 0.718.

(Mg2+):(Ca2+) = 0.0:1.0					
Expt #	g calcite / kg ASW	Ω(initial)	- log kn	n	R
SC62	0.500	3.92	7.70	5.95	1.00
			6.58	1.83	0.98
SC64	0.499	3.90	8.04	6.13	0.98
			6.78	1.84	0.99
SC66	0.496	10.58	6.58	1.70	1.00
SC68	0.546	9.91	6.65	1.64	0.99
SC70	0.998	4.06	7.70	4.60	1.00
			7.14	2.17	0.98
SC72	0.998	4.01	7.33	3.91	0.97
			6.53	2.19	0.99
SC74	1.388	10.86	6.87	2.34	0.99
SC75	0.997	11.16	6.41	1.93	0.99
SC76	5.000	3.52	6.42	4.21	0.95
			6.72	2.27	0.99
SC77	5.005	3.44	6.27	3.05	0.98
			6.45	2.10	0.99
SC78	5.012	10.39	6.70	1.95	1.00
SC79	5.003	10.73	6.66	2.32	1.00

Table 3.2 continued

(Mg2+):(Ca2+) = 2.96:1.0

Expt #	g calcite / kg ASW	Ω(initial)	- log kn	n	R
SC80	0.499	3.86	11.77	16.73	1.00
			7.54	2.67	0.95
SC81	0.502	3.89	9.27	8.18	0.95
			7.34	2.67	0.93
SC82	0.499	10.65	9.13	4.60	0.99
			7.85	2.92	0.99
SC83	0.558	10.60	8.42	6.76	0.98
			7.72	2.45	0.96
SC84	1.001	3.68	8.42	6.76	0.98
			7.35	3.20	0.96
SC85	1.007	4.11	9.07	7.53	0.98
			7.41	2.75	0.96
SC86	1.003	11.31	9.63	4.39	0.98
			7.85	2.31	0.98
SC87	1.002	9.40	9.10	3.40	0.95
			7.94	2.49	0.98
SC88	5.005	3.37	7.37	3.41	0.99
			7.29	2.72	0.98
SC89	5.001	3.53	7.50	3.40	0.98
			7.42	2.82	1.00
SC90	5.000	10.15	7.78	1.86	0.98
SC91	5.002	10.01	7.68	1.76	0.99

Table 3.2 continued

(Mg2+):(Ca2+) = 4.99:1.0

Expt #	g calcite / kg ASW	Ω(initial)	- log kn	n	R
SC92	0.499	3.91	13.44	18.51	0.99
			7.66	3.51	0.97
SC93	0.500	4.04	14.46	19.75	0.99
			7.86	3.54	0.97
SC95	0.573	8.70	12.87	9.24	0.99
			8.10	2.29	0.99
SC94	1.003	4.06	11.35	12.47	0.98
			7.81	2.80	0.97
SC97	1.003	3.58	11.84	16.59	0.98
			7.78	3.15	0.97
SC98	1.004	8.70	11.08	6.44	0.97
			8.18	2.38	0.99
SC99	0.968	8.64	11.31	7.97	1.00
			8.16	2.81	0.99
SC02	5.002	3.76	8.54	5.66	0.97
			8.02	2.47	1.00
SC03	5.002	3.77	8.92	7.35	0.95
			8.11	2.97	0.99
SC100	5.001	9.07	7.97	1.87	0.99

the bulk nucleation. A general agreement suggests that the crystal growth proceeds by incorporation of neutral molecules, as discussed in section 3.3.1, at kinks in a growth step on crystal surface *(Laitinen and Harris, 1977)*. Ions of opposite charge must combine stoichiomtrically at certain stage in the process to obtain an electrical neutrality in the crystal lattice. *Doremus, (1958)* suggested two ways of ion grouping on surface of the crystals: (a) formation of salt "molecule" which then diffuse to growth steps; (b) alternate incorporation of oppositely charged ions directly from adsorbed layer at a kink in growth step.

Probably, the reason for the large initial values of n_2 were caused by the formation of hydrated, non-neutral amorphous form of calcium and or magnesium (i.e. in presence of magnesium) carbonate (or bicarbonate) as a monolayer on the surface of the crystals, then gradually, transformed to a neutral molecule of unhydrated calcium and or magnesium carbonate, which is involved in the formation of crystal overgrowth. This was suggested from the disappearance of n_1 at high ionic products. This disappearance of n_1, at high pH was probably due to the presence of sufficient CO_3^{2-} species that could form $CaCO_3^o$ ion-pairs on the surface of the crystal because the stability constant of $CaCO_3^o$ is larger than the stability constant of $CaHCO_3^+$ *(Hawley, 1973)*. At low pH the concentration of HCO_3^- species was much higher than the concentrations of CO_3^{2-}, which led to the formation of more $CaHCO_3^+$ than $CaCO_3^o$. Apparently, the (Mg^{2+}) ion in solution, is involved in the reaction as the hydrated form depending upon its concentration in solution. This was shown by the increase of n_1, as well as n_2 with magnesium concentration.

Once the monolayer transformed into a neutrally charged interface between the bulk solution and the crystal surface, it regulated the crystal overgrowth. At this stage n_2 represented the real overgrowth reaction. Accordingly, by taking the overgrowth

Figure 3.4

The values of ns as a function of the initial pHi and the amount of calcite added in solutions of: (a) Mg-free ASW, (b) Mg:Ca = 3 and (c) Mg:Ca = 5.

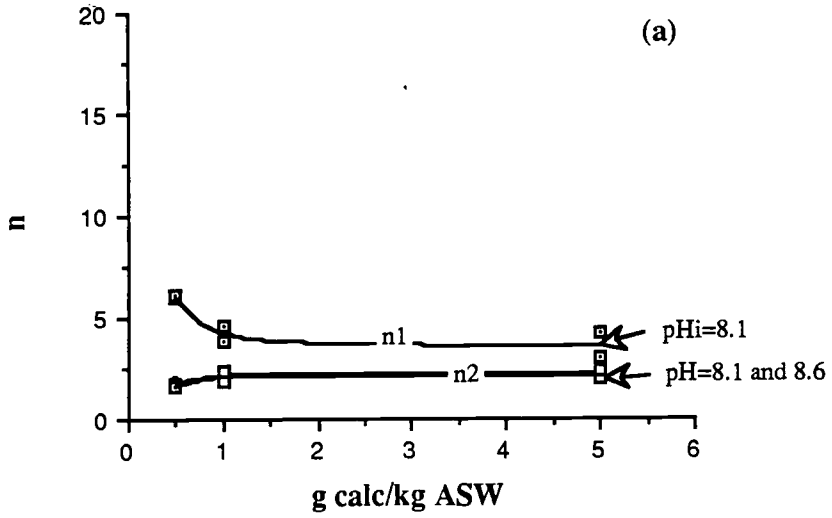
(a)
n
g calc/kg ASW
n1
n2
pHi=8.1
pH=8.1 and 8.6

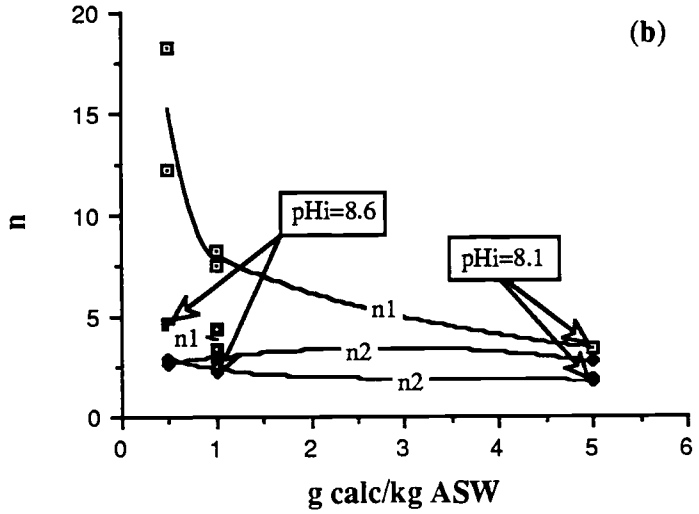
(b)
n
g calc/kg ASW
pHi=8.6
pHi=8.1
n1
n2

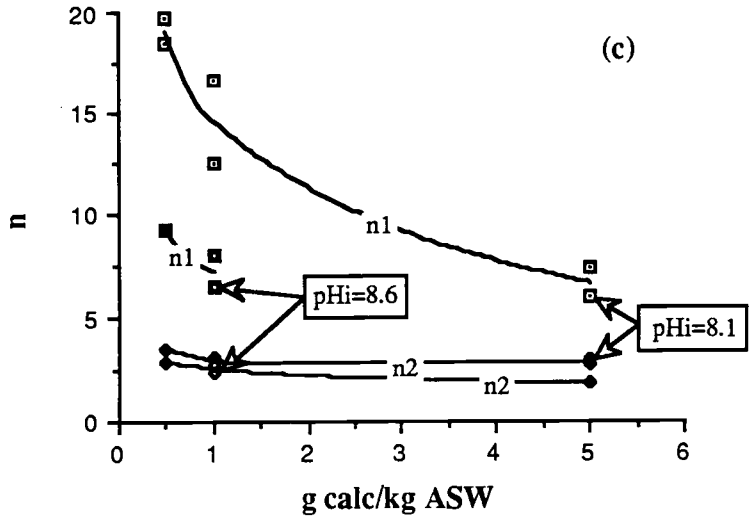
(c)
n
g calc/kg ASW
n1
pHi=8.6
pHi=8.1
n2

Figure 3.4

reactions at supersaturation of natural seawater, it is concluded that the order of the overgrowth reaction $n_2 = 2.07 \pm 0.17$ for Mg-free artificial seawater; $n_2 = 2.81 \pm 0.18$ for $(Mg^{2+}):(Ca^{2+}) = 2.96$ and $n_2 = 3.07 \pm 0.38$ for $(Mg^{2+}):(Ca^{2+}) = 5.03$. Interestingly, at high degree of supersaturtion and large surface area the total order of the reaction approached a second order in presence of magnesium ions in solution.

The presence of magnesium ions in solution affected the reaction rate as shown in Figure 3.5. The rate of the reaction was slowed down by a factor of 14 by going from a Mg-free artificial seawater to a magnesium concentration that is found in natural seawater.

3.6 Conclusion

Generally, the mechanism is a surface-controlled reaction. The total order of the reaction is a second order in Mg-free artificial seawater. In the presence of magnesium ions the order of the reaction is approximately third order reaction. The degree of saturation as well as the surface area are found to affect the order of the reaction. The reaction order tends to approach a second order at high degree of supersaturation and large surface area of calcite.

The overgrowth reaction rates of calcite decrease dramatically with the increase of magnesium ions in solutions, which confirms the involvement of magnesium ions in the overgrowth reaction in the form of magnesian calcite.

Figure 3.5.

The rate constants of calcite overgrowth as a function of magnesium-to-calcium concentration ratios in artificial seawater similar to natural seawater.

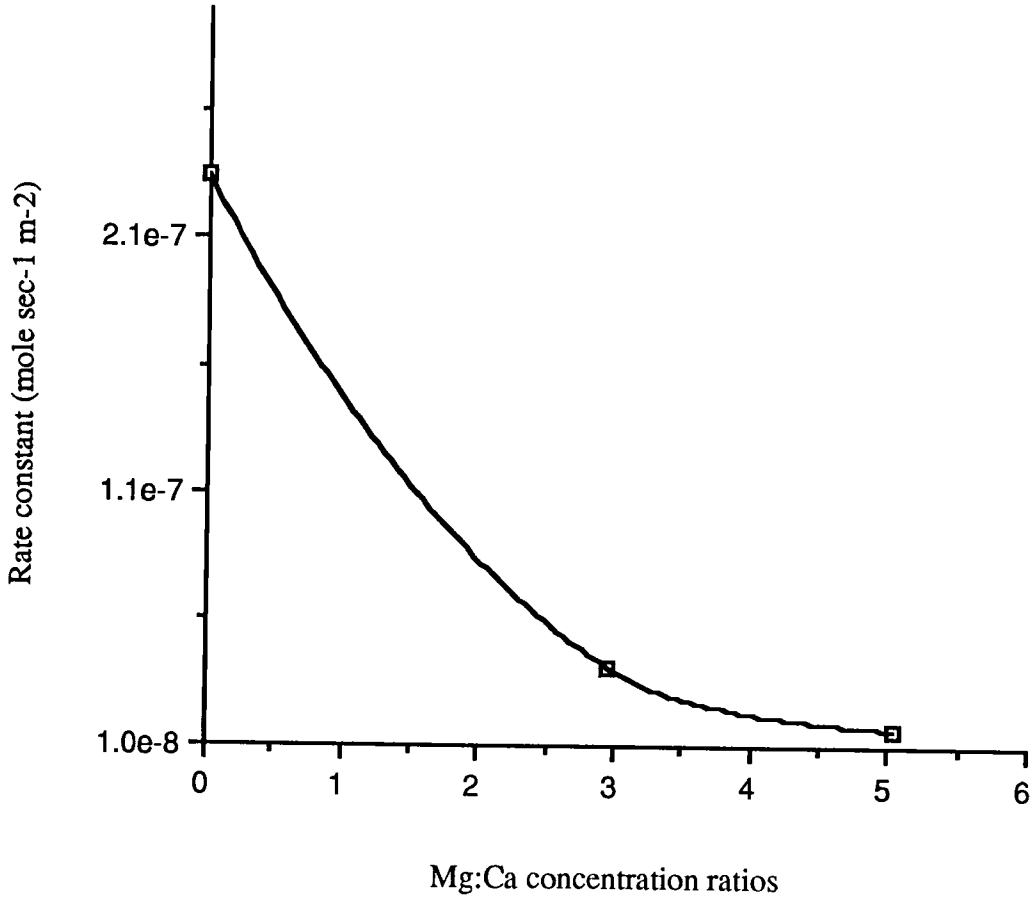
Rate constant (mole sec-1 m-2)
2.1e-7
1.1e-7
1.0e-8
0
1
2
3
4
5
6
Mg:Ca concentration ratios

Figure 3.5

Chapter 4.

THE SOLUBILITY OF CALCITE IN ARTIFICIAL SEAWATER AS A FUNCTION OF MAGNESIUM CONCENTRATIONS, IONIC PRODUCTS AND SOLID-TO-SOLUTION RATIOS: STATE OF THERMODYNAMIC EQUILIBRIUM.

4.1. Introduction

The degree of saturation of seawater or natural waters with respect to calcite is important for the prediction of the precipitation and the dissolution of $CaCO_{3(s)}$. It is also important because the degree of saturation is used as a parameter in the general equation for the rate of the growth and dissolution of minerals. Some natural waters such as springs, ground water, marine surface seawater and pore waters were reported to be supersaturated with respect to calcite. *(Weyl 1961, Cloud 1962a, Schmalz and Chave 1963, MacIntyre and Platford 1964, Barnes 1965, Berner 1966a; Plath et al 1982; Mucci and Morse, 1984b and many others).* Surprisingly, the availability of fine-grained size $CaCO_{3(s)}$ does not change the growth of cementation fabric *(Bathurst 1964 and 1975).* Additionally there are preserved skeletal aragonites from Tertiary and Mesozoic rocks *(Hall and Kennedy 1967).*

The retention of supersaturation of natural water and the very slow diagenetic transformation of sediments led many investigators to study the influence of organic and inorganic additives upon the chemical and physical behavior of calcite *(Pytkowicz, 1965; Jackson and Bischoff, 1971; Suess, 1970,1973).* The presence of metastable calcite phases indicates that, either a lack of equilibrium *(Krauskopf 1967)* or a compositional (multistate) thermodynamic equilibrium exists with respect to solid carbonate coating phase *(Wollast and Reinhard-Derie 1977; Pytkowicz and Cole, 1979; Pytkowicz, 1983b)* occur.

Different Mg-calcite minerals have different solubilities in solution and it was shown that their solubility increases with the increase of the Mg fraction in calcite *(Chave et al 1962).* It is known that the solubility of magnesian calcite overgrowth increases with the content of magnesium in solid solution *(Berner 1975, Thorstenson and Plummer 1977, Morse et al 1979, Schoonmacker 1981 and Koch and Disteche 1984; Walter and Morse, 1985; Pigott and Land,1986).* The values of apparent solubility products of calcite in seawater of 34.8 ‰ salinity were reported to be between $4.24X10^{-7}$ to $5.94X10^{-7}$

mole^2/kg^{2}SW (*Cloud 1962b, Moller and Parkh 1975, MackIntyre 1965, Plath et al 1980, and Morse et al 1980; Mucci and Morse, 1984b).* It is believed that the surface area of the mineral that is exposed to the solution plays an essential role on the equilibrium conditions *(Wollast and Reinhard-Derie, 1977; Wollast and Pytkowicz,1978; Pytkowicz and Cole, 1979; Mackenzie et al., 1982; Pytkowicz 1983b).*

The equilibrium states between calcium-magnesium carbonate mineral and aqueous solution at a given temperature and pressure are still ambiguous. It was shown that the stationary states of calcium carbonate in the presence of Mg^{2+} in solution are reaction-rate and kinetically controlled *(Weyl 1961;1966; Berner, 1978).* To explain the equilibrium state of calcite an stoichiometric saturation model was developed for a non-variable solid phase *(Thorstenson and Plummer, 1977).* They showed that magnesian calcite with < 5 mole% $MgCO_3$ is controlled by thermodynamic equilibrium and the occurrence of other compositions is a kinetic control. It has also been suggested *(Wollast and Reihard-Derie 1977; Pytkowicz and Cole, 1979; Pytkowicz, 1983)* that there is no single thermodynamic phase that is a stable one in the presence of solid solution.

The increase of magnesium to calcium concentration ratios in solution is believed to increase the mole% $MgCO_3$ in calcite (formation of magnesian calcite), the less stable than pure calcite *(Chave et al 1962; Plummer and Mackenzie, 1974; Berner, 1975; Moller and Parekh 1975, Moller and Rajagoplan, 1976, Wollast et al 1980).* It was also stated that the magnesian calcite is governed by the activity products $(^aCa^{2+})(^aCO3^{2+})$ rather than the Mg^{2+}:Ca^{2+} in aqueous phase *(Macknezie and Pigott 1982).*

The purpose of this work was to reassess in detail the effects of various magnesium concentrations, different surface areas of calcite in artificial seawater of two different degree of supersaturations with respect to calcite constant ionic strength of .718 at 25^{o}C upon the apparent solubility products of calcite. The ion association model was used in conjunction

with the mole fraction of $CaCO_{3(s)}$ in the calcite overgrowths to predict the activity coefficients of calcite and magnesite in the test solution.

4.2. Theory

In a closed system and in the presence of only CO_2 and $CaCO_{3(s)}$ as independent components in solution, the following reactions are involved:

$$H_2CO_3^* \quad \Longleftrightarrow \quad H^+ + HCO_3^- \qquad (4.1)$$

$$HCO_3^- \quad \Longleftrightarrow \quad H^+ + CO_3^{2-} \qquad (4.2)$$

or

$$CO_2 + H_2O + CO_3^{2-} \quad \Longleftrightarrow \quad 2HCO_3^- \qquad (4.2a)$$

$$H_2O \quad \Longleftrightarrow \quad H^+ + OH^- \qquad (4.3)$$

and

$$CaCO_{3(s)} \quad \Longleftrightarrow \quad Ca^{2+} + CO_3^{2-} \qquad (4.4)$$

where $H_2CO_3^*$ represents the sum of the species $H_2CO_3 + CO_{2(aq)}$.
The apparent solubility product of calcite, ${}^{(Ca)}K_{sp}'$, is defined as:

$${}^{(Ca)}K'_{sp} = (Ca^{2+})_{T,e}\,(CO_3^{2-})_{T,e} \qquad (4.5)$$

where the subscripts T,e refer to the total concentration of that species at equilibrium and the parenthesis represents the molalities.

4.2.1 Thermodynamic Equilibrium of Magnesian Calcite

The chemical potentials in the aqueous solution and in the solid phase must be the same at equilibrium. The following relationships are fulfilled in the case of magnesian calcite *(Wollast and Reihard-Derie, 1977; Pytkowicz, 1983b)*:

$$CaCO_{3(s)} \quad \Longleftrightarrow \quad Ca^{2+} + CO_3^{2-}; \qquad {}^{(Ca)}K_{so} = \frac{a_{Ca^{2+}} a_{CO_3^{2-}}}{a_{CaCO_{3(s)}}} \qquad (4.6)$$

and

$$MgCO_{3(s)} \quad \Longleftrightarrow \quad Mg^{2+} + CO_3^{2-}; \qquad {}^{(Mg)}K_{so} = \frac{a_{Mg^{2+}} a_{CO_3^{2-}}}{a_{MgCO_{3(s)}}} \qquad (4.7)$$

where ${}^{(Ca)}K_{so}$ and ${}^{(Mg)}K_{so}$ are the thermodynamic dissolution equilibrium constants for pure calcite and pure magnesite and ${}^{a}CaCO_{3(s)}$ and ${}^{a}MgCO_{3(s)}$ are their activities respectively, which can be expressed by:

$$a_{CaCO_{3(s)}} = \lambda_{CaCO_{3(s)}} x_{CaCO_{3(s)}} \qquad (4.8)$$

$$a_{MgCO3(s)} = \lambda_{MgCO3(s)}\, x_{MgCO3(s)} \qquad (4.9)$$

where $\lambda CaCO3_{(s)}$ and $\lambda MgCO3_{(s)}$ are the activity coefficients of the solid and $^{x}CaCO3_{(s)}$ and $^{x}MgCO3_{(s)}$ are the mole fractions.

If x is the mole fraction of $MgCO3_{(s)}$ in magnesian calcite, then (1-x) is the mole fraction of $CaCO3_{(s)}$ in the solid. I shall follow the approach of *Wollast and Reihard-Derie, (1977)*, developed for the dissolution of Mg-calcite, but with elaboration for precipitation as discussed by *Pytkowicz, (1983b)*. Generally, in the case of congruent precipitation in absence of initial magnesian calcite solid, the reaction is described by:

$$xMg^{2+} + (1-x)Ca^{2+} + CO_3^{2-} \Longleftrightarrow Mg_xCa_{(1-x)}CO3 \qquad (4.10)$$

The above equation is a mass balance equation, which can be represented by the conservation of mass as:

$$D_i = M + D \qquad (4.11)$$

where D_i and D are respectively, the number of moles of CaCO3 and MgCO3 in the initial solution that are available for the formation of magnesian calcite M, and the number of moles that remains in solution after magnesian calcite precipitation. Usually, the molal fractions of dissolved compounds are used to represent the behavior of magnesian calcite, and in this case:

$$y = \frac{(Mg^{2+})}{(Mg^{2+}) + (Ca^{2+})} \qquad (4.12)$$

$$(1-y) = \frac{(Ca^{2+})}{(Mg^{2+}) + (Ca^{2+})} \qquad (4.12)$$

Actually, the conservation of mass of magnesium is:

$$y_i D_i = xM + yD \qquad (4.14)$$

where y_i and y are the mole fractions of magnesium ion in the initial and the final solution, as described by equations (4.12) and (4.13). Through the manipulation of equation (4.11) and equation (4.14):

$$y = \frac{y_i D_i}{D} - \frac{x(D_i - D)}{D} \qquad (4.15)$$

Usually $D_i > D$.

The equilibrium relationship of equation (4.6) and equation (4.7) may be combined as:

$$\left(\frac{y}{1-y}\right) = \left(\frac{x}{1-x}\right)\left(\frac{\gamma Ca^{2+}}{\gamma Mg^{2+}}\right)\left(\frac{\lambda MgCO_{3(s)}}{\lambda CaCO_{3(s)}}\right)\left(\frac{{}^{(Mg)}K_{so}}{{}^{(Ca)}K_{so}}\right) \qquad (4.16)$$

where γ represents the activity coefficient in aqueous solution. A graphical diagram of y versus x is shown in Figure 4.1. If pure calcite seeds are used in a solution of a y_i mole fraction of magnesium, their surface magnesium content will increase because magnesian calcite coatings are formed. Therefore, the vector that corresponds to equation (4.15) faces downward as x increases during the process as illustrated in Figure 4.1. It should be noted that D decreases in solution during precipitation and the vector AC is not really a straight line, because the slope -(Di - D)/D and the intercept Di/D decreases as shown in Figure 4.1. (the opposite happens in a dissolution process).

When $CaCO_{3(s)}$ and $MgCO_{3(s)}$ form parts of a solution :

$${}^{(Ca)}K_{so} = \frac{(\gamma_{\pm}CaCO_3)^2\ {}^{(Ca)}K_{sp}}{\lambda CaCO_{3(s)}\ x CaCO_{3(s)}} \qquad (4.17)$$

and

$${}^{(Mg)}K_{so} = \frac{(\gamma_{\pm}MgCO_3)^2\ {}^{(Mg)}K_{sp}}{\lambda MgCO_{3(s)}\ x MgCO_{3(s)}} \qquad (4.18)$$

Figure 4.1

Graphical representation for the final composition of the solid and aqueous of precipitation reaction (adapted from Wollast and Reinhard-Derie, 1977).

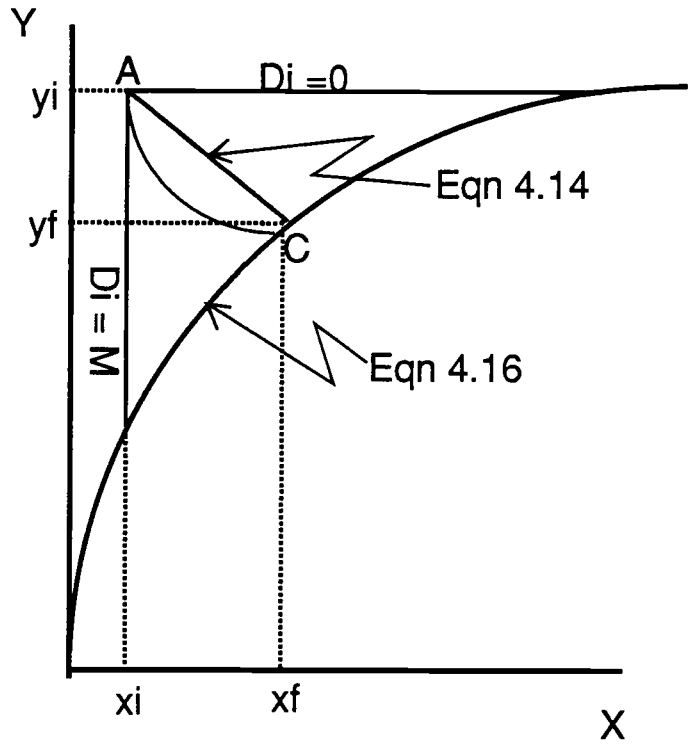

Figure 4.1

The mean activity coefficients of calcite, ($\gamma\pm CaCO_3$), and magnesite, ($\gamma\pm MgCO_3$), have to be estimated. The stoichiometric solubility of calcite, $^{(Ca)}K_{so}$, and of magnesite, $^{(Mg)}K_{so}$, can be measured. Because the composition of solid surface is not well known, x is difficult to be determined, unless it is compositionally homogenized, and only if the bulk value of x is assumed to be correct, then λ can be estimated.

4.2.2. Phase Rule and Degree of Freedom

The theoretical explanation for the equilibrium between a solid solution mineral and an aqueous phase can be approached by the application of the phase rule. According to the phase rule:

$$f = c - p + 2 \qquad (4.19)$$

where f is the number of degrees of freedom of a system when the concentration units in aqueous phase are mole fractions (x), c is the number of independent components, and p is the number of phases. Because the concentration units in aqueous phase are expressed in molar (M) or molal (m), an additional quantity, which is the total number of moles, is required to convert x into M or m. *(see Pytkowicz 1983a p192)*. Therefore, in terms of molalities :

$$f_m = f + 1 \qquad (4.20)$$

and

$$c_m = f_m - 2 \qquad (4.21)$$

where the term c_m is the number of compositional variables that may be specified.

For the system $CaCO_3$-$MgCO_3$-CO_2-H_2O with two solids, one liquid and one vapor pressure phases;

$$f = 4 - 4 + 2 = 2$$

$$f_m = 2 + 1 = 3$$

$$c_m = 3 - 2 = 1$$

If there is no vapor pressure phase, because the container of the solids and the solution is stoppered then:

$$f = 4 - 3 + 2 = 3$$

$$f_m = 3 + 1 = 4$$

$$c_m = 4 - 2 = 2$$

so extra quantity beyond the $\Sigma CO_2 + \Sigma H_2O$ must be specified.

If $Mg_xCa_{1-x}CO_3$ is the only solid as a solid solution in the presence of vapor pressure, the system is fixed if P,T, pH and x of the solid are specified. But in the absence of vapor pressure an additional degree of freedom must be specified such as CA or ΣCO_2. This shows that for each solid solution of a given composition y, there is only one equilibrium aqueous solution. This can be illustrated by x_{f1}, y_{f2} and x_{f1},y_{f2} in Figure 4.2. y_i is the initial supersaturated solution in which the initial amount of magnesian calcite precipitates towards equilibrium while y_{f1} and y_{f2} are the aqueous solutions in equilibrium with solids x_{f1} and x_{f2}.

4.2.3. The Long Hand Notations

For the system with four phases, vapor pressure, aqueous solution and two solids, the following equations are defined, if assuming that pH_20 and the activities coefficients are known:

$$P = pCO_2 + pH_2O \qquad (4.22)$$

$$(CO_2) = {}^{s}CO_2\, pCO_2 \qquad (4.23)$$

$$(H_2O) = k_{H2O}\, pH_2O \qquad (4.24)$$

$$(H_2CO_3) = K''_h\, (H_2O)(CO_2) \qquad (4.25)$$

$$(HCO_3^-) = \frac{K''_1\, (H_2CO_3)}{(H^+)} \qquad (4.26)$$

$$(CO_3^{2-}) = \frac{K''_2\, (HCO_3^-)}{(H^+)} \qquad (4.27)$$

$$(OH^-) = \frac{K''_w\, (H_2O)}{(H^+)} \qquad (4.28)$$

The charge balance is:

$$(H^+)+2(Ca^{2+})+2(Mg^{2+}) = (HCO_3^-)+2(CO_3^{2-})+(OH^-) \qquad (5.39)$$

The mass balances are:

$$\Sigma H_2O+\Sigma CO_2 = (H_2O)+(H^+)+(OH^-)+(CO_2)+(H_2CO_3)+(HCO_3^-)+(CO_3^{2-}) \qquad (5.30)$$

Figure 4.2

Triangular diagram for precipitation. It shows more than one possible equilibrium condition. (Multistate hypothesis).

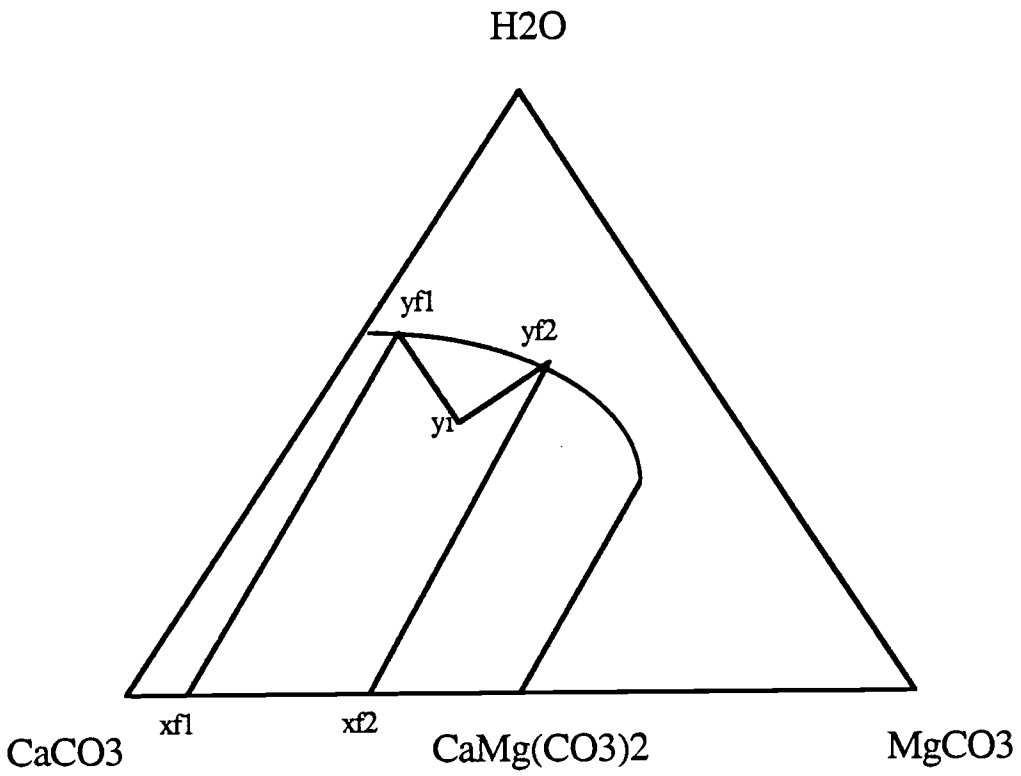

Figure 4.2

The charge balance is:

$$(H^+)+2(Ca^{2+})+2(Mg^{2+}) = (HCO_3^-)+2(CO_3^{2-})+(OH^-) \qquad (5.39)$$

The mass balances are:

$$\Sigma H_2O+\Sigma CO_2 = (H_2O)+(H^+)+(OH^-)+(CO_2)+(H_2CO_3)+(HCO_3^-)+(CO_3^{2-}) \qquad (5.30)$$

$$(Ca2+)_T = \frac{{}^{(Ca)}K_{sp}}{(CO32-)_T} \qquad (4.31)$$

and

$$(Mg2+)_T = \frac{{}^{(Mg)}K_{sp}}{(CO32-)_T} \qquad (4.32)$$

Therefore, there are 11 equations in 12 unknowns and the phase rule shows that there is an additional variable to be specified. If the vapor pressure is absent the first three equations (eg 4.22, 4.23 and 4.24) are neglected because pCO_2 and pH_2O are lost in the system. Then there are only eight equations in ten unknowns. Therefore, two compositional variable beside T, P should be specified (e.g. pH and CA or ΣCO_2 or ΣCO_2 and CA).

4.3. Experimental Procedure

4.3.1 Experiment

The experimental procedure was the same as described in chapter 3. After reaching the steady-state equilibrium the solution was filtered through a 0.45 μm Millipore filter papers. The unwashed seeds were collected, dried and stored for calcium and magnesium contents determinations. Atomic adsorption analysis was used to determine the final (Ca^{2+}) concentrations. The concentration of calcium at equilibrium of each solution was determined by diluting the solution to obtain a calcium concentration of about 1.0 ppm. The original test solution was used as an standard, from which two dilutions with calcium concentrations of 1.25 ppm and 0.9 ppm were prepared. Excess KCl (about 1000 ppm) was added to each solution as an ionizing suppressant to avoid the ionization of excess NaCl which may affect the (Ca^{2+}) and (Mg^{2+}) determinations. The concentration of (Mg^{2+}) at equilibrium was calculated by difference between the amount of the total (Mg + Ca) precipitated and the measured (Ca^{2+}) by A. A. analysis accordingly:

$$(Mg^{2+})_f = (Mg^{2+})_i + \{\Delta - [(Ca^{2+})_i - (Ca^{2+})_f]\} \qquad (4.33)$$

Usually, about 10mg of the seeds was dissolved by adding drops of 0.5N HCl and diluted to obtain about 1.0ppm Ca and another to obtain about 0.5ppm Mg to determine the calcium and magnesium content of overgrowth by AA's method. This was done by assuming that the magnesium content was compositionally, homogeneous in the overgrowth coatings. The residual (Na^{+}) concentration on calcite was also determined by AA's analysis to calculate the residual (Mg^{2+}) and (Ca^{2+}) from the concentration ratios of these major ions to (Na^{+}) in the original solution.

4.3.2 Calculation

The total CO_2,ΣCO_2, in mole/kgASW and the total alkalinity, TA, in equivalent/kgASW are defined by equations (2.21) and (2.22). Carbonate alkalinity,CA, in equivalent/kgASW is defined by equation (2.23). In terms of ionization fraction α_i, *(Butler, 1964; Snoeyink and Jenkins, 1980; Stumm and Morgan, 1982)*:

$$CA = \Sigma CO_2 (\alpha_1 + 2\alpha_2) \qquad (4.24)$$

where α_i is defined in chapter 2, represents the fraction of ith species of carbonic acid at a certain pH.

Since the precipitation or the dissolution of $CaCO_{3(s)}$ affects both the total carbon dioxide and the carbonate alkalinity, as describe in chapter 3, there will be a change in the ΣCO_2/CA ratio in solution. The following equation is obtained:

$$\Delta = CAi\left\{\frac{\left[\frac{1}{(\alpha_1 + 2\alpha_2)_i} - \frac{1}{(\alpha_1 + 2\alpha_2)_f}\right]}{2\left[\frac{1}{(\alpha_1 + 2\alpha_2)_f}\right] - 1}\right\} \qquad (4.35)$$

which is identical to equation (3.25), where the subscripts i and f refer to initial and final respectively and Δ is the number of moles of CO_3^{2-} species that is involved in the

formation or the dissolution of $CaCO_{3(s)}$ from the initial concentration i to the final concentration f.

The concentration of $(CO_3^{2-})_f$ at equilibrium can be calculated by the following equation:

$$(CO_3^{2-})_f = (\Sigma CO_{2i} + \Delta)(\alpha_2)_f \qquad (4.36)$$

It can also be calculated from:

$$(CO3^{2-})_f = (CA_i + 2\Delta)\left[\frac{K_2'}{(x)+2K_2'}\right]_f = Y \qquad (4.37)$$

The apparent solubility products is :

$$^{(Ca)}K_{sp} = (Ca^{2+})_f [Y] \qquad (4.38)$$

and

$$^{(Mg)}K_{sp} = (Mg^{2+})_f [Y] \qquad (4.39)$$

4.4. Results and Discussion

The results of the effects of magnesium-to-calcium concentration and the solid-to-solution ratios in ASW of two different degree of saturation and ionic strength of 0.718M at 25°C upon the apparent solubility products of calcite and magnesite are shown in Table 4.1. The apparent solubility products in ASW for a degree of supersaturation similar to natural seawater (IP = 9-20E-7 $mole^2/kg^2ASW$ which is equivalent to the degree of saturation (Ω = 3-4) versus magnesium concentrations are illustrated in Figure 4.3a, and in ASW for a high degree of supersaturation (IP = 28-50 $mole^2/kg^2ASW$ which is equivalent to the degree of saturation Ω=8.6-8.7) in Figure 4.3b.

Generally, the results in Table 4.1 show that there is an increase in the values of the apparent solubility products with an increase of magnesium concentration in solution. This trend is illustrated in Figures 4.3a and 4.3b. The increasing trend with higher magnesium concentration becomes more significant by increasing the degree of saturation in solution; in other words, the apparent solubility products increased significantly with magnesium concentration in solution at a higher degree of supersaturation as shown in Figure 4.3b. The increase in the degree of supersaturation had no significant change on apparent solubility products in the absence of magnesium in solution. This confirms that there is an effect of magnesium on the calcite solubility products. The increase in the surface area of calcite in solutions of low degree of saturation very slightly affected the values of apparent solubility products in the presence of magnesium in solution. But in a solution of high degree of supersaturation, the surface area of calcite showed a noticeable influence on the apparent solubility products. The small surface area showed a high values of apparent solubility products at a certain magnesium concentration and this values decrease with thesw increase of calcite surface area in solution of the same magnesium concentration.

Table 4.1

The apparent solubility products of calcite and magnesite as a function of Mg:Ca concentration ratios in ASW of two different degree of supersaturations and constant total ionic strength of 0.718 at 25°C.

$(Mg:Ca)_{soln} = 0:1$

Expt #	gcalcite / kg ASW	pH_i	pH_f	CA_i meq/kgASW (10^{+3})	$(Ca)_f$ mole/kgASW (10^{+3})	$(Mg)_f$	$^{(Ca)}K_{sp}$ (mole/kgASW)^2 (10^{+7})	$^{(Mg)}K_{sp}$
SC62	0.500	8.087	7.516	2.2935	9.6375	0.0	2.5314	0
SC64	0.492	8.096	7.527	2.2959	9.6372	"	2.5968	"
SC66	0.496	8.602	7.611	2.5062	9.4552	"	2.8071	"
SC68	0.492	8.585	7.619	2.4959	9.4552	"	2.8806	"
SC70	0.997	8.103	7.517	2.2979	9.6334	"	2.5314	"
SC72	0.997	8.099	7.513	2.2967	9.6338	"	2.5083	"
SC73	0.914	8.120	7.521	2.3024	9.6297	"	2.5495	"
SC74	1.388	8.612	7.608	2.5124	9.4370	"	2.7760	"
SC75	0.997	8.582	7.616	2.5031	9.4419	"	2.6217	"
SC76	5.000	8.080	7.554	2.2917	9.6464	"	2.7803	"
SC77	5.004	8.099	7.582	2.2967	9.6466	"	2.9676	"
SC76	5.012	8.614	7.630	2.5136	9.4391	"	2.9253	"
SC77	5.003	8.613	7.614	2.5130	9.4373	"	2.8154	"

Table 4.1. continued

$(Mg:Ca)_{soln} = 2.96:1$

Expt #	gcalcite / kg ASW	pH_i	pH_f	CA_i meq/kgASW (10^{+3})	$(Ca)_f$ mole/kgASW (10^{+3})	$(Mg)_f$ mole/kgASW (10^{+3})	$^{(Ca)}K_{sp}$ (mole/kgASW)^2 (10^{+7})	$^{(Mg)}K_{sp}$ (mole/kgASW)^2 (10^{+7})
SC80	0.499	8.096	7.531	2.2799	9.6314	28.8621	2.5314	8.1148
SC81	0.502	8.119	7.565	2.2287	9.7166	28.8621	3.1987	8.7798
SC82	0.499	8.626	7.668	2.5248	9.4970	28.8601	3.5420	10.027
SC83	0.558	8.640	7.644	2.5344	9.4834	28.8610	3.3221	9.4216
SC84	1.008	8.122	7.571	2.2876	9.6311	28.8608	3.2153	8.9040
SC85	1.001	8.157	7.573	2.2985	9.7064	28.8600	3.2390	8.9032
SC86	1.003	8.663	7.642	2.5508	9.4666	28.8620	3.2707	9.2975
SC87	1.002	8.634	7.690	2.5303	9.4094	28.8621	3.6872	10.537
SC88	5.005	8.105	7.595	2.2825	9.7263	28.8603	3.4484	9.4546
SC89	5.001	8.091	7.563	2.2785	9.7244	28.8622	3.1985	8.7702
SC90	5.000	8.628	7.614	2.5262	9.4017	28.8623	3.0790	8.8071
SC91	5.002	8.661	7.595	2.5242	9.5092	28.8622	3.0967	9.3946

Table 4.1. continued

$(Mg:Ca)_{soln} = 4.99:1$

Expt #	gcalcite / kg ASW	pH_i	pH_f	CA_i meq/kgASW (10^{+3})	$(Ca)_f$ mole/kgASW (10^{+3})	$(Mg)_f$ mole/kgASW (10^{+3})	$^{(Ca)}K_{sp}$ (10^{+7})	$^{(Mg)}K_{sp}$ $(mole/kgASW)^2$ (10^{+7})
SC92	0.499	8.152	7.586	2.3662	9.6724	49.0910	4.7224	23.968
SC93	0.500	8.145	7.561	2.3632	9.6700	49.0908	4.4525	22.604
SC94	1.003	8.124	7.539	2.3546	9.6741	49.0914	4.2426	21.529
SC95	0.513	8.619	7.744	2.6578	9.4097	49.0684	5.7292	29.876
SC97	1.004	8.119	7.586	2.3526	9.6860	49.0923	4.7609	24.130
SC98	1.004	8.620	7.714	2.6553	9.4029	49.0901	5.3289	27.809
SC99	0.968	8.616	7.817	2.6553	9.4277	49.0720	6.8234	35.563
SC100	1.001	8.612	7.689	2.6518	9.4050	49.0720	5.0424	26.309
SC02	5.002	8.122	7.559	2.3538	9.6854	49.0702	4.4666	22.645
SC03	5.002	8.122	7.589	2.3538	9.6854	49.0924	4.7922	24.290

Figure 4.3

The apparent solubility products of calcite as a function of Mg:Ca concentration and solid:solution ratios at two initial degree of supersatrution: a) low degree of supersaturation and b) higher degree of supersaturation.

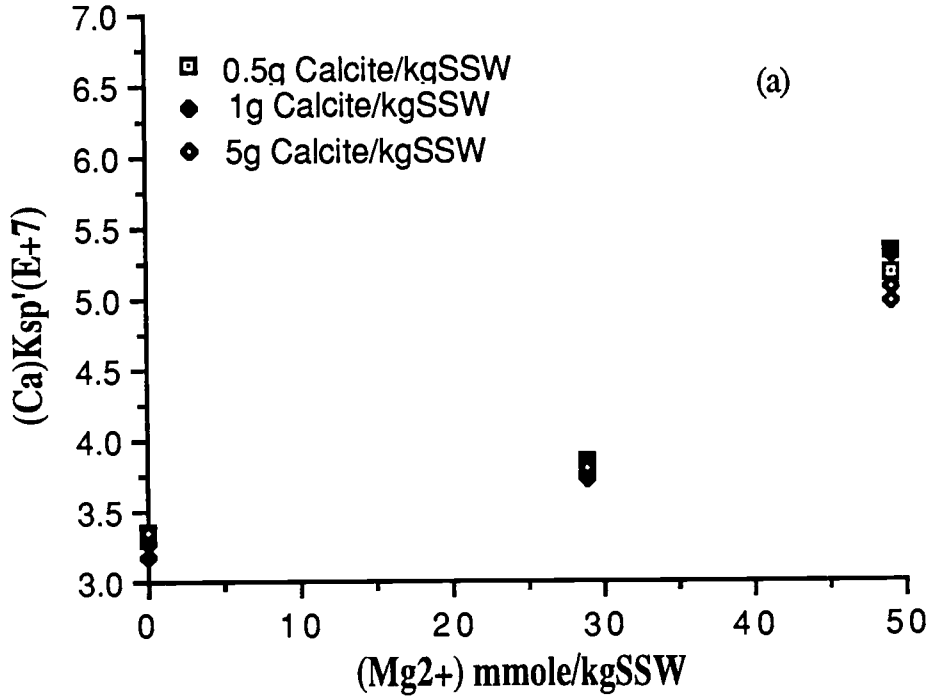
7.0
6.5
6.0
5.5
5.0
4.5
4.0
3.5
3.0
0.5g Calcite/kgSSW
1g Calcite/kgSSW
5g Calcite/kgSSW
(a)
(Ca)Ksp'(E+7)
0
10
20
30
40
50
(Mg2+) mmole/kgSSW

Figure 4.3

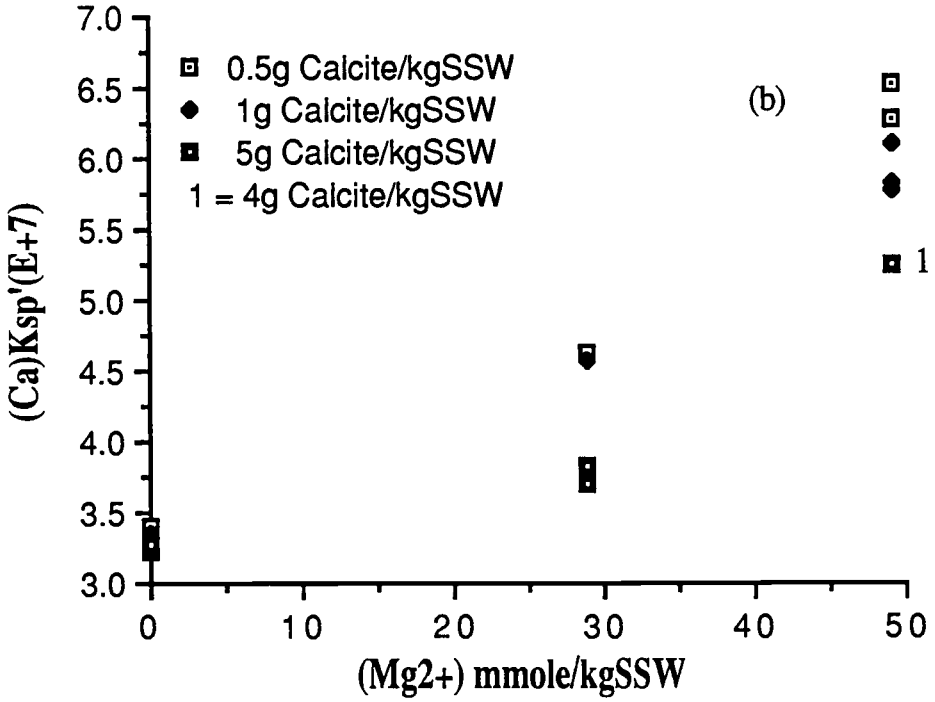

Figure 4.3 continued

The increase of solubility products with magnesium concentration in solution may be caused by an increase of the mole fraction of magnesium in the surface of calcite as a result of the overgrowth which enhances its solubility *(Chave et al, 1962; Morse et al., 1979; Schoonmacker, 1981; Mucci and Morse, 1984b; Koch and Disteche, 1984).* Actually, there were two forces enhancing the involvement of magnesium in overgrowth precipitation, the increase of magnesium concentration and the increase of apparent ionic products of carbonate in solution. It was noticed that the apparent ionic products increased by 84% with the increase of magnesium concentration in solution of the same pH from 0 to 0.05 mole l^{-1} as shown in Figure 4.4. The increase of magnesium fraction on calcite overgrowth surface was probably more effective upon the solubility products values than ion-pairing, because the activity of magnesian calcite overgrowth was not unity any more. The calcium fractions on calcite overgrowths which were determined by A. A. analysis are shown in Table 4.2. The results showed an increase of $^{x}MgCO_3$ on calcite overgrowth coatings with the increase of Mg:Ca concentration ratios in ASW.

If the activity of magnesian calcite was about unity and did not really affect the solubility of the solid phase and the increase of the solubility of calcite in Table 4.1 was mainly caused by ion-pairs formation, then the free solubility products of calcite, $^{(Ca)}K_{sf}$, as well as magnesite, $^{(Mg)}K_{sf}$, in different solutions could be expressed by :

$$^{(Ca)}K_{sf} = (Ca^{2+})_{f,e}\,(CO_3^{2-})_{f,e} \qquad (4.40)$$

Figure 4.4

The apparent ionic products of calcite versus (Mg^{2+}) concentration in ASW of two pH values.

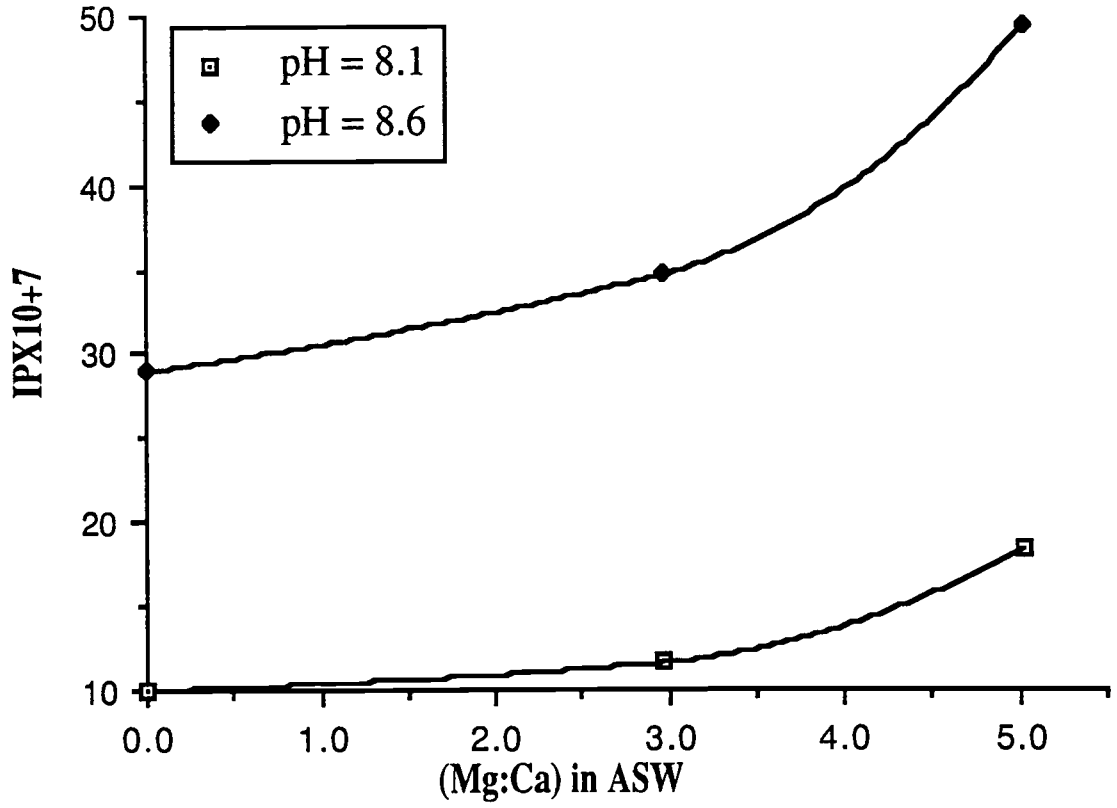

Figure 4.4

Table 4.2

The mole fraction $CaCO_{3(s)}$ in calcite overgrowth coatings as a function of Mg:Ca concentration ratios in ASW.

$(Mg:Ca)_{soln} = 2.96:1$		
Expt #	$^{x}CaCO_{3(s)}$	Method
SC80	0.946	A. A. analysis
SC81	0.946	"
SC86	0.944	"
SC87	0.946	"
SC89	0.947	"
SC90	0.948	"
SC91	0.947	"
$(Mg:Ca)_{soln} = 4.99:1$		
Expt #	$^{x}CaCO_{3(s)}$	Method
SC92	0.926	A. A. analysis
SC93	0.924	"
SC95	0.916	"
SC96	0.918	"
SC97	0.928	"
SC98	0.926	"
SC100	0.922	"
SC02	0.928	"
SC03	0.929	"

and

$$^{(Mg)}K_{sf} = (Mg^{2+})_{f,e}\,(CO_3^{2-})_{f,e} \qquad (4.41)$$

They may have the same values or very slight change with the increase of (Mg^{2+}) in solution because of $MgCO_3^+$, $MgCO_3^o$, $MgCaCO_3^{2+}$ and $MgCO_3^{2+}$ ion-pairs formation. The free and ion-pairs species were calculated for only those experiments of lower degrees of supersaturation (that is, to avoid the kinetic control conditions) by using the MICROQL program *(Westall 1979)*. The method is discussed in appendix 4.1. The values of the free solubility products expressed in -log K_{sf} are listed in Table 4.3. It is noticed that the values of $^{(Ca)}K_{sf}$ and $^{(Mg)}K_{sf}$ increased by 113% with the increase of (Mg^{2+}) from 0 to 0.05 mole l^{-1} ASW. However the free ionic products increased by only 38% with the same increase of (Mg^{2+}). This indicates that the increase of K_{sf} value is, probably, a result of the increase of the magnesian calcite dissolution.

The thermodynamic solubility products of calcite can be calculated from the relations:

$$^{(Ca)}K_{so} = a_{Ca^{2+}}\,a_{CO_3^{2-}} \qquad (4.42)$$

$$^{(Ca)}K_{so} = (\gamma Ca^{2+})_{T,e}(Ca^{2+})_{T,e}\,(\gamma CO_3^{2-})_{T,e}(CO_3^{2-})_{T,e} \qquad (4.42a)$$

$$^{(Ca)}K_{so} = (\gamma Ca^{2+})_{F,e}(Ca^{2+})_{F,e}\,(\gamma CO_3^{2-})_{F,e}(CO_3^{2-})_{F,e} \qquad (4.42b)$$

and the same relations are appropriate for magnesite.

The free activity coefficient of CO_3^{2-}, $(\gamma CO_3^{2-})_F$ was calculated from:

Table 4.3

The free solubility products of calcite and magnesite, represented by pK_{sf}, as a function of Mg:Ca concentration ratios in ASW.

$(Mg:Ca)_{soln}$ =0:1

Expt #	-log $(Ca^{2+})_F$	-log $(CO_3^{2+})_{F,e}$	$p^{(Ca)}K_{sf}$	$p^{(Mg)}K_{sf}$
SC62	2.380	4.600	6.980	-
SC64	2.378	4.589	6.967	-
SC66	2.397	4.550	6.947	-
SC70	2.378	4.600	6.978	-
SC72	2.371	4.604	6.975	-
SC73	2.378	4.597	6.975	-
SC74	2.380	4.555	6.935	-
SC75	2.380	4.579	6.959	-
SC76	2.378	4.661	6.939	-
SC77	2.371	4.534	6.905	-
SC78	2.390	4.533	6.924	-
SC79	2.387	4.549	6.936	-

Table 4.3 continued

$(Mg:Ca)_{soln}$ =2.96:1

Expt #	$-\log (Ca^{2+})_{F,e}$	$-\log (Mg^{2+})_{F,e}$	$-\log (CO_3^{2+})_{F,e}$	$p^{(Ca)}K_{sf}$	$p^{(Mg)}K_{sf}$
SC80	2.339	1.819	4.547	6.885	6.365
SC81	2.365	1.819	4.514	6.878	6.333
SC84	2.339	1.819	4.509	6.848	6.329
SC85	2.365	1.819	4.508	6.873	6.328
SC88	2.353	1.819	4.485	6.838	6.304
SC89	2.335	1.819	4.515	6.875	6.335
SC90	2.379	1.820	4.519	6.898	6.339
SC91	2.376	1.820	4.537	6.913	6.357

$(Mg:Ca)_{soln}$ =4.99:1

Expt #	$-\log (Ca^{2+})_{F,e}$	$-\log (Mg^{2+})_{F,e}$	$-\log (CO_3^{2+})_{F,e}$	$p^{(Ca)}K_{sf}$	$p^{(Mg)}K_{sf}$
SC92	2.312	1.566	4.345	6.657	5.911
SC93	2.311	1.566	4.366	6.679	5.932
SC94	2.311	1.566	4.385	6.697	5.951
SC97	2.311	1.566	4.342	6.654	5.908
SC02	2.311	1.566	4.366	6.677	5.932
SC03	2.312	1.566	4.334	6.651	5.906

$$(\gamma CO_3^{2-})_F = \frac{(\gamma CO_3^{2-})_T (CO_3^{2-})_T}{(CO_3^{2-})_F} \qquad (4.43)$$

The value of $(\gamma CO_3^{2-})_T$ in different Mg:Ca concentration ratios in ASW are listed in Table 2.5 and $(CO_3^{2-})_F$ were calculated as described in appendix 4.1. The free activity coefficients of magnesium and calcium cations, represented by $(\gamma M^{2+})_F$, were calculated from the equation:

$$(\gamma M^{2+})_F = \frac{(\gamma_{\pm} MCl_2)_F^3}{(\gamma_{\pm} KCl)_F} \qquad (4.44)$$

where $(\gamma_{\pm})_F$ represents the free mean activity coefficients.

The free mean activity coefficients of KCl, $CaCl_2$ and $MgCl_2$ were calculated from the general equation of the activity of an electrolyte MCl_q which could be expressed in two equivalent ways:

$$a_{MClq} = \gamma M_T (M)_T [\gamma Cl_{,T} (Cl)_T]^q \qquad (4.45a)$$

$$a_{MClq} = \gamma M_F (M)_F [\gamma Cl_{,F} (Cl)_F]^q \qquad (4.45b)$$

by combining equations (4.45a) and (4.45b), they yield:

$$(\gamma_{\pm}MCl_q)_F = (\gamma_{\pm}MCl_q)_T \left[\frac{(M)_T(Cl)_T^q}{(M)_F(Cl)_F^q}\right]^{(1/q+1)} \qquad (4.46)$$

To apply equation (4.46), first the effective ionic strength for each solution was calculated from:

$$I_e = 0.5\,[\Sigma(F)Z_{F,i}^2 + \Sigma(ip)Z_{ip}^2] \qquad (4.47)$$

where the concentrations of free, (F), and ion-pairs, (ip), were calculated by MICROQL program as described in appendix 4.1. Second, different effective ionic strength were used to calculate the equivalent total ionic strength of KCl, $MgCl_2$ and $CaCl_2$. In this case the same iterative procedure, which was described by *Johnson, (1979 p88)*, was used to estimate the stability constants K^*_{MCl}. The stability constants were estimated from *Johnson and Pytkowicz (1978)* following the equation:

$$\ln K^*_{MCl} = A_k + B_k Ie + C_k I_e^2 \qquad (4.48)$$

The constants A_k, B_k and C_k are given in Table 4.4. Then, the effective ionic strengths were plotted versus the total ionic strength of KCl, $MgCl_2$ and $CaCl_2$ and least square method was used to fit the data. The following equation was obtained to calculate the equivalent total ionic strength of the electrolyte salts:

$$I_{T,MClq} = \frac{I_{e,MClq} - \beta_o}{\beta_1} \qquad (4.49)$$

Table 4.4

The constants of equation (4.48) for KCl^o, $MgCl^+$ and $CaCl^+$ ion pairs (From Johnson and Pytkowicz, 1978).

Ion pairs	A	B	C
KCl^o	-0.280	-0.718	0
$MgCl^+$	0.736	0.028	-0.467
$CaCl^+$	0.961	-0.004	-0.426

The constants β_o = 0.083, 0.107 and 0.1099 and β_1 = 0.6737, 0.5166, and 0.475 for KCl, $MgCl_2$ and $CaCl_2$ respectively. The total mean activity coefficients of KCl, $MgCl_2$ and $CaCl_2$ were calculated from Culberson equation *(Pytkowicz et al, 1977)* after converting ionic strength to molality scale:

$$\log (\gamma_{\pm} MCl_q)_T = \frac{A I_T^{0.5}}{1 + B I_T^{0.5}} + C I_T + D I_T^{1.5} + E I_T^2 \qquad (4.50)$$

and I_T is the total ionic strength. The constants of this equation are listed in Table 4.5.

At this point, equation (4.46) could be used to calculate $(\gamma_{\pm} MCl_q)_F$, which was finally used to calculated the single free activity coefficient of the cation (M^{2+}). The values of estimated mean free activity coefficients of KCl, $MgCl_2$ and $CaCl_2$ and the free single activity coefficients of Ca^{2+} and Mg^{2+} of different Mg:Ca concentration ratios in ASW in molal scale are listed in Table 4.6.

The thermodynamic solubility products of calcite and magnesite calculated according to equation (4.42b) in which the activity of the solid phase was assumed to be one, are shown in Table 4.7. The data show an increase of the thermodynamic constants values with Mg:Ca concentration ratios in ASW. This indicates that the activity of the solid phases are more than one. By assuming that the activity of the solid was about unity for both $^{(Ca)}K_{so}$ at zero (Mg2+) and $^{(Mg)}K_{so}$ = 1.07 E-8 (mole/kg $H_2O)^2$ *(from Robie and Waldbaum, 1968; Garrels and Christ, 1965)*, then the activities of the solid phases as a result of the impurities were calculated from:

Table 4.5

The constants of equation (4.50) used to calculate mean total activity coefficients of electrolyte of interest (From Pytkowicz et al., 1977).

Electrolyte	A	B	C	D	E
KCl	-0.5108	1.307	0	0	0.002075
$MgCl_2$	-1.0216	1.800	-0.03365	0.1156	-0.04101
$CaCl_2$	-1.0216	1.501	0.07898	-0.01545	0

Table 4.6

The estimated mean total and free activity coefficients of KCl, $MgCl_2$ and $CaCl_2$, and the free activity coefficients of Mg^{2+}, Ca^{2+} and CO_3^{2-} as a function of Mg:Ca concentration ratios in ASW.

		KCl		$MgCl_2$		$CaCl_2$				
(Mg:Ca) Ratio	I_e	$(\gamma\pm)_T$	$(\gamma\pm)_F$	$(\gamma\pm)_T$	$(\gamma\pm)_F$	$(\gamma\pm)_T$	$(\gamma\pm)_F$	$(\gamma Mg)_F$	$(\gamma Ca)_F$	$(\gamma CO3)_F$
0:1	0.610	0.619	0.803	0	0	0.4506	0.6959	0	0.4197	0.07105
3:1	0.596	0.621	0.800	0.4749	0.698	0.4513	0.6922	0.4253	0.4146	0.06119
5:1	0.583	0.623	0.799	0.4753	0.695	0.4520	0.6926	0.4158	0.4158	0.04070

Table 4.7

Estimated Kso of calcite and magnesite , assuming that the activity of the solid was unity. The values in the last two columns are the predicted values of the solid activity precipitated from different Mg:Ca concentration ratios in ASW.

$(Mg:Ca)_{soln} = 0:1$

Expt #	$^{(Ca)}K_{so}$ (mole/kgASW)^2 (10^{+9})	$^{(Mg)}K_{so}$ (10^{+8})	$^{a}CaCO_{3(s)}$	$^{a}MgCO_{3(s)}$
SC62	3.1392	-	1	-
SC64	3.2167	-	1	-
SC70	3.1392	-	1	-
SC72	3.1600	-	1	-
SC73	3.1600	-	1	-

$(Mg:Ca)_{soln} = 2.96:1$

Expt #	$^{(Ca)}K_{so}$ (mole/kgASW)^2 (10^{+9})	$^{(Mg)}K_{so}$ (10^{+8})	$^{a}CaCO_{3(s)}$	$^{a}MgCO_{3(s)}$
SC80	3.3078	1.1225	1.0657	1.0491
SC81	3.3637	1.1083	1.0624	1.1293
SC85	3.4013	1.2200	1.0753	1.1402
SC89	3.3876	1.2036	1.0710	1.1249
SC90	3.2116	1.1906	1.0154	1.1127
SC91	3.1041	1.1428	0.9814	1.068

Table 4.7 continued

$(Mg:Ca)_{soln}$ = 4.99:1

Expt #	$^{(Ca)}K_{so}$ (mole/kgASW)^2 (10^{+9})	$^{(Mg)}K_{so}$ (mole/kgASW)^2 (10^{+8})	$^{a}CaCO_{3(s)}$	$^{a}MgCO_{3(s)}$
SC92	3.7221	2.0744	1.1767	1.9387
SC93	3.5390	1.9765	1.1189	1.8472
SC94	3.3971	1.8919	1.0740	1.7681
SC97	3.7521	2.0879	1.1863	1.9513
SC02	3.5529	1.9765	1.1233	1.8472
SC03	3.7721	2.0994	1.1926	1.9621

$(Mg:Ca)_{soln}$ = 1:0

Expt #	$^{(Ca)}K_{so}$ (mole/kgASW)^2 (10^{+9})	$^{(Mg)}K_{so}$ (mole/kgASW)^2 (10^{+8})	$^{a}CaCO_{3(s)}$	$^{a}MgCO_{3(s)}$
1	-	1.07	-	1

1 = the value is calculated from $^{(Mg)}K_{so}$= 2.82 $^{(Ca)}K_{so}$ according to Robie and Waldbaum (1968) and Garrels and Christ (1965).

$$a_{CaCO_{3(s)}} = \frac{{}^{(Ca)}K_{so(Mg=0)}}{{}^{(Ca)}K_{so(Mg:Ca)}} \qquad (4.51)$$

and

$$a_{MgCO_{3(s)}} = \frac{{}^{(Mg)}K_{so(Ca=0)}}{{}^{(Mg)}K_{so(Mg:Ca)}} \qquad (4.52)$$

where the subscripts (Mg=0), (Ca=0) and (Mg:Ca) are respectively the K_{so} values when $(Mg^{2+}) = 0$, $(Ca^{2+}) = 0$ and Mg:Ca concentration ratios in the solution. The activities of the solids phases are shown in Table 4.7

The activity coefficients of the solid phases were calculated from equation 4.8 and equation 4.9. These values as well as the mole fraction of magnesium in solution at equilibrium, y_f, and the mole fraction of $CaCO_{3(s)}$, $(1-x_f)$, in calcite overgrowths are listed in Table 4.8. The large increase of $\lambda MgCO_{3(s)}$ in the solid is probably because of the effect of magnesium on the crystal lattice of calcite. The incorporation of smaller magnesium ion in the crystal lattice causes a distortion of the lattice as described in chapter 1 and leads to a nonideal solid solution formation.

Because of the incongruent dissolution and precipitation of magnesian calcite *(Plummer and Mackenzie, 1974; Wollast and Rienhard-Derie, 1977; Wollast et al., 1980)*, the solid-solution thermodynamic solubility product of magnesian calcite, ${}^{(Mg\text{-}calc)}K_{so}$, is represented by the following equation:

$$^{(Mg\text{-}calc)}K_{so} = \frac{(a_{Mg^{2+}})^{y_e}(a_{Ca^{2+}})^{1-y_e}(a_{CO_3^{2+}})}{(a_{MgCO_3^{2+}})^{x_e}(a_{CaCO_3^{2+}})^{1-x_e}} \qquad (4.53)$$

according to the following mass balance equilibrium reaction:

$$y_e Mg^{2+} + (1-y_e)Ca^{2+} + CO_3^{2-} \Longleftrightarrow Mg_{x_e}Ca_{(1-x_e)}CO_3 \qquad (4.54)$$

The equivalent expression of equation (4.53) is:

$$^{(Mg\text{-}calc)}K_{so} =$$

$$\frac{(\gamma_{Mg^{2+}})_{F,e}^{y_e}(Mg^{2+})_{F,e}^{y_e}(\gamma_{Ca^{2+}})_{F,e}^{1-y_e}(Ca^{2+})_{F,e}^{1-y_e}(\gamma_{CO_3^{2+}})_{F,e}(CO_3^{2+})_{F,e}}{(a_{MgCO_3^{2+}})^{x_e}(a_{CaCO_3^{2+}})^{1-x_e}} \qquad (4.55)$$

The following general equilibrium reaction equation for magnesian calcite is usually used:

$$x_e Mg^{2+} + (1-x_e)Ca^{2+} + CO_3^{2-} \Longleftrightarrow Mg_{x_e}Ca_{(1-x_e)}CO_3$$

and its thermodynamic solubility product is expressed as:

$$^{(Mg\text{-}calc)}K_{so} =$$

$$\frac{(\gamma_{Mg^{2+}})_{F,e}^{x_e}(Mg^{2+})_{F,e}^{x_e}(\gamma_{Ca^{2+}})_{F,e}^{1-x_e}(Ca^{2+})_{F,e}^{1-x_e}(\gamma_{CO_3^{2+}})_{F,e}(CO_3^{2+})_{F,e}}{(a_{MgCO_3^{2+}})^{x_e}(a_{CaCO_3^{2+}})^{1-x_e}} \qquad (4.56)$$

Table 4.8

The activity coefficients of calcite and magnesite, estimated from $x_f = {}^{x}MgCO_{3(s)}$ and $(1-x_f) = {}^{x}CaCO_{3(s)}$ as a function of Mg:Ca concentration ratios in ASW.

$(Mg:Ca)_{soln} = 2.96:1$					
Expt #	y_f	${}^{x}CaCO_{3(s)}$	${}^{x}MgCO_{3(s)}$	$\lambda CaCO_{3(s)}$	$\lambda MgCO_{3(s)}$
SC80	0.750	0.947	0.053	1.1253	19.7943
SC81	0.750	0.946	0.054	1.1230	20.9130
SC85	0.750	0.948	0.052	1.1343	21.9827
SC89	0.750	0.949	0.051	1.1286	22.0569
SC90	0.749	0.949	0.051	1.0700	21.8176
SC91	0.749	0.951	0.049	1.0320	21.7959
$(Mg:Ca)_{soln} = 4.99:1$					
Expt #	y_f	${}^{x}CaCO_{3(s)}$	${}^{x}MgCO_{3(s)}$	$\lambda CaCO_{3(s)}$	$\lambda MgCO_{3(s)}$
SC92	0.835	0.924	0.076	1.2735	25.5092
SC93	0.835	0.925	0.075	1.2096	24.6293
SC94	0.835	0.926	0.074	1.1598	23.8932
SC97	0.835	0.926	0.074	1.2811	26.3689
SC02	0.835	0.929	0.071	1.2091	26.0169
SC03	0.835	0.928	0.072	1.2851	27.2514

Another type of thermodynamic solubility product equation, used in literature is defined by the ion activity product, (IAP) equation (9) in the introduction, which is similar to equation (4.56) except that the activity of solid magnesian calcite is assumed to be one. This type of equation is expressed as:

$$^{(Mg\text{-}calc)}K_{so} = (IAP)$$

$$(\gamma Mg^{2+})_{F,e}{}^{x_e}(Mg^{2+})_{F,e}{}^{x_e}(\gamma Ca^{2+})_{F,e}{}^{1-x_e}(Ca^{2+})_{F,e}{}^{1-x_e}(\gamma CO_3{}^{2+})_{F,e}(CO_3{}^{2+})_{F,e}$$

The three types of the above equations were used to estimate the values of thermodynamic solubility products of magnesian calcite as a function of Mg:Ca concentration ratios in ASW. The results are shown in Table 4.9 and Figure 4.6. The results of equation 4.56 and the equation defined by (IAP) showed no significant change in $^{(Mg\text{-}calc)}K_{so}$ as a function of Mg:Ca concentration ratios in solution because that the equilibrium reaction is treated as a congruent reaction. The solid-solution equilibrium reaction of magnesian calcite is is attributed to an incongruent reaction and equation (4.55) is more realistic. This suggests that there are more than one thermodynamic (multistate) equilibrium and, probably, that the composition of outer-most surface layer of magnesium calcite, which is in contact with the bulk solution, is of higher magnesium concentration. The Auger microanalysis showed that the magnesium concentration is much higher than calcium in the outer-most layer (~70-100 Angstrom) *(Mucci et al., 1985).*

Finally, in ASW of magnesium-to-calcium concentration ratio of 5, the apparent solubility products was $10^{-6.299}$, in agreement with $Ksp'=10^{-6.3}$ found by *Koch and Disteche (1984).* They related that to surface overgrowth of 2 to 3 mole% magnesium carbonate. But according to my results I related that to surface overgrowth of about 7.4 mole% $MgCO_3$. *Mucci et al (1985),* using Scanning Auger Microanalysis, showed that the $(Mg^{2+}:Ca^{2+})$ concentration on $CaCO_{3(s)}$ surface increased with the increase of

Table 4.9

The estimated thermodynamic solubility products of magnesian calcite as a function of Mg:Ca concentration ratios in ASW, calculated by equation (4.55), equation (4.56) and the equation defined by (IAP).

Expt #	$(Mg:Ca)_{soln}$ Ratio	$^{(Mg\text{-}calc)}Kso\ (10^{+9})$ Eqn (5.55)	Eqn (5.56)	(IAP)
SC62	0	3.160	3.160	3.160
SC81	2.96:1	7.756	3.310	3.525
SC85	2.96:1	8.237	3.378	3.600
SC89	2.96:1	8.288	3.551	3.813
SC89	2.96:1	8.385	3.355	3.421
SC92	4.99:1	10.68	3.418	4.177
SC93	4.99:1	12.84	3.485	4.049
SC94	4.99:1	12.81	3.471	3.868
SC97	4.99:1	12.80	3.466	4.266
SC02	4.99:1	12.81	3.453	4.019
SC03	4.99:1	12.81	3.458	3.458

Figure 4.5

The thermodynamic solubility products as a function of Mg:Ca concentration ratios in ASW, represented by equations (4.55), (4.56) and (9) (see text).

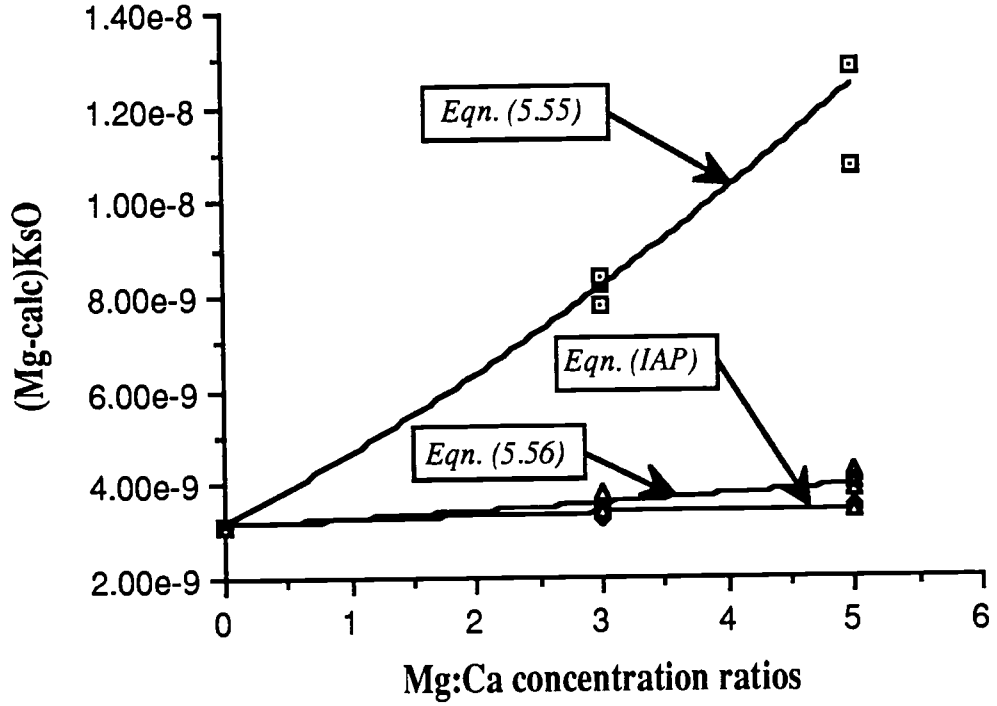
1.40e-8
1.20e-8
1.00e-8
8.00e-9
6.00e-9
4.00e-9
2.00e-9
(Mg-calc)KsO
Eqn. (5.55)
Eqn. (IAP)
Eqn. (5.56)
0
1
2
3
4
5
6
Mg:Ca concentration ratios

Figure 4.5

(Mg^{2+}:Ca^{2+}) concentration in solution. They strongly suggested that magnesium calcite overgrowth was in an exchange equilibrium with the solution from which it precipitated and that it was representative of the solubility controlling phase. The results reported here suggested that there were two types of controlling factors; the thermodynamic and the kinetic controls in agreement with *Pytkowicz and Cole, (1979)*: (1) the thermodynamic control was effective at a low degree of saturation, whereby the increase of surface area showed a very slightly change, and (2) the kinetic control whereby the increase in surface area played a significant role on the steady-state equilibrium constant; the latter was effective at higher degree of supersaturation.

4.5 Conclusion

One can conclude that in the natural environment where the degree of saturation is close to saturation level the inorganic precipitation of magnesian calcite tends to approach thermodynamic equilibrium, but where the degree of saturation is high enough to enhance the formation of high magnesian calcite overgrowth, or biogenic precipitation of high magnesian calcite, the kinetic control on equilibrium is favored. The kinetically controlled steady-state may approach the thermodynamic equilibrium, if enough time is given or any process becomes effective that causes changes in the composition of the system.

Another conclusion is that the apparent solubility products values measured in laboratory experiment could be applied to environments of low degree of saturation as well as to natural systems where there are large solid surface in contact with the solution such as in sediments or places where there are suspended particles. At high degrees of saturation and in environments where there are small amount of particles with overgrowths of a high mole fraction of magnesium carbonate, such as in surface of the open ocean, the apparent solubility products measured in laboratory are questionable.

Chapter 5.

POSSIBLE EFFECTS AND APPLICATION OF THE ABOVE STUDIES IN VARIOUS NATURAL WATERS (PORE WATER AND OPEN WATER AS WELL AS LAKES, RIVERS AND UNDERGROUND WATERS).

Recently, scientific workers have increasingly, focued on the changes of atmospheric CO_2 and the hydrospheric Mg:Ca activity ratio, through geological time and their effects on the physicochemically precipitated, shallow-marine ooids and cements *(Sandberg, 1975; Wilkinson, 1979; Mackenzie and Pigott, 1981; Wilkinson et al., 1985; Wilkinson and Given, 1986; Scoffin, 1987; Nancollas and Brand, 1989).* Accordingly, two periods, defined by carbonate deposits have been introduced to the literature: the ***aragonite sea***, which is the period of low sea-level, low atmospheric pCO_2 and high Mg:Ca concentration ratios, and the ***calcite sea***, which is the period of sea-level highstand, high atmospheric pCO_2 and low Mg:Ca concentration ratios*(Mackenzie and Pigott, 1981; Sandberg, 1983;1985; Wilkinson et al., 1985).* These periods are also proposed to occur during the emergent mode and submergent mode respectively as illustrated in Figure 5.1. It is suggested that the reaction rate of growing carbonate crystals influences the crystal morphology, mineralogy and the size of the crystal *(Folk, 1974; Lahann, 1978; Given and Wilkinson, 1985; Wilkinson and Given, 1986; this work).* It should be emphasized that the change of CO_2 influences mainly the degree of saturation of the solution with respect to carbonate minerals.

The effects of changing pCO_2 and Mg:Ca concentration ratios and other potential factors like temperature (references cited in Introduction and outline; *Burton and Walter 1987*) have been demonstrated in this laboratory study (chapter 1 and chapter 4). The results show that the system $CaCO_3$-$MgCO_3$-H_2O in presence of a solid phase is controlled by kinetics, especially in the presence of Mg^{2+} and a high degree of supersaturation, as well as by thermodynamic limiting factors. Magnesium ion is the main agent that causes the shift towards the kinetic control. In natural water of low magnesium concentration, such as rivers, lakes, meteoric-vadose environments, where the ratio of magnesium-to-calcium concentration is usually less than 0.5, the laboratory studies show that the behavior of the system tends to approach an equilibrium state with lower magnesian

Figure 5.1

Diagrammatic models of lowstand and highstand geochemical processes adapted from Mackenzie and Pigott, (1981) and Wilkinson et al., (1985):

a) Aragonite Seas; during the emergent mode pCO_2 deceases, because of subaerial oxidation of sulfides, erosion of carbonate and metal silicates and increase of photosynthesis. Magnesium uptake is reduced at cooler ridges and the silicates weathering adds more magnesium ions.

b) Calcite Seas: during the submergent mode increase of metamorphic reactions at subduction zones, reduction of sulfate and deposition of carbonates in epicontinentals, decrease of photosynthesis conversion of plagioclase and mafic to chlorite and epidote and removing magnesium at hydrothermal vents. These reaction depress magnesium concentration and liberate H^+ and Ca^{2+}.

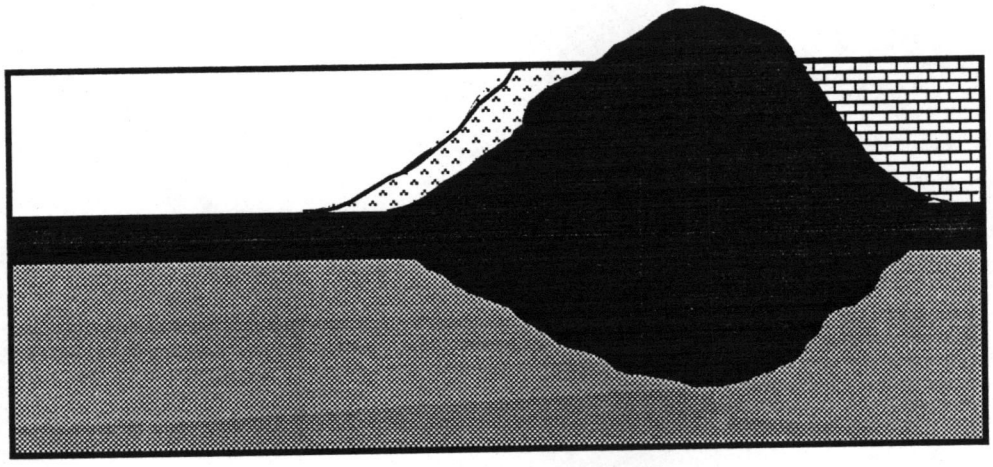

Figure 5.1

ARAGONITE SEAS: ***(Emergent Mode)***

(1) Emergence of terrestrial materials; increases of sulphide oxidation:

$$4FeS_2 + 15O_2 + 8H_2O \Rightarrow 2Fe_2O_3 + 8SO_4^{2-} + 16H^+$$

(2) Erosion of carbonates:

$$CaCO_3 + CO_2 + H_2O \Rightarrow Ca^{2+} + 2HCO_3^-$$

(3) Erosion of metal-silicates:

$$MeSiO_3 + CO_2 \Rightarrow MCO_3 + SiO_2$$

(4) Increase of photosynthesis:

$$CO_2 + H_2O \xrightarrow{\text{nutrients}} CH_2O + O_2$$

(5) Evaporites precipitation:

$$Ca^{2+} + SO_4^{2-} \Rightarrow CaSO_4$$

Net Reaction:

$$4FeS_2 + 8CaCO_3 + 16MSiO_4 + 23CO_2 + 15H_2O \Rightarrow$$
$$2FeO_3 + 16MCO_3 + 8CaSO_4 + 16SiO_2 + 15CH_2O$$

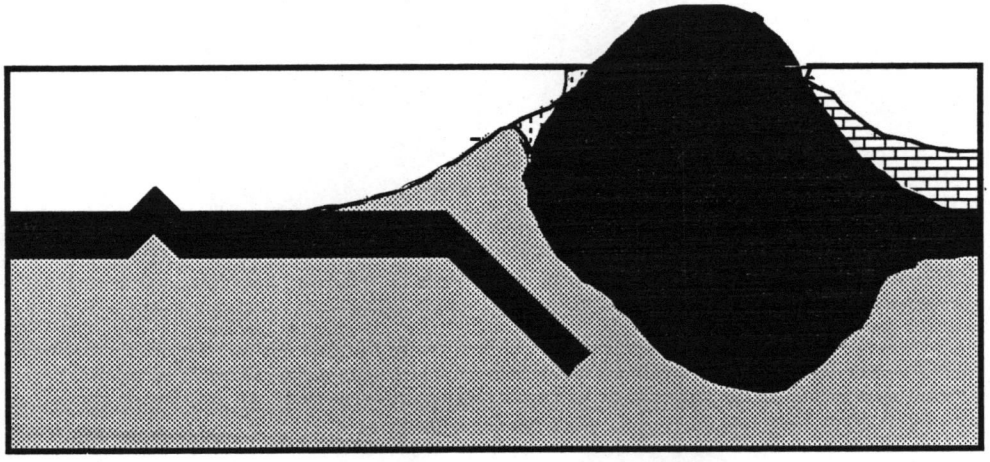

Figure 5.1 continued

CALCITE SEAS: ***(Submergent Mode)***

(1) High input of diagenetic and metamorphic CO2 to ocean-atmosphere system:

$$MeCO_3 + SiO_2 \Rightarrow MeSiO_2 + CO_2$$

(2) Erosion of sulphate and organic carbon and precipitation of carbonate and pyrite:

$$2Fe_2O_3 + 15CH_2O + 8CaSO_4 \Rightarrow$$
$$8CaCO_3 + 4FeS_2 + 7CO_2 + 15H_2O$$

(3) Restriction of terrestrial biota; nutrients supply to oceans decreased; oxidation increased:

$$CH_2O + O_2 \Rightarrow CO_2 + H_2O$$

Net Reaction:

$$CO_2 + 2F_2O_3 + 8CaSO_4 + 8MgSiO3 + 15CH_2O \Rightarrow$$
$$4FeS_2 + 8CaMg(CO_3)_2 + 8SiO_2 + 15H_2O$$

calcite. At this low magnesium-to-calcium concentration ratio and a high degree of supersaturation, probably, more than one thermodynamic equilibrium state is reached depending upon the solid-to- solution ratios which leads to different lower mole% $MgCO_3$ in calcite as illustrated in Figures 4.1 and 4.2. The equant morphological feature of low magnesian calcite is possible in such environments where the magnesium concentration is low. However, there are significant exceptions where the acicular crystals are found *(Longman, 1980; Binkley et al., 1980)*. Both, the equant morphology and low magnesian calcite favor the thermodynamic equilibrium over the kinetic steady-state.

In marine environments, where the magnesium concentration is five times the concentration of calcium, both kinetics and thermodynamics controls may coexist. In marine-shallow waters, hypersaline lacustrine or brines, where the degree of saturation is high (because of the increase of the temperature and photosynthesis which reduce CO_2 gas) one will expect the formation of high magnesian calcite and/or aragonite, which possibly precipitates as overgrowth on suspended skeletal and nonskeletal particles or in the form of biogenic skeletons, because inorganic spontaneous precipitation is still impossible according to this study and the results in chapter 1. These types of precipitates are kinetically favored. Acicular morphology of high magnesian calcite is expected as shown in section 1.4.3, although, in some sediments there are some high magnesian calcites which exhibit equant morphologies *(Al-Hashimi, 1977; James and Ginsburge, 1979; Warme and Schneidermann, 1983; Pierson and Shinn, 1983)*. If a precipitate of magnesian calcite reached the sediments, it is expected to dissolve and reprecipitate into another magnesian calcite as demonstrated in section 1.4.2. Because of respiration and oxidation processes in sediments the transformation processes maybe much effective. A lower magnesian calcite is probably formed according to the multistate equilibrium, because the solid to solution ratio is larger in sediments.

In various environments there are some natural processes which may influence the chemical composition of the local aqueous environment. These processes can be biological activities which affect the CO_2 concentration during the photosynthesis and oxidation reactions. The excess of atmospheric CO_2 as a result of the increase fossil fuel CO_2 ($FFCO_2$) penetrates the oceanic surface waters to a depth of 500 m *(Takahashi et al., 1982; Chen, 1982)* such that the saturation depth with respect to calcite was about 100-150m deeper before the Industrial Revolution *(Feely and Chen, 1982)*. The submarine hydrothermal activities, showed significant sources and sinks for several components of seawater *(Corliss et al 1979, Edmond et al 1979)*. The long period geological events reflected by the basalt reactions are found to affect the chemical composition of the solution during hot-temperature seawater-basalt interaction and due to different minerals interaction *Mackenzie and Piggot (1981)*. They concluded that the CO_2 levels were higher prior to the formation of Carboniferous ooid and skeletal parts. Later CO_2 levels fell and aragonite and magnesian calcite of greater than 8 mole % were formed.

Now suppose that a given magnesian calcite is at equilibrium with seawater. There is no reason for geological conversion to a single stable phase, such as low-magnesian calcite or a dolomite, in term of multistate equilibrium. This can be seen in Figure 5.2 and Figure 4.1. In the case of 2 solution of composition w_1 and w_2, precipitation will start and reach an equilibrium with y_1 and y_2 as shown in Figure 5.2. If the composition of the solution is changed, such as the increase or the decrease of magnesium-to-calcium ratio by any process in sediment, y_1 or y_2 moves towards y_3, where dolomite precipitates theoretically, and y_1 or y_2 moves to the left and becomes low-magnesian calcite. Another factor which may cause such diagenetic processes is the increase of the solid-to-solution ratio in old sediments and in their pore water *(Wollast and Pytkowicz, 1978)*. The phase rule tells us that the degree of freedom $f = 3$, for the system $CaCO_3$-$MgCO_3$-H_2O, if only

Figure 5.2

Triangular diagram to show that there are more than one final solid solution thermodynamic equilibrium.

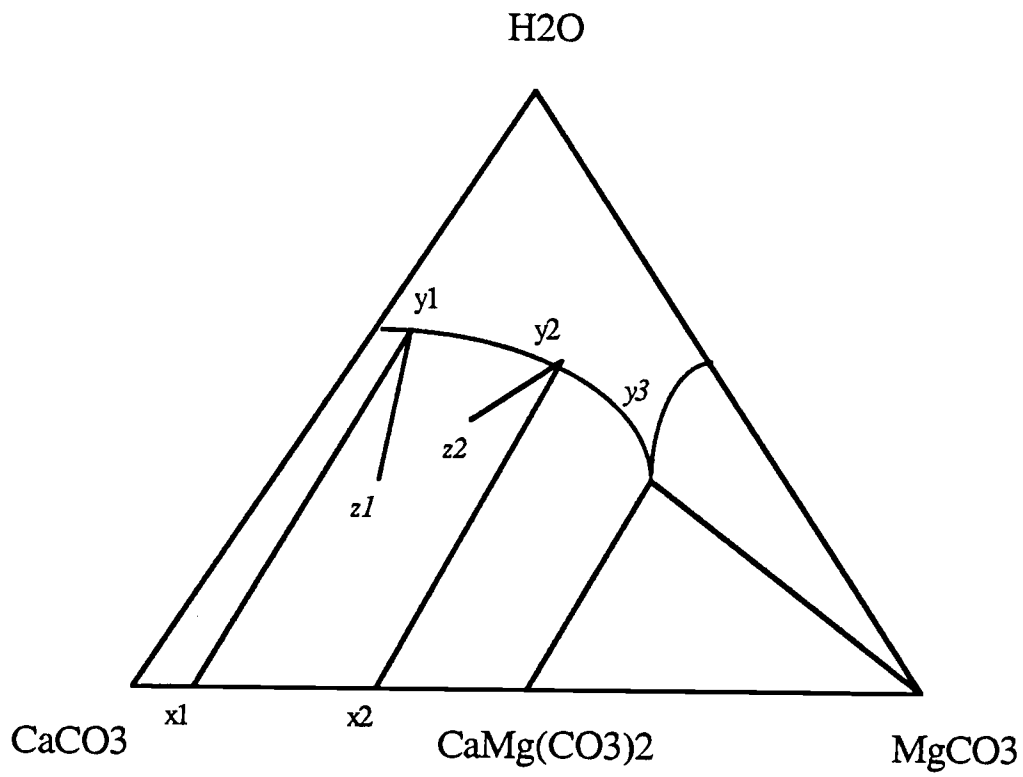

Figure 5.2

one solid, one aqueous and a vapor phase are present in the system. Therefore one compositional variable which is x_e is needed to fix the system. In the case of the presence of two solids, one aqueous and one vapor pressure, $f = 2$ and the system is fixed by T and P. This is only valid and true if the pH is always constant.

BIBLIOGRAPHY

Al-Hashmi, W.S. (1977). Recent carbonate cementation from seawater in some weathered dolostones, Northumberland, England. J. Sed. Petrology 47, 1375-1391.

Am. Chem Soc. 44:877-898.

and calcium, at 25°C and 0.72 ionic strength Ph.D. thesis Oregon State Univ.

Anderson, D. H. and Robinson, R. J. (1946). Rapid electrometric determination of alkalinity of seawater. Industrial and Engineering Chemistry. 18: 767-769

Anderson, L. G. and Dyrssen, D. (1987). Formation of chemogenic calcite in super-anoxic seawater- Framvaren Southerm Norway. Mar. Chem. 20:361-376.

aqueous solution. Ph.D. Thesis, Oregon State Univ. Corvallis 116pp.

Back, W. (1963). Intern Associ. Sci. Hydrology. VIII Annee. No 3. 43.

Barnes, I. (1965). Geochemistry of Birch Creek Inyo County, California a Travertime depositing Creek in an arid climate. Geochim Cosmochim Acta 29:85-112.

Bates R. G. C. (1973) . Determination of pH, Theory and Practice ed. 2 John Wiley Interscience. New York, N.Y. 479pp.

Bathurst, R. G. C. (1964). The replacement of aragonite by calcite in molluscan shell wall in: Approaches to Paleoecology. J Imbrie and N. D. Newell eds John Wiley and Sons, New York 357-367.

Bathurst, R. G. (1975). Carbonate sediments and their diagnosis, Development in Sedimentology 12. 2nd Ed. Elsverier Publishing Company N. Y. 658pp.

Ben-Yaakov, S. and M. B. Goldhaber (1973) . The influence of sea water composition on apparent constants of carbonic system. Deep-Sea Res. 20:87-99.

Berner, R. A. (1966a.). Chemical diagnesis of some modern carbonate sediments. Am. J. Sci 264:1-30.

Berner, R. A. (1966b.). Diagenesis of magnesium in seawater with mineral grains. Science 153:188-191.

Berner, R. A. (1975.). The role of magnesium in crystal growth of calcite and aragonite from seawater. Geochim. Cosmochim Acta, 39:489-504.

Berner, R. A., and Morse, J. W. (1974). Dissolution kinetics of calcium carbonate in seawater. IV Theory of calcite dissolution. Am. J. Science 274:108-134.

Berner, R.A. (1967). Comparative dissolution characteristics of carbonate minerals in the presence and absence of aqueous magnesium ion. Amer. J. Sci. 265, 45-70.

Berner, R.A. (1968). Calcium carbonate concretions formed by the decomposition of organic matter. Science 159:195-197.

Berner, R.A. (1971). Principles of chemical sedimentology. McGraw-Hill, New York, 240pp.

Berner, R.A. (1978). Equilibrium, kinetics and the precipitation of magnesian calcite from seawater. Amer. J. Sci. 278, 1435-1477.

Binkley, K.L., B.H. Wilkinson and R.M. Owen (1980). Vadose beachrock cementation along a southeastern Michigan marl lake. J. Sed. Petrology. 50, 953-962.

Bischoff, J. L. (1968). Kinetics of calcite nucleation: Magnesium ion inhibition and ionic strength catalysts. Geophys. Res. 73:3315-3322.

Bischoff, J. L. and Fyfe, W. S. (1968). The aragonite-calcite transformation. Am. J. Sci 266:65-79.

Blaedel, W. J. and Meloche, V. W. (1957). Elementary quantitative analysis: Theory and practice. Evanston, Illinois, Row Peterson.

Boettcher. A. L. and Wyllie, P. J. (1968). The calcite- aragonite transition measured in the system CaO-CO2-H2O. J. Geol. 76:314-330

Broecker, W. S. and Peng, T. H. (1982). Tracers in the sea. Eldigio Press, Palisades, New York 690 pp.

Broecker, W. S. and Peng, T. H. (1987). The role of CaCO3 compensation in the glacial to interglacial atmospheric CO2 change. Global Biogeochem. Cycles. 1:15-29.

Broecker, W. S. and Takahashi, T. (1966). Calcium precipitation on the Bahamas Banks, Geophys. Res. 71:1575-1602.

Broecker, W. S., Takahashi, T., Simpson, H. J. and Peng, T. H. (1979). Fate of fossil fuel carbon dioxide and the global carbon cycle. Science 206:409-418.

Bronsted, J.N. (1922.) Studies on solubilities.4 Principle of specific interactions of ions. J. Am. Chem. Soc. 44:877-898.

Brooks, R., Clark, L. M. and Thurston, E. F. (1951). Calcium carbonate and it hydrates. Phil. Trans. Roy, Soc. London. Ser. A. 243:145-167.

Burton, E. A. aand Walter, L. M. (1987). Relative precipitation rates of aragonite and Mg calcite from seawater. Temperature or carbonate ion control? Geology 15:11-114.

Butler, J. N. (1964). Ionic Equilibrium: A mathematical approach. Reading Massachusetts. Addison-Wesley.

Butler, J. N. (1982). Carbon dioxide equilibrium and their applications. ed. Addison-Wesley. Reading, Massachusetts. 259pp.

Chave, K. E. (1952). A solid solution between calcite and dolomite. J. Geol. 60:190-192.

Chave, K. E. (1954a;b). Aspects of the biochemistry of magnesium 1. Calcareous and marine organism 2. Calcareous sediments and rocks. J. Geol 62:266-283, 587-599.

Chave, K. E. (1965). Carbonates: association with organic matter in surface seawater. Science 148:1723-1424.

Chave, K. E. (1981). Summary of background information on Mg-calcites. In Garrels, R. M and Mackenzie, F.T. eds. Some aspects of the role of the shallow ocean in Global carbon dioxide uptake. U.S.D.O.E. Conf. 8003115, Nat'l Tech Inform. Service Springfield Virginia. pA4-A9.

Chave, K. E. and Suess (1970). Calcium carbonate saturation in seawater: Effects of dissolved organic matter. Limnol. Oceanogr. 15:633-637.

Chave, K. E., K. S. Deffeyes, P. K. Weyl, R. M. Garrels and M. E. Thompson (1962). Observations on the solubility of skeletal carbonate in aqueous solutions. Science 137:33-34

Chave, K.E. and Schmalz R.F. (1966). Carbonate-seawater interactions. Geochim. Cosmochim. Acta. 30, 1037-1048.

Chave, K.E. and Suess E. (1967). Suspended minerals in seawater. Trans. N.Y. Acad. Sci. 29,991-1000.

Chen, C. T. A. (1982). On the distribution of anthropogenic CO2 in the Atlantic and South Ocean. Deep-Sea Res. 29:563-580.

Christ, C.L. and Hostetler (1970). Studies, in the systems Mg0-SiO2-CO2-H2O (II): The activity -product constant of magnesite. Amer. J. Sci. 268, 439-453.

Christiansen, J.A. and Nielsen A.E. (1951). On the kinetics formation of precipitates of sparingly soluble salts. Acta Chem. Scand. 5, 673-675.

Clark, P. S. (1957). A note on calcite-aragonite equilibrium. Am. Mineralogist. 42:564-566.

Cloud, P. E. (1962a). Environment of calcium carbonate deposition west of Andros Island, Bahamas, U.S. Geol. Surv. Prof. paper 350: 138pp.

Cloud, P. E. (1962b). Behavior of calcium carbonate in seawater. Goechim. Cosmochim Acta. 26:867-887.

Corliss, et al. (1979). Submarin thermal springs on Glapagaos Rift. Science. 203:1703-1083.

Culberson, C.; Pytkowicz, R. M. and Hawley, J. E. (1970). Seawater alkalinity determination by pH method. J. Mar. Res. 28: 15-21.

Culberson, C. H. and Pytkowicz, R. M. (1973). Ionization of water in seawater. Mar. Chem. 1:309-316.

Dana, S. E. and Ford, W. E. (1951). A textbook of mineralogy with an extended treatise on crystallography and physical mineralogy ed. John Wiley an Sons. Inc. New York.

Davies, C. W. and Jones, A. L. (1955). The precipitation of silver chloride from aqueous solutions part 2. Kinetics of growth of seed crystal, Trans. Faraday Soc. 51:812-817.

de Boer, R. B. (1977). Influence of seed crystals on the precipitation of calcite and aragonite. Am. J. Sci. 277: 38-60.

Deer, W. A., Howie, R. A. and Zussam, J. (1962). Rock- Forming minerals 5 Longmans, London 371pp.

Doremus, R. H. (1958). Precipitation kinetics of ionic salts from solution. J. Phys. Chem. 62: 1968-1075.

Dufour, L. and Defay, R. (1963). Thermodynamic of Clouds. Acad. Press. New York.

Dyrssen, D. and Sillen, L. G. (1967). Alkalinity and total carbonate in seawater. A plea for p-T independent data. Tellus, 19:113-121.

Edmond, J. M., et al., (1979). Ridge crest hydrothermal activity balance of major and minor elements in the oceans: The Glapagos data. Earth Planet. Lett. 46:1-18.

Elgquist, . . and Wedlborg, . . (1975). Stability of ion pairs from gypsum solubility. Degree of ion pair formation between the major constitueints of seawater. Mar. Chem. 3:215-225.

Evans, R.C. (1966). An introduction to crystal chemistry. Cambridge University Press. Cambridge, Great Britain, 410pp.

Feely, R. A. and Chen, C. T. A. (1982). The effect of excess CO2 on the calculated calcite and aragonite saturation horizons in Northeast Pacific. Geophys. Res. Lett. 9:1294-1297.

Fine, M.F. (1964). Introduction to phase transformations in condensed systems. New York, Macmillan Co.

Folk, R.L. (1974). The natural history of crystalline calcium carbonate: Effect of magnesian content and salinity. J. Sed. Petrol. 44, 40-53.

Folk, R.L. (1978). A chemical model for calcite crystal growth and morphology control . J. Sed. Petrol. 48, 145-146.

Garrels, R. M , Thompson, M. E. and Siever R. (1961). Control of carbonate solubility by carbonate complexes. Am. J. Scie 259:24-24.

Garrels, R. M and Thompson, M. E. (1962). A chemical model for seawater at 25oC and one atmosphere total pressure. Am. J. Sci. 260:57-66.

Garrels, R. M. and Christ, C. L. (1968). solution, minerals and equilibria. Harper and Row, New York.

Given, R.K. and B.H. Wilkinson (1985). Kinetic control of morphology, composition, and mineralogy of abiotic sedimentary carbonates. J. Sed. Petrol. 55, 109-119.

Goldsmith, J. R. and Heard, H. C. (1961). Lattice constants of calcium-magnesium carbonates. Am. Mineralogist 46:453-547.

Gran, G. (1952). Determination of equivalence point in potentiomtric titration Part. II Analyst. 77: 661-671.

Guggenheim, E. A. (1935.) The specific thermodynamic properties of aqueous solution of strong electrolytes. Phil. Mag. 19:588-643.

Hall, A and J. Kennedy (1967). Aragonite in Fossils, Proc. Roy Soc. Ser. B 168:377-412.

Harned H. S. and Bonner (1945) .The first ionization of carbonic acid in aqueous solution of sodium Colorado J. Am. Chem. Soc.67: 1026-1031.

Harned H. S. and R. Davies Jr. (1943) . The ionization constant of of carbonic acid in water and the solubility of carbon dioxide in water and aqueous solutions from 0 to 50°C. J. Am. Chem. Soc 65: 2030-2037.

Harned H. S. and S. R. Scholes (1941) .The ionization constant of HCO_3^- from 0 to 50°C. J. Am. Chem. Soc. 63, 1706-1709.

Hawley, J. E. (1973). Bicarbonate and carbonate ion association with sodium, magnesium and calcium at 25oC and 0.72 ionic strength. Ph.D. thesis Oregon State University, Corvallis 71pp.

Hawley, J. E. and Pytkowicz (1973.) Interpretation of pH measurements in concentrated electrolyte solutions. Mar. Chem. 1:245-250.

Herman, J. S. and Lorah, M. M. (1988). Calcite precipitation rates in the field: measurement and prediction for travertine-depositing stream. Geochim. Cosmochim Acta. 52: 2347-2355.

Horne, R. A. (1970). In Advances in Hydroscience. Chow, V. T. ed. vol. 6 p119-122.

House, W. A. (1981). Kinetics of crystallization of calcite from calcium bicarbonate solutions. J. Chem Soc. Faraday Trans. 77: 341-359.
hypothesis. Mar. Chem. 1:251-256.

Ingle, S. E., Culberson, C. H., Hawley, J. E. and Pytkowicz, R. M. (1973). The solubility of calcite in seawater at atmospheric pressure and 35‰ salinity. 1:295-307.

Inskeep, W. P. and P. R. Bloom, (1985). An evaluation of rate equations for calcite precipitation kinetics at pCO2 less than 0.01 atm and pH greater than 8. Geochim Cosmochim Act. 49:2165-2180.

Jackson, T.A. and J. L. Bischoff (1971). The influence of amino acids on kinetics of crystallization of aragonite to calcite. J. Geol. 79: 493-497.

James, N.P. and R.N. Ginsburg (1979). The seaward margin of Belize barrier and atoll reefs. Int. Assoc. Sed. Spec. Pub. No. 3, 191pp.

Jamieson, J. C. (1953). Phase equilibrium in the system calcite-aragonite. J. Chem. Phys. 2:1385-1390.

Jamieson, J. C. (1957). Introductory studies of high-pressure polymorphism to 24,000bars x-ray diffraction with some comments on calcite II. J. Geol. 56:334-343.

Johnson, K. S. and Pytkowicz, R. M. (1978). Ion association of Cl^- with H^+,K^+,Ca^{2+} and Mg^{2+} in aqueous solutions at 25°C. Am. J. Sci. 278:1428-1447.

Johnson, K. S., R. Voll, C. A. Curtis and R. M. Pytkowicz (1977). A critical examination of NBS pH scale and determination of titration alkalinity. Deep Sea Res. 24:915

Kashehiev, D. (1969). Nucleation at existing cluster size distributions. Surface Sci. 18: 293-297.

Katz, A (1973). The interaction of magnesium with calcite during crystal growth at 25-29oC and one atmosphere. Geochim et Cosmochim Act. 37:1563-1586.

Keltz, K and Mckenzie, J. A (1982) Diagenetic dolomite formation in Quatenary anoxic diatomaceous muds, Initial reports DSDP 64, Part 2 Washington D.C. U.S. Government Printing Office pp 553-570

Kester D. R., Duedall, J. W., Conners, D. N. and Pytkowicz, R . M.(1967) Preparation of artificial seawater. Limnol. Oceanogr. 12:176-179.

Kester, D. R. (1969). Ion association of sodium, magnesium and calcium with sulfate in aqueous solution. Ph. D. thesis. Oregon State University, Corvallis 116pp.

Kester, D. R. and Pytkowicz R. M. (1967). Determination of the apparent dissociation constants of phosphoric acid in seawater. Limnol. and Oceanogr. 12:243-252.

Kester, D. R. and Pytkowicz R. M. (1969.) Sodium magnesium and calcium sulfate ion-pairs in seawater at 25oC. Limnol. and Oceanogr. 14:686-692.

Kitano, Y. (1962). The behavior of various inorganic ions in the separation of calcium carbonate from a bicarbonate solution: Chem. Soc. Japan. Bull. 35:1973-1980.

Kitano, Y. and Hood D.W. (1962). Calcium carbonate crystal forms formed from seawater by inorganic processes. J. Oceanogr. Soc. Japan. 18, 35-39.

Kitano, Y. and Hood, D. W. (1965). The influence of organic material on the polymorphic crystallization of carbonate. Goechim. Cosmochim Acta. 29:29-40.

Kitano, Y., Park, K. and Hood D. W. (1962). Pure Aragonite synthesis J. Geophys Res. 67:4873.

Koch, B. and A. Disteche (1984). Pressure effect on magnesian calcite coating calcite and synthetic magnesian calcite seed added to seawater in a closed system. Goechim. Cosmochim Acta 48:583-589.

Krauskopf, K (1967). Introduction to geochemistry. McGraw-Hill. New York 721pp.

Kulm, L. D., Suess, E and Thornburg, T. M. (1984) Dolomites in organic-rich muds of the Peru forearc basins; Analogue to the monterey Formation. In Garrison, R. E.

Kastner, M. and Zenger, D.H. eds Dolomites of the Monterey Formation and other organic rich units. SEPM Pacific Section 41, 29-49.

Lahann, R.W. (1978a). A chemical model for calcite crystal growth and morphology control. J. Sed. Petrol. 48, 337-341.

Lahann, R.W. (1978b). (Reply). A chemical model for calcite crystal growth and morphology control. J. Sed. Petrol. 48, 146-147.

Laitinen, H. A. and Harris, W. E. (1975). Chemical Analysis: An advanced text and Reference. 2nd Ed. Mcgraw-Hill Inc. New York. p 143-165.

Land, L. S. (1967). Diagenesis of skeletal carbonate. J. Sed. Pet. 37: 914-930.

Lasaga, A. C. (1981). Rate laws of chemical reactions. In Kinetics of geochemical processes. Reviews in Mineralogy Vol. 8. Ed. A. C. Lasaga and R. J. Kirkpatrick. 1-67. Mineral. Soc. Amer.

Leitmeir, H. (1910). Neves. Tahris. mineral. Vol. 1, p. 9.

Leyendekkers, J. V. (1972.) The chemical potentials of seawater components. Mar. Chem 1:75-88.

Lippman, F. (1960). Versuch Zun Aufklarung der Bildungsdeingungen von Kalzit under Aragonite. Fortschr. Miner. 38:156-161.

Longman, M.W. (1980). Carbonate diagenetic textures from nearshore diagenetic environments. Amer, Assoc, Petrol. Geology. Bull. 64, 461-487.

Lowenstam, H. A. (1955). Aragonite needles secreted by algae and some sedimentary implications. J. Sediment Petrol. 25:270-272.

Lowenstam, H. A., and Epstein, S (1957). On the origin of sedimentary aragonite needles of the Great Bahamas Bank. J. Geol 65:364-375.

Lyman, J (1956.) Buffer mechanism of seawater. Ph. D. thesis Univ. of California Los Angeles. 196pp.

MacIntyre, W. G. (1965). The temperature variation of calcium carbonate in seawater. Fish. Res. Board Canada Manuscript report Ser. 200, 153pp.

MacIntyre, W. G. and R. F. Platford (1964). Dissolved CaCO3 in Labrador Sea. J. Fish. Res. Bd. Canada. 21:1475-1480.

Mackenzie, F.T. and J.D. Pigott (1981). Tectonic controls of Phanerozoic sedimentary rock cycling, J. Geol. Soc, London 138, 183-196.

Macknezie, F. T., Bischoff, W. D., Bishop, F. C., Loijens, M., Schoonmaker, J. and Wollast, R. (1982). Magnesium calcite: Low-Temperature occurrence, solubility, and solid solution behavior. Reeder, R. J. ed. Carbonates mineralogy and chemistry Reviews in Mineralogy 11 P. H. Ribbe series ed. p97-144.

McDully, R.E. and Gieskes, J.M. (1976) Calcium and magnesium profile in DSDP interstial waters. Diffusion or reactions? Earth Planet. Sci. Lett. 33:873-886.

Mehrbach, C . (1973.) Measurements of apparent dissociation constants of carbonic acid in seawater at atmospheric pressure M.S. thesis Oregon State Univ. Corvallis 47pp.

Mehrbach, C., C.H. Culberson, J.E. Hawley, and R. M. Pytkowicz (1973). Measurements of apparent dissociation constants of carbonic acid in seawater at atmospheric pressure. Limnol. Oceanogr. 18:897-907.

Miller, G. R. and Kester, D. R. (1975). Sodium fluoride ion-pairs in seawater. Marine Chem. 4:67-82.

Milliman, J. D. (1967). Carbonate sedimentation on Hogsty Reef, a Bahamian atoll. J. Sediment Petrol. 37:658-676.

Milliman, J. D. (1974). Marine carbonates. Part 1. of Recent sedimentary carbonates. Spring-Verlag: Berlin 375pp.

Moberly, R. (1968). Composition of magnesian calcites of algae and pelecypods by electron microprobe analysis. Sedimentology 11:61-82.

Moller, P. and G. Rajagapolan (1975). Zeitsch, Physik. Chem., Nerve, Folge 74.

Moller, P. and Parkh P. P. (1975). Influence of magnesium on ion activity product of calcite and carbonate dissolved in seawater: a new approach. Mar. Chem. 3:63-70.

Monaghan, and Lytle (1956). the origin of calcareous oolith. J. Sed. Petrol. 26, 111-118

Morse, J. W. (1983). Kinetics of calcium carbonate dissolution and precipitation. In review in mineralogy (VII) .Reeder, R. J. ed. carbonate mineralogy and chemistry. Reviews in Mineralogy 11. Ribbe, R. H. Series ed. p227-264.

Morse, J. W. and Berner, R. A. (1979). The chemistry of calcium carbonate in deep oceans. In Jenne, E. Ed., Chemical modeling- speciation, sorption solubility and kinetics in aqueous systems. Am. Chem. Soc. Washington D. C. p499-535.

Morse, J. W., Mucci A. and Millero F. J. (1980). The solubility of calcite and aragonite in seawater of 35 %o salinity and 25oC and atmospheric pressure. Geochim Cosmochim Act 44: 85.

Morse, J. W.,Mucci A.,Walter, M.L. and Kaminsky (1979). Magnesian interaction with surface of calcite in seawater. Science 205:904-905.

Mucci, A. and Morse J. W. (1984a). The incorporation of Mg2+ and Sr2+ into calcite overgrowths: Influences of growth rate and solution composition. Geochim. Cosmochim. Acta.47, 217-133.

Mucci, A. and Morse J. W. (1984b). The solubility of calcite in seawater solutions at various magnesian concentrations. It = 0.697m at 25oC and one atmosphere total pressure. Geochim. Cosmochim. Acta. 48:815-822.

Mucci, A., Morse J. M. and Kaminsky M. S. (1985). Auger spectroscopy analysis of magnesium calcite overgrowths precipitated from seawater and solution of similar composition. Am. J. Sci 285:289-305.

Muller, G., Irion, G. and Forstner, V. (1972). Formation and diageneisis of inorganic Ca-Mg-carbonate in Lacustrine environment. Naturwissenschaften 59, 158-164.

Murray, J.W. (1967). The decomposition of calcite and aragonite in coves. J. Geol. 62, 481-492.

Murry, C. N. and J. P. Riley (1971). The solubility of gases in distilled water and seawater-IV. Carbon dioxide. Deep-Sea Research 18:533-543.

Nancollas, G. H. and Purdie, N. (1964). Kinetics of crystal growth. Quart. Rev. (London) 18:1-20.

Nancollas, G. H. and Reddy, M. M. (1971). The crystallization of calcium carbonate. II Calcium growth mechanism. J. Colloid. Interface Sci. 37: 824-830.

Nancollas, R. B. and Brand, U. (1989). Secular Variation of calcium carbonate mineralogy; and evaluation of ooid and micrite chemsitries. (in press).

Newkirk, J.B. (1957). General Theory, mechanism and kinetics: From precipitation from solid solution. 6-40. Series of 9 lectures presented to AMS during natural Congress. Nov. 4-8, 1957. Am. Soc. for Metal, Cleveland, Ohio.
of strong electrolytes Phil. Mag. 19:588-643.

Pantin, H. M. (1965). the effect of adsorption on the attainment of physical and chemical equilibrium in sediments. N. Z. J. Geophys 8:453-464.

Pierson, B J. and Chinn E.A. (1983). Distribution and preservation of carbonate cements in Pleistocene limestone of hogsty Reef atoll, southeastern Bahamas (abstract). Am. Assoc. Petroleum Geologist Bull. 67, 534pp.

Pigott, J. D. and Land, L. S. (1986). Interstitial water chemistry of Jamaica Reef sediment: Sulfate reduction and submarine cementation. Mar. Chem. 19:355-378.

Pitzer, K.S. (1971) . Thermodynamics of electrolytes.I Theoretical basis and general equations. J. Phys. Chem. 77:268-277.

Plath, D. C. and Pytkowicz, R. M. (1982). The solubility of Aragonite in seawater at 25oC and 32.62%o salinity. Mar. Chem. 10:3-7.

Plath, D. C., Johnson, K. S. and Pytkowicz R. M. (1980). The solubility of calcite in seawater with respect to salinity and temperature. Mari. Chem. 10:9-.

Plummer, L. N. and Back, W. (1982). The mass balance approach: Application to interpreting the chemical evolution of hydrologic system. Am. J. Sci. 280: 130-142.

Plummer, L. N. and Mackenzie, F. T. (1974). Predicting mineral solubility from rate data: Application to the dissolution of magnesian calcites. Am. J. Sci. 274: 61-83.

Plummer, L. N.; Parkhurst, D. L. and Wigley, T. M. L. (1979). Critical review of kinetics of calcite dissolution and precipitation. In Jenne, E. Ed., Chemical modeling speciation, sorption, solubility, and kinetics in aqueous systems. Am. Chem. Soc.: Washington D. C. p537-573.

Plummer, L. N.; Wigley, T. M. L. and Parkhurst, D. L. (1978). The kinetics of calcite dissolution in CO2-seawater system at 5oC to 60oC and 0.0 to 1.0 atm CO2. Am. J. Sci. 278: 179-216.

Pytkowicz, R. M (1965). Rates of inorganic calcium carbonate nucleation. j. Geol. 3:196-199.

Pytkowicz, R. M (1973). Calcium carbonate retention in superstaruted seawater. Am. J. Sci 273:515-522.

Pytkowicz, R. M. (1969.) Use of apparent equilibrium constants in chemical oceanography, geochemistry, and biochemistry. Geochem. J. 3:181-184.

Pytkowicz, R. M. and Conners, N (1964). High pressure solubility of calcium carbonate in seawater. Science 144:840-841.

Pytkowicz, R. M. and Hawley, (1974). Bicarbonate and carbonate ion-pairs in a model of seawater at 25oC. Limnol. and oceanogr. 19:223-234.

Pytkowicz, R. M. and Kester D. R. (1969.) Harned's rule behavior of NaCl-NaSO4 solution explained by ion association model. Am. J. Sci. 267:217-229.

Pytkowicz, R. M. and M. Cole (1979). Equilibrium and kinetic problems in mixed electrolyte solutions. In Newman, S. A. ed.Thermodynamics of aqueous systems with industrial applications ACS Symposium Ser., 133:643-652.

Pytkowicz, R. M.(1975). Activity coefficients of bicarbonates and carbonates in sheather. Limnol. and Oceanogr. 20:971-975.

Pytkowicz, R. M., Atlas, E. and Culberson, C. H. (1977). Some concentrations of chemical equilibrium in the oceans. Oceanogr. Mar. Biol. Ann. Rev. 15: 11-45.

Pytkowicz, R. M., S. E. Ingle and C. Mehrbach (1974 .). Invariance of apparent equilibrium constants with pH. Limnol. and Oceanogr. 19:665-669.

Pytkowicz, R.M. (1969). Chemical solution of calcium carbonate in seawater. Am. Zoologist. 9, 673-679.

Pytkowicz, R.M. (1983a). Equilibria, non-equilibria, and natural waters. vol. I. ed. John Wiley Interscience, New York, 353pp.

Pytkowicz, R.M. (1983b). Equilibria, non-equilibria, and natural waters. vol. II. ed. John Wiley Interscience, New York, pp.

Pytkowicz, R.M. and Cole (1979). Equilibrium and kinetic problem in mixed electrolyte solutions. In Newmann, S.A. ed. Thermodynamics of Aqueous Systems with Industrial Applications. Am. Chem Soc. Symp. Ser. 133, 643-652.

Reddy, M. M. (1983). Characterization of calcite dissolution and precipitation using an improved experimental technique. Sci. Geol. Mem. 71: 109-117.

Reddy, M. M. and Nancollas, G. H. (1971). The crystallization of calcium carbonate. I Isotopic exchange and kinetics. J. Colloid. Interface Sci. 36: 166-172.

Reddy, M. M. Plummer, L. N. and Busenberg, E. (1981). Crystal growth of calcite from calcium bicarbonate solutions at 25°C: A test of calcite dissolution model. Geochim Cosmochim. Acta. 45: 1281-1289.

Riley, J. P. and Skirrow, G. (1975). Chemical Oceanography eds. Academic Press Inc. London 647pp.

Robie, R. A. and Walbaum, D. R. (1968). Thermodynamic properties of minerals and related substances at 298.15 oK and one atmosphere. Goel. Survey Bull. Washington. 1259.

Robinson, R. A. (1954). The vapor pressure and osmotic equivalence of seawater. J. Mar. Ass. U. K. 33:449-455.

Robinson, R. A. and R. H. Stokes (1968). Electrolyte solutions 2nd ed. Butterworths

Robinston, R. A. and R. H. Wood. (1972). Calculation of the osmotic and activity of seawater at 25oC. J. Solution Chem. 1:481-488.

Sandberg, P.A. (1975). New interpretation of Great Salt Lake ooids and of ancient nonskeletal carbonate mineralogy. Sedimentology 22, 499-537.

Sandberg, P.A. (1983). An oscillating trend in Phanerozoic nonskeletal carbonate mineralogy. Nature 305, 19-22.

Sandberg, T. P. (1958). Nonskeletal aragonite and pCO2 in Phanerozoic and Proterozoic. In The carbon cycel and atmospheric CO2 natural variation Archean to present. E. T. Sundquist and W. S. Broecher, (eds) American Geophyical Union Monograph 32:585-594.

Sayles, F.L. and W.S Fyfe (1973). Low-magnesian calcite limestones forming at deep-sea floor, Tongue of the ocean, Bahamas. Sedimentology 25, 675-702.

Schmalz, R. F. (1967). Kinetics and diagensis of carbonate sediments. J. Sediment Petrol. 37:60--67.

Schmalz, R. F. and K. E. Chave (1963). Calcium carbonate: Factors affecting saturation in ocean waters off Bermuda. Science. 139:1206.

Schoonmacker, J. E. (1981). Magnesian calcite-seawater reaction: solubility and recrystallization behavior. Ph. D. Thesis, Nothrwestern University.

Scoffin, T. P. (1987). An introduction to carbonate sediments and rocks. Blackie p708-730.

Silliman, B. (1846). On the chemical composition of calcareous corals. Am. J. Science 1:189-199.

Simkiss, K. (1964). Variation on crystalline from calcium carbonate from artificial seawater. Nature 201:492.

Sjoberg, E. L. (1976). A fundamental equations for calcite dissolution kinetics. Geochim Cosmochim Acta. 40: 441-447.

Smith, A. D. and Roth, A. A. (1979). Effect of carbon dioxide concentration on calcification in the red coralline algae Bossiella orbigniana. Mar. Biol. 52:217-225.

Sneoyink, V. L. and D. Jenkins (1980). Water chemistry, New York Wiley. 463pp.

Stern, K. H. and Amis, E. S. (1959). Ionic Size. Chemical Reviews. 59:1-64.

Stockman, K. W. Ginsburg, R. N. and Shinn, E. A. (1967). The production of lime mud by algae in south Florida. J. Sediment. Petrol. 37:633-348.

Stumm, W. and J.W. Morgan (1982). Aquatic Chemistry: An introduction emphasizing chemical equilibria in natural waters. 2nd ed. Interscience, New York. 780pp.

Suess, E. Von Huene, et al., (1987) Proc. Init. Repts ODP. 112 Site 685.

Suess, E. (1970). Interaction of organic compounds with calcium carbonate. I Association phenomena and geochemical implications. Geochim, Cosmochim. Acta 34:157-168.

Suess, E. (1973). Interaction of organic compounds with calcium carbonate. II Organo-carbonate association in recent sediments. Geochim, Cosmochim. Acta 37:2435-2447.

Taft, W.H. (1963). Cation influence on diagenesis of carbonate sediments (abstract). Geol. Soc. Am. Spec. Paper 76. (Abstract for 1963).

Taft, W.H. and J.W. Harbaugh (1964). Modern carbonate sediments of southern Florida, Bahamas, and Espititu Santo island, Baja California: a comparison of their mineralogy and chemistry Stanford University Publ. University Series Geol. Sci. 8:1-133.

Takahashi, T. , Williams, R. T. and Bos, D. L. (1982). Carbonate chemistry: In W. S. Broecker, D. W. Spencer, and H. Craig. (eds) GEOSECS. Pacific Expidition.V3. Hydrographic Data. NSF. Washington 78-82.

Thorstenson, D. C. and L. N. Plummer (1977). Equilibrium criteria for two component solids reacting with fixed composition in an aqueous phase example: the magnesian calcite. Amer. J. Sci. 277:1203-1223.

Toschev, S. (1973). In Crystal Growth. P. Hartman (ed.) Elsevier, New York.

V*on Breymann, M. T. (1988)* Magnesium in hemipelagic Environments: Surface reactions in the sediment-pore water system. Ph. D. Thesis Oregon State Univ. Corvallis 224pp.

Walter, L. M. and Morse, J. W. (1984). Magnesian calcite stabilities:. A reevaluation. Geochim. Cosmochim. Acta. 48:1059-1069.

Walter, L. M., and Morse, J. W. (1985). The dissolution kinetics of shallow marine carbonates in seawater: A laboratory study. Geochim Cosmochim Acta. 49: 1503-1513.

Warme, J.E. and Schneiderman, N. (1983). Patch-Reef cementation: Holocene of Eniwetock atoll and Jurassic of Morocco (Abstract). Am. Assoc. Petrol. Geol Bull. 67, 565pp.

Westall, J. (1979). MICROQL. A chemical equilibrium program in basic. Chemistry Detaprtment, Oregon State University, Corvallis. 41pp.

Weyl, P. K. (1958). The solution kinetics of calcite. J. Geol. 69:32-44.

Weyl, P. K. (1961). The carbonate satratometer. J. Geol. 69:32-44.

Weyl, P. K. (1964). The solution solution alternation of carbonate sediments and skeletons. In approaches to Paleoecology, Imbrie, J. and Newell, N ed. John Wiley and Sons. New York. 345-356.

Weyl, P. K. (1966). Environmental stability of earth's surface chemical consideration. Geochim Cosmochim. Acta. 30:663-679.

Weyl, P.K. (1967). The solution behavior of carbonate materials in seawater. Int'l. Conf. Tropical Oceanogr. University of Miami, Miami, Florida, 178-228.

Whitfield, M. (1973.) A chemical model for sea water based on Bronsted-Guggenheim hypothesis. Mar. Chem. 1:251-256.

Wilkinson, B.H. (1979). Biomineralization, paleo-oceanography, and the evolution of calcareous marine organisms. Geol.. 7, 524-527.

Wilkinson, B.H., Roberts M.O. and Alan, R. C. (1985). Submarine hydrothermal weathering, Global eustasy, and carbonate polymorphism in Phanerozoic marine oolites. J. Sed. Petrol. 55, 171-183.

Wollast, R. (1971). Kinetics aspects of the nucleation and growth of calcite from aqueous solutions. In carbonate cements. O. P. Bricher (ed). John Hopkins University Studies in Geology. 19. p264-273.

Wollast, R. and Pytkowicz R. M. (1978). Carbonate equilibrium and phase rule. Geochim J. 12:199-200.

Wollast, R. and Reinhard-Derie D. (1977). Equilibrium and mechanism of dissolution of magnesium calcites. In The Fate of Fossil Fuel CO2 in Oceans, N. R. Andersoen and A. Malahoff, eds. Plenum. Press. New York 479-492.p.

Wollast, R., Garrel, R. M. and Mackenzie, F. T. (1980). Calcite-seawater reaction in ocean surface waters. Am. J. Sci. 280:831-848.

Appendix 2.1

pC-pH diagram

pC-pH diagram of carbonic acid in seawater of 35‰ salinity. Total CO_2 is 2.3 mmole/kgSW, K_1'=9.972E-7 and K_2'=7.651E-10 (from Mehrbach, 1973) and K_W= 2.399E-14 (Culberson et al., 1970), showing the various equivalent points.

In terms of carbonate alkalinity, CA, the points a, b, and c correspond to the expressions: CA=$(HCO_3^-)+2(CO_3^{2-})$, CA= $(H_2CO_3^*)+(CO_3^{2-})$ and CA=$-2(H_2CO_3^*)-(HCO_3^-)$, respectively.

APPENDICES

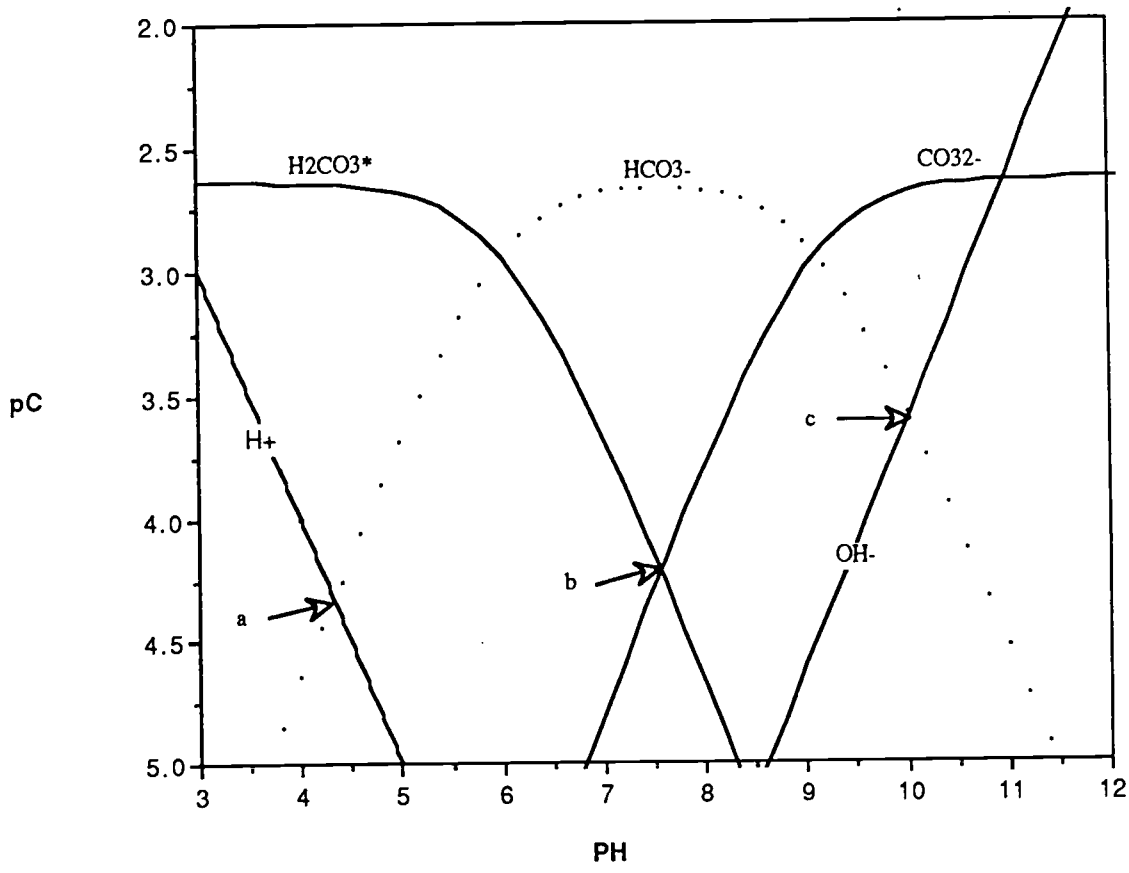
2.0
2.5
3.0
3.5
4.0
4.5
5.0
pC
H2CO3*
HCO3-
CO32-
H+
OH-
a
b
c
3
4
5
6
7
8
9
10
11
12
PH

Appendix 2.2

Derivation of the equation (2.24)

$$(x) = \frac{\Sigma CO_2 K_1'}{CA} \quad K_1'$$

Appendix 2.2.

At low pH ranges where the concentration of CO_3^{2-} is almost zero, one can treat the carbonic acid as monoprotic acid. The following difinitions and equations are possible:

$$\Sigma CO_2 = (H_2CO_3^*)+(HCO_3^-) \qquad (2a)$$

and

$$CA = (HCO_3^-) \qquad (2b)$$

Also total CO_2 is expressed by the following equation:

$$\Sigma CO_2 = \Sigma CO_2 \frac{(H^+)}{((H^+)+K_1)} + (HCO_3^-) \qquad (2c)$$

by rearrangement:

$$(HCO_3^-) = \Sigma CO_2 \frac{1-(H^+)}{(H^+)+K_1} \qquad (2d)$$

and

$$\Sigma CO_2K_1 = (HCO_3^-)[(H^+)+K_1] \qquad (2e)$$

The following equation is obtained by substitution equation (2b) in equation (2e) and rearrangement:

$$(H^+) = \frac{\Sigma CO_2K_1}{CA} - K_1 \qquad (2f)$$

Appendix 2.3

Composition of ASW for K1' and K2' measurements

Appendix 2.3 continued

Salt	Molarity $X10^{+3}$
NaCl	402.7
Na_2SO_4	027.7
KCl	008.9
$NaHCO_3$	002.29
KBr	000.81
NaF	000.072
$SrCl_2$	000.152*
Ionic strenth	497.91

* Added from prestantradized stock solution.

Appendix 3.1

Determination of the specific area of calcite.

Appendix 3.1

The specific area of synthetic calcite per g of calcite was determined from it's density and the volume of the calcite crystal. The density of calcite, $\rho_{(calc)} = 2.71\ g\ c^{-3}$. The average volume of the crystal, $V_{(mean)} = 54.71\ \mu m^3 = 5.471 \times 10^{-17}\ m^3$. It was determined from SEM images. From the density of calcite the volume per g is:

$$\frac{1}{\rho_{(calc)}} = \frac{10^{-6}\ m^3}{2.71\ g} = 3.69 \times 10^{-7}\ m^3/g \qquad (4.1a)$$

The numbers of crystals that may fill $3.69 \times 10^{-7}\ m^3/g$ is:

$$\frac{3.69 \times 10^{-7}\ m^3/g}{5.471 \times 10^{-17}\ m^3} = 6.745 \times 10^{+9}\ \text{crystals/g.}$$

From the average surface area of the crystal, $A_{(mean)} = 87.253\ \mu m^2/crystal = 8.725 \times 10^{-11}\ m^2/crystal$, the specific surface area, A, is:

$$A = (8.725 \times 10^{-11}\ m^2/\text{crystal})\ (6.745 \times 10^{+9}\ \text{crystals/g}) = 0.589\ m^2/g.$$

Appendix 4.1

MICROQL program

Example of the chemical equilibrium calculation by MICROQL program (Westall, 1979).

Appendix 4.1: continued

The chemical species of ASW, were calculated by MIQROQL basic program described by Westall (1979). The experiment SC97 is shown here as an example.

The Stability constants of ionic pairs are represented by the general equation:

$$K^*_{(MnXm)} = \frac{(M_nX_m^{[m-n]})}{(M)_F^n(X)_F^m} \quad (4.1A)$$

The components and the species as well as their equilibrium constants are shown in Table 4.1A. The out put of Table 4.1A. is shown in Table 4.2A.

Table 4.1A

Equilibrium of the experiment SC97. (For more details see Westall 1979).

	COMPONENTS										
	1	2	3	4	5	6	7	8	9		
SPECIES	Na^+	Mg^{2+}	Ca^{2+}	K^+	Cl^-	$SO4^{2-}$	$CO3^{2-}$	F^-	H^-	Log K	Ref.
1. Na^+	1	0	0	0	0	0	0	0	0	0	
2. $NaCl^o$	1	0	0	0	1	0	0	0	0	-0.484	1
3. $NaSO_4^-$	1	0	0	0	0	1	0	0	0	0.305	2
4. $NaHCO_3^o$	1	0	0	0	0	0	1	0	1	5.383	5
5. $NaCO_3^-$	1	0	0	0	0	0	1	0	0	0.628	5
6. NaF^o	1	0	0	0	0	0	0	1	0	1.337	6
7. Mg^{2+}	0	1	0	0	0	0	0	0	0	0	
8. $MgCl^+$	0	1	0	0	1	0	0	0	0	0.263	1
9. $MgSO_4^o$	0	1	0	0	0	1	0	0	0	1.010	2
10 $MgHCO_3^+$	0	1	0	0	0	0	1	0	1	6.145	5
11 $MgCO_3^o$	0	1	0	0	0	0	1	0	0	2.050	5
12 $Mg_2CO_3^{2+}$	0	2	0	0	0	0	1	0	0	2.587	5
13 $MgCaCO_3^{2+}$	0	1	1	0	0	0	1	0	0	2.018	5
14 MgF^o	0	1	0	0	0	0	0	1	0	1.988	9
15 Ca^{2+}	0	0	1	0	0	0	0	0	0	0	
16 $CaCl^+$	0	0	1	0	1	0	0	0	0	0.358	1
17 $CaSO_4^o$	0	0	1	0	0	1	0	0	0	1.033	3
18 $CaHCO_3^+$	0	0	1	0	0	0	1	0	1	6.228	5
19 $CaCO_3^o$	0	0	1	0	0	0	1	0	0	2.447	5
20 CaF^o	0	0	1	0	0	0	0	1	0	0.653	6
21 K^+	0	0	0	1	0	0	0	0	0	0	
22 KCl^o	0	0	0	1	1	0	0	0	0	-0.297	1
23 KSO_4^-	0	0	0	1	0	1	0	0	0	0.265	4
24 HCl^o	0	0	0	0	1	0	0	0	1	-0.752	1
25 Cl^-	0	0	0	0	1	0	0	0	0	0	
26 SO_4^{2-}	0	0	0	0	0	1	0	0	0	0	
27 $H_2CO_3^*$	0	0	0	0	0	0	1	0	2	15.082	7
28 HCO_3^-	0	0	0	0	0	0	1	0	1	9.418	7
29 CO_3^{2-}	0	0	0	0	0	0	1	0	0	0	
30 F^-	0	0	0	0	0	0	0	1	0	0	
31 OH^-	0	0	0	0	0	0	0	0	-1	-13.62	8
32 H^+	0	0	0	0	0	0	0	0	1	0	
Total Conc:	0.4908		0.009686		0.5802		0.0020389	0.0			
(Molar)		0.04909		0.0095		0.027		0.00209			

Guess (log C_T):	-1	-2	-3	-3	-1	-2	-3	-5	-7.586

(1) Johnson and Pytkowicz, (1978).
(2) Pytkowicz and Kester, (1968).
(3) Kester and Pytkowicz, (1968).
(4) Elgquist and Wedborg, (1978).
(5) Pytkowicz and Hawley, (1974).
(6) Miller and Kester, (1975).
(7) From Chapter 2.
(8) Culberson et al, (1973).

Species	Matrix										log K	C	log C
1	1	0	0	0	0	0	0	0	0	0		.414151466662	-.382840797335
2	1	0	0	0	1	0	0	0	0		-.484	6.60389751142E-2	-1.18019967535
3	1	0	0	0	0	1	0	0	0		.305	1.05279446587E-2	-1.97765640665
4	1	0	0	0	0	0	1	0	1		5.383	1.19694720418E-7	-6.92192500534
5	1	0	0	0	0	0	1	0	0		.628	8.11101107969E-5	-4.09092500536
6	1	0	0	0	0	0	0	1	0		-1.337	3.84737652903E-7	-6.41483530879
7	0	1	0	0	0	0	0	0	0	0		2.42141953926E-2	-1.61592995744
8	0	1	0	0	1	0	0	0	0		.263	2.15630983906E-2	-1.66628883545
9	0	1	0	0	0	1	0	0	0		1.01	3.12071733403E-3	-2.50574556675
10	0	1	0	0	0	0	1	0	1		6.145	4.04562695789E-8	-7.39301416548
11	0	1	0	0	0	0	1	0	0		2.05	1.25310030168E-4	-3.90201416547
12	0	2	0	0	0	0	1	0	0		2.587	1.04485464343E-5	-4.9809441229
13	0	1	1	0	0	0	1	0	0		2.018	4.99513754151E-7	-6.30145254895
14	0	1	0	0	0	0	0	1	0		1.988	4.75417901939E-5	-4.32292446888
15	0	0	1	0	0	0	0	0	0	0		4.29103064896E-3	-2.36743838348
16	0	0	1	0	1	0	0	0	0		.358	4.75557175004E-3	-2.32279726149
17	0	0	1	0	0	1	0	0	0		1.033	5.83103981993E-4	-3.23425399279
18	0	0	1	0	0	0	1	0	1		6.228	8.67915428155E-9	-8.0615225915
19	0	0	1	0	0	0	1	0	0		2.447	5.53958726893E-5	-4.25652259151
20	0	0	1	0	0	0	0	1	0		.653	3.89553494982E-7	-6.40943289494
21	0	0	0	1	0	0	0	0	0	0		7.48944430506E-3	-2.1255504045
22	0	0	0	1	1	0	0	0	0		-.297	1.83692200829E-3	-2.73590928251
23	0	0	0	1	0	1	0	0	0		.265	1.73633686557E-4	-3.76036601381
24	0	0	0	0	1	0	0	0	1		-.752	2.23172727916E-9	-8.651358878
25	0	0	0	0	1	0	0	0	0	0		.486005430505	-.313358878011
26	0	0	0	0	0	1	0	0	0	0		1.25946003386E-2	-1.89981560931
27	0	0	0	0	0	0	1	0	2		15.083	3.75754537951E-5	-4.42509420601

28	0	0	0	0	0	0	1	0	1	9.148	1.68234782871E-3	-2.77408420803
29	0	0	0	0	0	0	1	0	0	0	4.61228135538E-5	-4.33608420803
30	0	0	0	0	0	0	0	1	0	0	2.01839187175E-5	-4.69499451143
31	0	0	0	0	0	0	0	0	-1	13.62	1.60694125301E21	21.206
32	0	0	0	0	0	0	0	0	1	0	2.59417936212E-8	-7.58600000003

COMPONENTS: MATRIX T, LOG(X), Y

1	.4908	-.382840797334	-1.929797E-12
2	.0490923	-1.61592995744	4.847E-13
3	.009686	-2.36743838348	8.1582E-14
4	.0095	-2.12555040449	-9.3E-14
5	.5802	-.313358878011	0
6	.027	-1.89981560931	-1.E-13
7	.00203898	-4.33608420802	4.38E-14
8	.0000685	-4.69499451143	5.93E-14
9	0	-7.586	-1.60694125301E21